Physics Lib.
DO NOT TAKE FROM LIBRARY
JUL 23 1935
cop 2

THE PHYSICAL REVIEW

VOLUME 48 *Second Series* NUMBER 2

JULY 15, 1935

Published for the

AMERICAN PHYSICAL SOCIETY

by the

AMERICAN INSTITUTE OF PHYSICS
Incorporated

LANCASTER, PA., AND NEW YORK, N. Y.

THE AMERICAN PHYSICAL SOCIETY

OFFICERS OF THE SOCIETY

R. W. WOOD, *President*
The Johns Hopkins University
Baltimore, Maryland

F. K. RICHTMYER, *Vice President*
Cornell University
Ithaca, New York

W. L. SEVERINGHAUS, *Secretary*
Columbia University
New York, New York

G. B. PEGRAM, *Treasurer*
Columbia University
New York, New York

JOHN T. TATE, *Editor*
University of Minnesota
Minneapolis, Minnesota

L. B. LOEB, *Local Secretary for the Pacific Coast*
University of California
Berkeley, California

THE PHYSICAL REVIEW

BOARD OF EDITORS

JOHN T. TATE, *Editor*

J. W. BUCHTA, *Assistant Editor*

Associate Editors

K. K. DARROW
J. C. HUBBARD
A. E. RUARK
A. ELLETT
L. A. TURNER
G. E. UHLENBECK
W. V. HOUSTON
R. S. MULLIKEN
I. I. RABI

THE PHYSICAL REVIEW, which was established in 1893, is a journal of experimental and theoretical physics. It is published for the American Physical Society by the American Institute of Physics Incorporated. There are two volumes annually with twelve issues in each volume.

Manuscripts for publication should be submitted to John T. Tate, University of Minnesota, Minneapolis, Minnesota.

Proof and all correspondence concerning papers in the process of publication, should be addressed to the Editorial Secretary, American Institute of Physics, 11 East 38th Street, New York, New York.

Subscription price: United States and Possessions and Canada, $15.00; Foreign, $16.50. Subscriptions and orders for back numbers should be addressed to Prince and Lemon Streets, Lancaster, Pennsylvania, or to the American Institute of Physics, 11 East 38th Street, New York, New York.

Advertising is not accepted for the *Physical Review* but attention is called to the *Review of Scientific Instruments with Physics News and Views*, a companion publication of the Institute, and a medium through which the field of physics can be reached most effectively. Rates and other information will be furnished on request to the Editorial Secretary.

Changes of address and complaints of failure to receive the *Physical Review*, in the case of members of the American Physical Society, should be addressed to the Treasurer; in the case of other subscribers, to the Editorial Secretary. New copies can be sent free in response to complaints of non-delivery only if notice of non-delivery is received within three months of date of issue.

The Physical Review is published semi-monthly at Prince and Lemon Streets, Lancaster, Pennsylvania.

Entered at the Post Office at Lancaster, Pennsylvania, as second class matter.

Acceptance for mailing at special rate of postage provided for in section 1103, Act of October 3, 1917, authorised September 6, 1926.

THE
PHYSICAL REVIEW
A Journal of Experimental and Theoretical Physics
VOL. 48, NO. 2 JULY 15, 1935 SECOND SERIES

The Variation of Sparking Potential with Intense Ultraviolet Illumination

HARRY J. WHITE, *Department of Physics, University of California*
(Received April 29, 1935)

The static sparking potential has been found to be lowered by illuminating the cathode of a spark gap with intense ultraviolet light, an auxiliary spark gap being used as the source of ultraviolet illumination. The photoelectric current released from the cathode of the illuminated gap was about 10^6 times larger with this source than with a quartz mercury arc for illumination. The amount of lowering of the sparking potential was found to increase as the intensity of the spark illumination was increased and reductions up to about 10 percent were noted in air. The reduced sparking potentials in air were found to be a function of gas pressure times gap length and therefore obey Paschen's law. The approximate law for the amount of lowering of the sparking potential can be expressed by the condition that a certain number remains constant. This number is the number of positive ions generated by electron collision in the gas as the result of a given number of photoelectrons being liberated at the cathode by one flash of the illuminating spark. One may interpret this as meaning that the breakdown is a space charge phenomenon and that some fixed value of the field is necessary for breakdown to occur. Then if the distribution of the space charge does not change appreciably, the amount necessary to produce the given field will be constant.

THE static sparking potential of a spark gap may be defined as the smallest potential difference which, when applied to it for an indefinite length of time, will cause a spark to pass. The results of many experiments[1] show that the sparking potential depends on the nature and pressure of the gas surrounding the electrodes, on the geometry and separation of the electrodes, but apparently for pressures above about 1 cm not on the electrode material.[2]

The effect of ultraviolet illumination on sparking potentials has been somewhat in doubt. It is well known that such illumination decreases the time lag,[3, 4] a fact which complicates any experiment designed to test the effect on the sparking potential. Most investigators find that ultraviolet illumination has no measurable effect on sparking potentials, but exceptions have been reported. Herweg[5] found a lowering of about 5 percent by illuminating a 3 mm gap in air at atmospheric pressure with a zinc arc. However, the arc was very close to the gap and the resultant heating of the gas could have produced the effect observed. Masch[6] reports that he observed a lowering of 3 percent by illuminating a gap in air with a quartz mercury arc, although the many previous observers have found no such effect. Hammerschaimb[7] on the other hand showed that intense x-radiation reduced the sparking potential of a short gap in nitrogen at *10 atmospheres pressure* by about 3 percent.

The researches referred to above have used relatively weak intensities of illumination. If really intense illumination is used, the photo-

[1] See, for example, Thomson, *Conduction of Electricity in Gases*, 3d ed., Vol. 2, p. 470.
[2] L. B. Loeb, Phys. Rev. **38**, 1891 (1931); L. J. Neuman, Proc. Nat. Acad. Sci. **15**, 259 (1929).
[3] Defined as the average time spent in awaiting a spark after a given potential is applied to a gap. For definiteness the manner of applying the potential must be specified, i.e., impulse or static potential.
[4] K. Zuber, Ann. d. Physik **76**, 231 (1925); A. Tilles, Phys. Rev. **46**, 1015 (1934).
[5] J. Herweg, Physik. Zeits. **7**, 925 (1906).
[6] K. Masch, Archiv. f. Elektrotechnik **26**, 589 (1932).
[7] Hammerschaimb, Archiv. d. Sci. Phys. et Nat., Ser. [5] **5**, 292 (1923).

charge released from the cathode might be expected to be large enough to have an appreciable effect on the sparking potential of a gap (see for example an analysis by Loeb[8]). The present paper describes the results obtained by using a spark gap as a source of ultraviolet illumination and noting its effect on the sparking potential of a second gap. Measurements of the photo-charge released from brass by this source of illumination and by illumination from a quartz mercury arc show the former to be 10^6 times as intense.

Apparatus

A schematic diagram of the apparatus is shown in Fig. 1. G_1 and G_2 are the two spark gaps, G_1 being the source of ultraviolet radiation and G_2 the gap under observation. G_1 consists of spherical brass electrodes 2 cm in diameter in air at atmospheric pressure. It is fired by the $\frac{1}{2}\mu$fd condenser C_2 and is set to break down at about 17,000 volts. The electrodes of G_2 are interchangeable and are enclosed in a glass chamber which is a part of a vacuum system. The electrodes, the gap distance, the gas and the pressure of G_2 are thus all readily varied.

The potential applied to G_2 is measured by a voltmeter consisting of a 50 megohm Taylor high voltage resistor, R_4, and a milliammeter. The condenser C_2 which is shunted across R_4 reduces the alternating-current ripple voltage to less than 0.1 percent of the steady voltage. The accuracy of the voltmeter is such that the potential could be read to the nearest 100 volts.

G_1 is placed about 30 inches above G_2 and the radiation from its spark is focused on the tip of the cathode of G_2 by the quartz lens, L. A quartz window in the glass chamber enclosing G_2 enables the ultraviolet to reach the cathode. A right-angle quartz prism could be placed between G_1 and L to reflect the light from a quartz mercury arc onto the cathode of G_2. The intensity of the radiation incident on G_2 could be varied by interposing various screens at S. The photocurrents released from the cathode of G_2 were measured by replacing the anode with a collecting electrode which was connected to an electrometer.

[8] L. B. Loeb, Science **69**, 509 (1929).

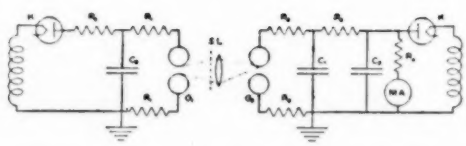

Fig. 1. Schematic diagram of apparatus. $R_1=4\Omega$, $R_2=25\Omega$, $R_3=5\times10^8\Omega$, $R_4=5\times10^7\Omega$, $C_1=0.008\mu$fd, $C_2=C_3=0.5\mu$f.

Measurements and Results

The measurements were taken with the purpose of comparing the sparking potentials of G_2, using first the auxiliary gap and second the quartz arc as sources of illumination, under various conditions as to gap length, pressure and intensity of illumination of G_2. In observing the sparking potential for the spark illumination, the gap G_1 was set to spark intermittently at intervals of a few seconds, and the potential of G_2 raised very slowly to the sparking point. The sparking potential for the arc illumination was obtained by interposing the quartz prism and again raising the potential until sparking occurred.

It was found that the spark illumination always reduced the sparking potential appreciably, but that, starting with a clean cathode surface, succeeding sparks required slight increases in voltage. Examination of the cathode surface after sparking showed that the first spark struck near the center and that the succeeding ones grouped about the first, no two ever striking in the same place. This suggests that the partial oxidation of the surface where the spark struck reduced the photo-emission there and thus made it unfavorable for another spark. As a result the next spark would have to take a slightly longer path and would thus require a somewhat higher voltage. With the arc illumination the spark always struck approximately the same place on the cathode and no increase in sparking potential with succeeding sparks was noted. The above effect made it necessary to clean the cathode after each comparison measurement of the sparking potential. With this precaution very consistent results were obtained, the sparking potential with a given set of conditions varying less than $\frac{1}{2}$ percent on repeated measurements.

Reduction of the sparking potential with the spark illumination was observed to occur with all

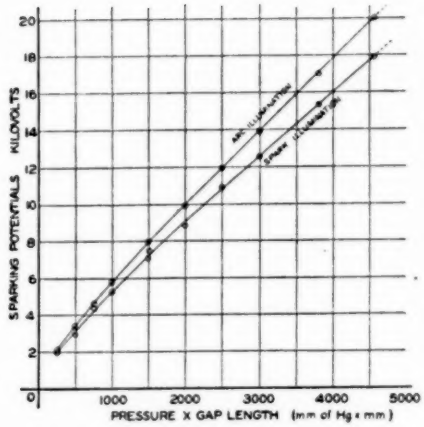

FIG. 2. Sparking potential for spark (intense) and arc (weak) illuminations.

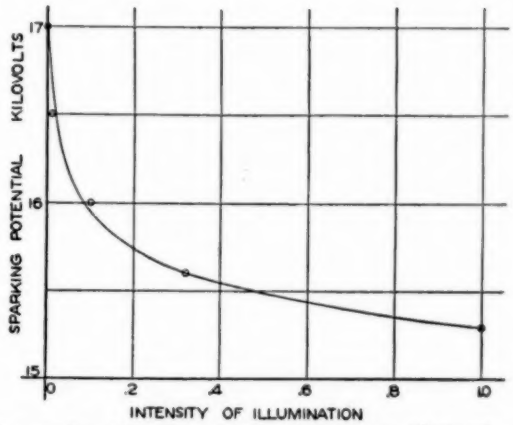

FIG. 3. Sparking potential as a function of intensity of illumination. Air at atmospheric pressure, approximately uniform field, 5 mm gap.

of the several gases tested, these being helium, carbon dioxide and air. Detailed measurements were carried out only for air, as this is the only gas for which the Townsend coefficient for ionization by collision by electrons is known accurately in the range of X/p involved.[9] All of the variable factors were found to affect the amount of lowering of the sparking potential, as will be described below.

(1) *Variable gap length and pressure, constant illumination intensity and approximately uniform field.* The electrodes were 4 cm brass spheres and gap lengths up to 6 mm were used so that the field near the axis of the spheres was nearly uniform. The sparking potential for weak illumination and uniform fields satisfies Paschen's law, i.e.,

$$V = f(pd)$$

where V = sparking potential; p = pressure (temperature supposed constant); d = gap length. It was found that this law was also obeyed for the reduced sparking potentials obtained with the intense illumination. Fig. 2 shows sparking potential plotted as a function of pressure times gap length for both the arc and the spark illuminations. The lowering of the sparking potential by the spark illumination is about 10 percent for the larger values of pd and about 5 percent for the smaller values. Reducing the intensity of the spark illumination gives curves similar to the one plotted but lying closer to the arc illumination curve.

[9] F. Sanders, Phys. Rev. **44**, 1020 (1933).

(2) *Variable intensity of illumination, constant value of pd and approximately uniform field.* The sparking potential for a 5-mm gap at atmospheric pressure is plotted as a function of intensity of illumination in Fig. 3. The maximum intensity is arbitrarily taken as unity, while the zero of intensity is sensibly that of the arc. The breakdown potential decreases with increasing illumination intensity. No significance should be attached to the shape of the curve near the zero of intensity because of the contraction of the scale there. Thus an intensity of 0.01 is still 10^4 times that of the arc.

The lowering of the sparking potential by illumination is due to the release of photoelectrons from the cathode, so that the spark mechanism is fundamentally affected. The normal spark breakdown is probably the result of space charge fields arising in the gap as a result of the large difference in the drift velocities of electrons and positive ions in the electric field.[10] Hence one may assume that the reduced potential breakdown is also a space charge phenomenon.

Now, whatever the detailed mechanism of the breakdown is, the space charge field will be approximately proportional to the amount of space charge present if its distribution is not changed appreciably. Then as a rough criterion for a spark in a given gap, one can set as the sparking condition that the number of positive ions be constant. Then if N_0 electrons leave the cathode in a time

[10] L. B. Loeb, J. Frank. Inst. **205**, 305 (1928); von Hippel and Franck, Zeits. f. Physik **57**, 696 (1929); Schumann, Zeits. f. tech. Physik **11**, 194 (1930).

small compared to the migration time of the positive ions, the number of positive ions produced by collision and giving rise to the space change will be

$$N = \int_0^{N_0} \exp\left(\int_0^d \alpha dx\right) dN_0,$$

where α = Townsend coefficient for ionization by collision for electrons, d = gap length. In this expression α is a function of the field and hence will vary as the field is modified by space charge.

Attempts have been made by von Hippel and Franck,[10] Schumann[10] and more recently by Sämmer[11] to calculate the field in a gap as modified by space charge. For simplicity one may assume as a first approximation that α is not modified by space charge formation and hence is independent of N_0. Further the value of α will be taken for the initial field across the gap. Then the integral $\int_0^d \alpha dx$ can be evaulated from the known field in the gap and Sanders' data.[9] The field is very nearly uniform so that one may place $\int_0^d \alpha dx = \alpha d$.

Applying the criterion for sparking mentioned above, we have

$$N = N_0 \exp \alpha d = \text{const.} = N_{00} \exp \alpha_0 d,$$

where N_0 and α are taken for any intensity, I, and N_{00} and α_0 are the corresponding values for the maximum intensity of illumination, I_0. Taking logarithms one has

$$\alpha - \alpha_0 = \frac{1}{d} \log \frac{N_{00}}{N_0} = \frac{1}{d} \log \frac{I_0}{I},$$

since the number of photoelectrons, N_0, is proportional to the intensity, I.

The ratio I_0/I can be calculated from the screen apertures, while α and α_0 are obtained by noting the breakdown potentials and referring to Sanders'[9] data. Thus $(\alpha - \alpha_0)$ plotted as a function of $\log I_0/I$ should give a straight line of slope $1/d$. Such a plot is shown in Fig. 4 for two values of gap length, d. The curves are quite accurately straight lines down to low values of intensity (large values of I_0/I), but their slopes are somewhat less than the corresponding values of $1/d$.

The agreement with the assumption of constant space charge is very good in the region of large intensities. The discrepancy in the slopes is to be expected as the integral $\int_0^d \alpha dx$ will not be

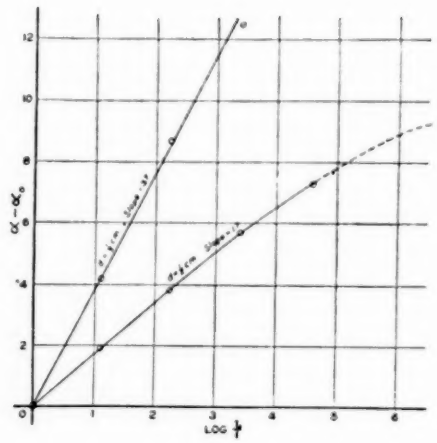

FIG. 4.

constant for all the photoelectrons, N_0, but will be modified by formation of space charge which will effectively shorten the gap and increase the field. The effect of field distortion on the integral $\int_0^d \alpha dx$ has been discussed by Rogowski.[12] He shows, for the region of field strengths involved here, that $\int_0^d \alpha dx$ is increased by field distortion. Hence this integral will increase progressively as the flow of photoelectrons continues, and the previously assumed constant α, taken for the initially uniform field, will be somewhat less than the true average value of α. Hence d will, in the curves, appear to be increased and the corresponding slope decreased.

For large values of I_0/I, i.e., small intensities, the value of $(\alpha - \alpha_0)$ falls below the linear relation of Fig. 4 and approaches a constant value for which α has the value corresponding to normal breakdown. This is in agreement with the fact that the sparking potential is not appreciably affected by illumination of small intensity. The significance of this may be seen by regarding it from another viewpoint suggested by Professor L. B. Loeb as follows. The number of positive ions or electrons produced by collision ionization is $N = N_0 e^{\alpha d}$. One may write $N_0 = e^{\gamma d}$, so that $N = e^{(\alpha+\gamma)d}$. Then for small illumination intensities N_0 will be small, and consequently γ will be negligible compared to α. However, for very intense illumination, N_0 will be large and γ will be comparable to α. Hence in the region of large intensities of illumination, increasing N_0 allows α

[11] J. Sämmer, Zeits. f. Physik **81**, 440 (1933).

[12] W. Rogowski, Archiv. f. Elektrotechnik **22**, 551 (1931).

to decrease correspondingly, but for small intensities $\gamma \ll \alpha$ and no such effect will be observed. The smaller intensities affect only the time lag of the spark. This has recently been discussed by Tillies.[4]

Only relative values of the intensity of illumination have been considered so far. The actual values of the intensity in terms of the number of photoelectrons released at the cathode is of interest. The charge reaching a collecting electrode placed 2 mm from the cathode was measured as a function of field and extrapolated to the fields existing at breakdown, the gas and pressure being the same as for sparking. That such extrapolation is legitimate has been shown by Bradbury.[13]

The charge released by one flash of the illuminating spark, using the full available intensity, was about 3×10^{8} electronic charges. The illumination probably lasts about 10^{-5} second, so that the average current is about 5×10^{-6} ampere. With the arc illumination the current was about 3×10^{-12} ampere. Hence about 10^{6} times as many electrons are released by the spark as by the arc in the same time. The spark falls on the cathode in such a way that only about 2 or 3 percent of the light is near the tip where the field is strongest. Thus only about 10^{7} electrons are effective in causing breakdown.

The total number of positive charges generated by these electrons is $N=N_0e^{\alpha d}$. For a 5 mm gap in air at atmospheric pressure the value of αd for normal breakdown is about 12. Hence

$$N=10^{7}e^{12}\cong10^{12}$$

and

$$q=Ne=10^{12}\times4.8\times10^{-10}\cong500 \text{ e.s.u.}$$

This charge, confined to the small region of space in which it is generated, would produce very large field strengths near it. Thus if it were confined to a sphere of radius 2 mm, the field at the surface of the sphere would be

$$E=q/r^{2}=500/(0.2)^{2}=12{,}500 \text{ e.s.u.}\cong 4\times10^{6} \text{ volts/cm.}[14]$$

Such a field appears unlikely and must mean that the charge produced does not exist in the gap at any one time as assumed. Thus in a qualitative way one sees that for large values of intensity of illumination, the value of α may be materially reduced and breakdown still occur. α is an exponential function of the field in the range of field strengths involved,[8] so that even if it decreases by a rather large amount, only a relatively small reduction in the breakdown potential will occur.

The law governing the reduction of the sparking potential, using the very short flash of illumination provided by a spark source, appears to be a very simple one. The assumption used in obtaining the equation of the curves of Fig. 4 was that the total charge generated by the photoelectrons is a constant. In view of the fact that the reduced sparking potentials closely satisfy Paschen's law, one can say that $N=$constant governs the breakdown in a uniform field under all conditions for this type of illumination.

This may be interpreted as meaning that static breakdown is a space charge phenomenon, and further that for the cases where the distribution of the space charge does not change appreciably, the amount of space charge generated at breakdown must be approximately constant.

I wish to express my appreciation to Professor L. B. Loeb for his assistance in interpreting the results of this paper and for many valuable discussions, and also to Dr. A. M. Cravath at whose suggestion the detailed measurements were made. My thanks are also due to Mr. R. R. Wilson who has helped in making the measurements and has drawn the figures.

[13] N. Bradbury, Phys. Rev. **40**, 980 (1932).

[14] Of course such a concentration of charge as this would mean an impossibly high potential. This calculation is illustrative only. The point is that very high fields would occur in the neighborhood of the charge in view of the exponential law of increase of both α and the charge. However, very large fields may actually occur and would give an easy way of explaining ionization of the gas by positive ions or of the liberation of electrons from the cathode by impact of the positive ions, as the ions would gain an energy of about 40 volts in a single free path in a field of the magnitude mentioned above. The existence of large fields becomes plausible in view of recent results of Posin in this laboratory which indicate strongly that Townsend's coefficient for ionization by positive ions, β, is dependent on pressure as well as x/p, which can only mean that β is space charge conditioned if present at all.

Yield of Alpha-Particles from Lithium Films Bombarded by Protons

R. G. Herb, D. B. Parkinson and D. W. Kerst, *University of Wisconsin, Madison, Wisconsin*

(Received April 24, 1935)

The absolute yield of alpha-particles from a thick target of lithium bombarded by protons has been determined using proton energies up to a maximum of 400 kv. The values obtained for the yield in alpha-particles per 10^9 protons, at several different voltages are 16.3 at 250 kv, 33.4 at 300 kv, 58.0 at 350 kv and 92.8 at 400 kv. The yields of several thin films have been studied in considerable detail. Results show that the thin film yield increases linearly with voltage from 180 kv up to 400 kv and at the upper voltage shows no tendency to approach a constant value. The thin film yield curves were smooth, giving no evidence for the existence of resonance levels.

Introduction

MUCH work has already been done on the disintegration of lithium by high energy protons showing conclusively that a Li^7 nucleus, when disintegrated, breaks up into two alpha-particles each with a range of 8.5 cm. The yield of alpha-particles has been studied as a function of the energy of the bombarding protons using both thick and thin targets of lithium. Cockcroft and Walton[1] studied the yield of 8.5 cm alpha-particles from a thick target of metallic lithium with various values of the proton energy from about 70 kv up to a maximum of 500 kv. Using a thick target of lithium fluoride Henderson[2] determined the yield of 8.5 cm alpha-particles at six different proton energies, ranging from about 430 kv up to 1200 kv. From an analysis of his thick target data Henderson concluded that the thin film yield should reach a constant value at 400 kv. Oliphant and Rutherford[3] bombarded a thin film of lithium oxide and studied the probability of disintegration using very intense proton streams but with a maximum energy of 200 kv. They found that the probability of disintegration is still increasing at their highest voltage but from the shape of the curve they concluded that the yield of alpha-particles should reach a constant value or even decrease as the energy of the protons increases above 200 kv.

In an attempt to remove the uncertainty which still exists as to the form of the yield curve we have studied several thin films using protons with accurately determined energies from about 100 kv up to 400 kv. We have also examined the yield over the whole range of voltage available at closely spaced voltages to determine whether or not resonance levels exist for penetration of protons into the Li^7 nucleus. Another object of this research was to determine the absolute yield of a thick target of lithium prepared by evaporation under good vacuum conditions and then bombarded without being exposed to air.

[1] J. D. Cockcroft and E. T. S. Walton, Proc. Roy. Soc. **A137**, 229 (1932).
[2] M. C. Henderson, Phys. Rev. **43**, 98 (1933).
[3] M. E. Oliphant and Lord Rutherford, Proc. Roy. Soc. **A141**, 259 (1933).

Apparatus and Method

A. Production and measurement of high potential

The source of high potential is a Van de Graaff generator operating in a steel tank under moderately high air pressure. Details of the construction and operation of this apparatus will be published in *The Review of Scientific Instruments*. The maximum steady voltage obtainable is at present limited to about 400 kv by breakdowns in the accelerating tube. During a run the voltage can generally be held constant to within about one percent. A generating voltmeter similar to the type developed by Kirkpatrick and Miyake[4] has been found very satisfactory for the measurement of the voltage. This instrument was calibrated at potentials up to 40 kv by means of a bank of carefully measured high resistances. A sphere gap which had been checked with the resistance measurements at low potentials was used to extend the calibration curve up to 100 kv. The scale was found to be accurately linear in this range. Assuming linearity over the entire range the calibration curve was extrapolated up to 400 kv. This assumption of linearity was then proved valid in the following way. The molecular ions (H_2^+) and atomic ions (H_1^+) were separated by a magnetic analyzer and were brought

[4] D. Kirkpatrick and J. Miyake, Rev. Sci. Inst. **3**, 1 (1932).

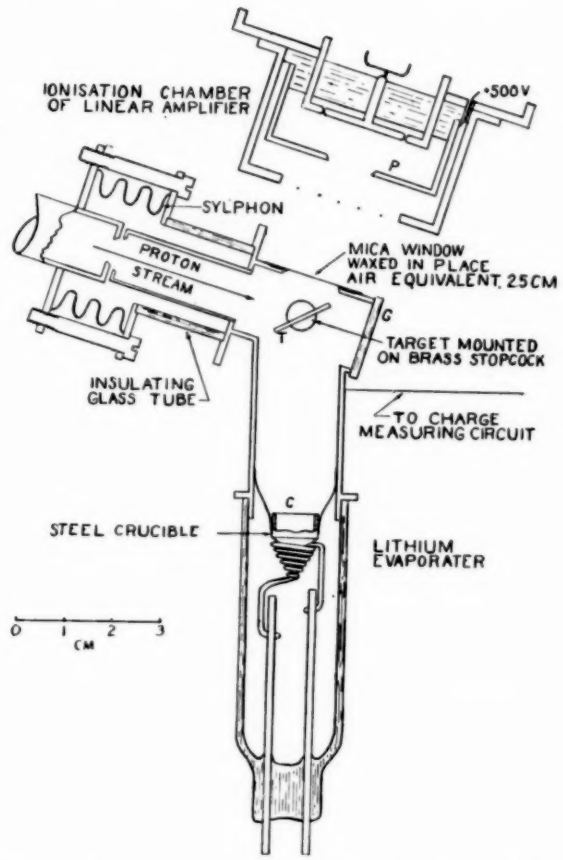

FIG. 1. Arrangement of target, counter and lithium evaporator.

alternately through a $\frac{1}{4}$-inch hole on to a glass plate G, Fig. 1, waxed to the target chamber, where they caused rather bright fluorescence. With the voltage at V_1 the molecular beam was brought to an accurately determined position M on the glass plate G. Leaving the magnetic field fixed the voltage was increased until the H_1^+ beam was at position M. If V_2 was this second voltage its value, providing the voltmeter is linear, should be given by $V_2=2V_1$. With several different voltages between 125 kv and 200 kv for V_1 the values determined for the ratio were $V_2/V_1=2\pm0.04$. A slight wavering of the fluorescent spot prevented more accurate determinations.

B. Target arrangement and counter

The target chamber with the apparatus for evaporation of lithium and for counting of alpha-particles is shown in Fig. 1. A heavy sheet of nickel T mounted on a ground brass stopcock can be turned from the outside to a horizontal position to receive a coat of lithium and then to the position shown in Fig. 1 for the bombardment with protons. Alpha-particles from the lithium pass through a mica window into the ionization chamber of a linear amplifier. The mica window was sufficiently large so that the effective solid angle was determined only by the opening in the plate P of the ionization chamber. This opening was covered by a copper screen for most of the experiments but an unscreened hole (diameter 0.953 cm) with beveled edges was used in determining the absolute yield. A large unscreened opening will cause a nonuniform field in the ionization chamber which might give an inaccurate count. To investigate this possibility a smaller opening was tried (diameter 0.418 cm). No difference in yield could be detected.

For the first part of the work on thick films a linear amplifier similar to that of Dunning[5] was used. It is equipped with a Cenco high impedance counter and a cathode-ray oscillograph. This arrangement was fairly satisfactory for counting-speeds up to 300 per minute. To permit faster counting a scale counter has been devised by one of us which counts every nth particle where n can be adjusted to any desired value. Generally n was set at about 12. Tests over a period of two months show that the scale remains sufficiently constant with time. Regularly spaced pulses generated by a thyratron circuit are accurately counted by this instrument at speeds of 120 per second. With alpha-particles it is satisfactory up to speeds of 2000 per minute. A circuit diagram and details of operation will be published in *The Review of Scientific Instruments*. As an additional check the regular "scale of one" counter was used occasionally when the absolute yield was of importance.

C. Measurement of proton current

Fig. 2 shows the general arrangement used to measure the number of protons incident on the target during a given time interval. G_1 is a Leeds and Northrup galvanometer, sensitivity 4.66 $\times10^{-10}$ amp. per millimeter. G_2 is a ballistic galvanometer, sensitivity 2.98×10^{-9} coulombs per millimeter. C_2 is a low leak condenser, capacitance 8 mfd. C_1 is a condenser with a

[5] J. R. Dunning, Rev. Sci. Inst. **5**, 137 (1934).

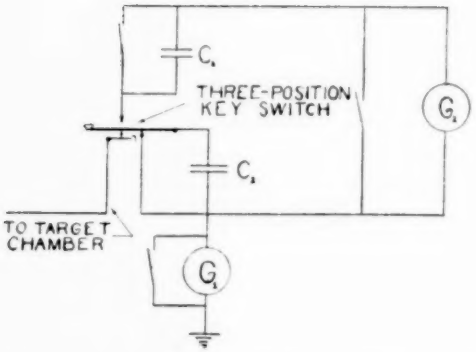

FIG. 2. Circuit for measuring the total number of protons incident on the target during a given time interval.

capacitance chosen to give suitable deflections of the ballistic galvanometer for the time interval and proton current desired. The charge and discharge key is a modification of the Kempe type.

In making a yield determination the arm of the key is depressed to its lowest position, shorting the condenser C_2 and grounding the target chamber through G_1, which now registers the proton current. At $t=0$ the first catch is released and the arm snaps up to the central position. The proton current now flows on to C_2 with G_1 still recording the magnitude of the current. At the end of the time interval the second catch is released. The arm snaps against its upper contact disconnecting the target chamber completely and discharging C_2 into C_1 through the ballistic galvanometer. If Q is the total charge originally on C_2, then the charge q sent through the ballistic galvanometer and measured is given by $q=QC_1/(C_1+C_2)$. Additional points on the key short the Cenco impulse counter except when the arm is at its central position. Thus the counter registers only those disintegrations caused by the charge accumulated on C_2. From the deflection of G_2 and the values of C_1 and C_2 the total charge is easily computed. This system is much more accurate and easier to use than a single current-reading galvanometer.

D. Evaporation of lithium

Considerable difficulty was experienced in obtaining good coats of evaporated lithium. For thick film work a piece of lithium of about $\frac{1}{4}$ cc was put in the crucible C, Fig. 1. The filament temperature was increased slowly for about two days to permit sufficient outgassing so that when evaporation started the pressure could be kept below 2×10^{-5} mm of Hg. With pressures below about 4×10^{-5} mm of Hg the lithium evaporated onto the plate T, Fig. 1 in a white matt surface. At higher pressures the film was dark and gave a lower yield when bombarded with protons. The rate of evaporation was difficult to control. Often after several hours of slow evaporation the rate suddenly rose by a large factor and the pressure became sufficiently high to give a dark colored film.

RESULTS

A. Thick films

Curve A, Fig. 3 shows the data for several runs on a thick target. The first run, shown by dots (increasing voltage) and circles (decreasing voltage) was taken a few hours after evaporation of a fresh lithium surface with good vacuum conditions. For most of these points about 10,000 alpha-particles were counted. Only two points have counts below 5000 and for many the count was above 12,000. The two sets of points check each other very well and fall on a smooth curve. Two days later another run was taken on the same surface using a proton beam with voltages from 340 kv down to 161 kv (shown by triangles). The yield was quite accurately the same as for the first run, showing that the target had not changed appreciably with time. For the lower part of the curve the molecular beam was used instead of the proton beam for the following reason. The accelerating tube depends on corona discharge for the proper potential distribution to give good focusing and does not work well below 150 kv. Since a 300-kv molecular ion consists of two protons, each with an energy of 150 kv the molecular beam can be used at high voltages to give low energy protons. The curve for the molecular ions joins onto the proton beam data satisfactorily.

At 251 kv the yield of alpha-particles per 10^9 protons for the three runs plotted is 17.0, 16.4 and 16.8. At 358 kv the two values are 62.2 and 63.0. A few days later the yield was lower and the data were inconsistent; a brown spot had developed on the target where the ion beam had hit. A fresh film was now evaporated under very good vacuum conditions. It gave a yield of 18.0

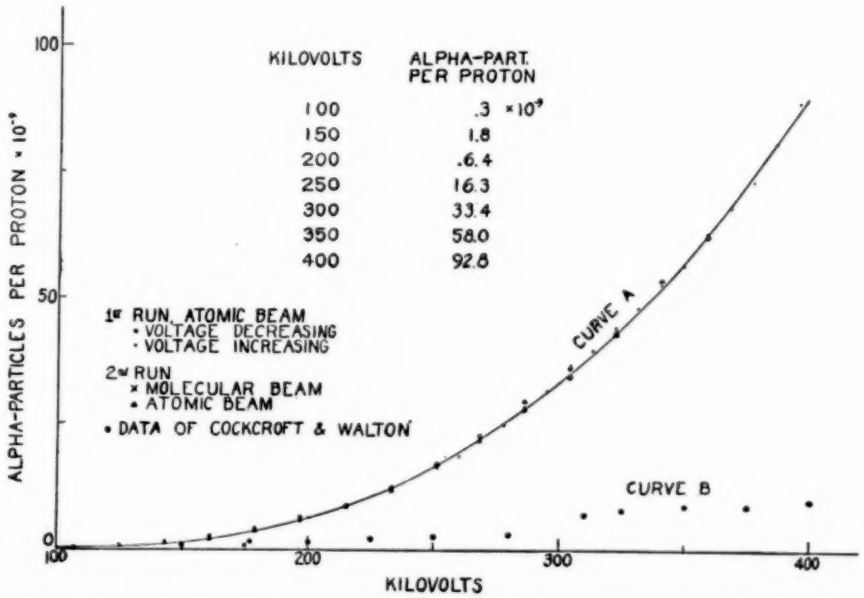

FIG. 3. Yield of alpha-particles from thick films of lithium bombarded by protons. Curve A is a plot of the data obtained at this laboratory. Curve B shows the data of Cockcroft and Walton.

at 251 kv and 62.5 at 358 kv. The increase in yield at the lower voltage may have been due to less surface contamination of the lithium target for the second film, since surface contamination is more important at low voltages. The true yield for a pure lithium film may therefore be somewhat higher at low voltages than the values indicated by the curve and table of Fig. 3. During the measurements the distance from the center of the target to the ionization chamber was 43 ± 0.7 mm. This uncertainty and the uncertain purity of the target are the most serious factors limiting the accuracy of the absolute yield determinations.

Curve B of Fig. 3 shows the yields obtained by Cockcroft and Walton with a target of lithium metal. Most of their values are smaller by a rather large factor than those obtained at this laboratory (curve A, Fig. 3). Henderson, using a target of lithium fluoride obtained values in good agreement with Cockcroft and Walton's data. This was unexpected but could be satisfactorily explained, as Henderson pointed out, by assuming that the lithium target used by Cockcroft and Walton was covered with a layer of lithium hydroxide. Lithium fluoride has 12 electrons per lithium nucleus, while pure lithium has only 3. Since fast protons lose their energy principally to the external electrons, a proton absorbed by lithium fluoride will on the average have had only $\frac{1}{4}$ as many close encounters with lithium nuclei as one absorbed in pure metal. Lithium hydroxide also has 12 external electrons per lithium nucleus and should therefore give the same yield as lithium fluoride, but $\frac{1}{4}$ the yield of pure lithium. Assuming that the target used by Cockcroft and Walton was effectively composed of lithium hydroxide, their yield values should be $\frac{1}{4}$ as large as the values obtained at this laboratory with pure lithium. A comparison of curves A and B of Fig. 3 shows this to be only approximately true.

B. Thin films

Several different geometrical arrangements were used for the thin film work. Five films were studied with the apparatus shown in Fig. 4. With this arrangement the effective solid angle subtended by the ionization chamber was sufficiently large to permit fast counting on a very thin film. A hole ($\frac{3}{8}$ in. diameter) in the end plate of the evacuated chamber is closed by a mica film waxed to the plate. The inner surface of the mica is coated with lithium by evaporation in a separate apparatus before being waxed into position. A mica film with an absorption of 2 or 3

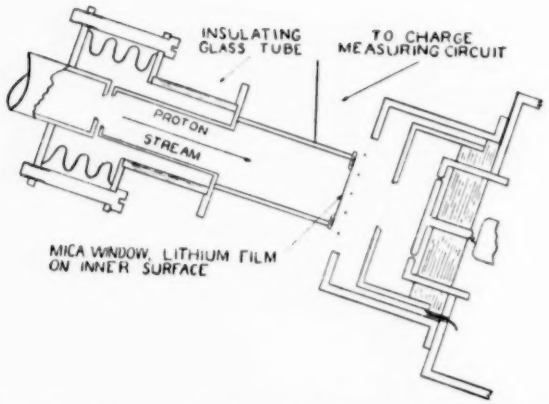

FIG. 4. Arrangement of target and counter for the study of thin films of lithium oxide on mica.

cm air equivalent is sufficiently strong to withstand the air pressure and of the right thickness to stop all protons but transmit the 8.5-cm alpha-particles. Of the five lithium films studied with this apparatus, I and II were prepared by evaporation of lithium on to bare mica. When exposed to the air the lithium quickly became oxidized and then probably changed over slowly into the hydroxide. Inconsistent yield curves from these nonconducting films and visible sparking along their surfaces indicated that charging up of the mica might have objectionable effects. To eliminate this possibility of inaccuracy films III, IV and V were first coated with a very thin semi-transparent layer of silver. For films III and IV the lithium was evaporated onto the silver surface. With film V the lithium and silver were on opposite surfaces. Both methods eliminated excessive surface charges and the yield curves obtained were similar.

The data obtained in a detailed study of film III (lithium hydroxide on silver) are shown in Fig. 5 by dots and crosses, where dots represent yields determined with H_1^+ ions incident on the target and crosses give yields obtained with H_2^+ ions. Two separate runs were taken for both the atomic and molecular ion data. In both cases the second run was taken at only a few voltages (those showing two dots or two crosses) as a check on the detailed data of the first runs. The excellent agreement between atomic and molecular ion data provides more evidence confirming the linearity of the voltmeter. All of the data from film III fall quite accurately onto the smooth curve which has been drawn in. Within the limits of experimental accuracy, the yield of alpha-particles is a linear function of the energy of the bombarding protons in the voltage range from 180 kv up to the maximum obtainable.

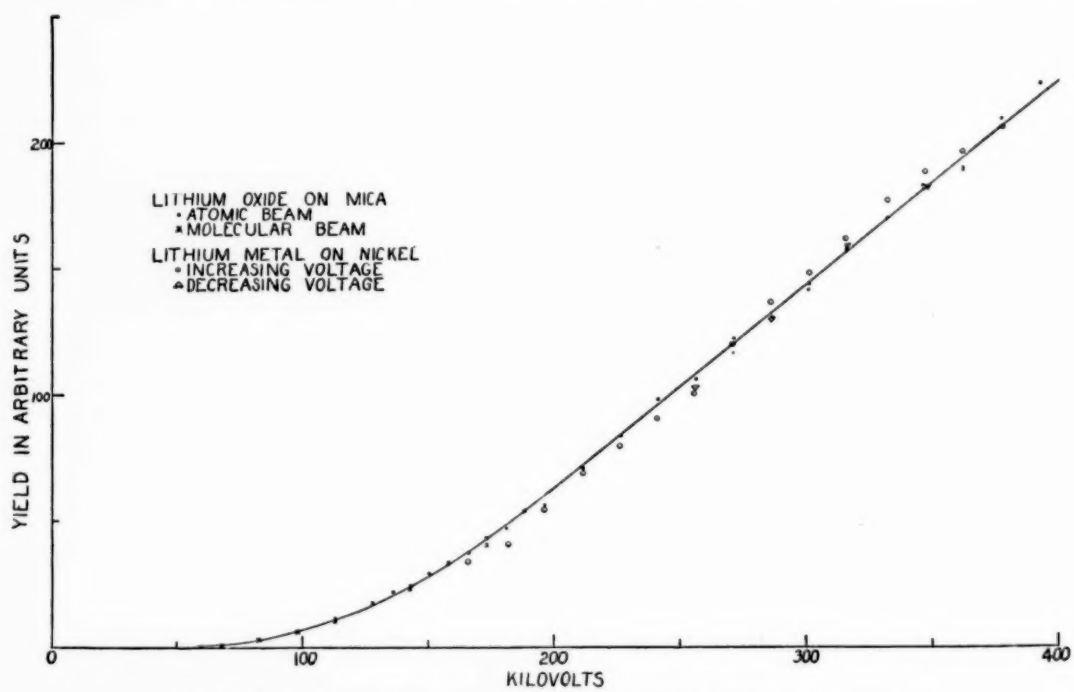

FIG. 5. Yield of alpha-particles from thin films of lithium bombarded by protons.

Above 180 kv the curve was drawn in with a straight edge. This linear increase of yield up to 400 kv indicates that the potential barrier of the lithium 7 nucleus for penetration of a proton is considerably higher than had been expected. The curve gives no evidence for the existence of resonance levels.

A study of the yield of a thin film of lithium should determine the probability of disintegration of lithium nuclei as a function of the energy of the protons causing disintegration. If the film being studied is sufficiently thick to decrease the energy of 300 kv protons to 250 kv, then protons in the entire range from 300 kv to 250 kv are causing disintegration and the yield obtained will determine only an average disintegration probability for proton energies in this range. For determining the true probability of disintegration as a function of the energy of the protons a film should be only infinitesimally thick. The yield which would be obtained from such a film will be called the true thin film yield. To find whether or not the lithium oxide film used gave accurate values for the true thin film yield, its stopping power for protons was determined in the following manner. At 256 kv this film gave an absolute yield of 0.35 (yields given in units of "alpha-particles per 10^9 protons"). The thick film yield at this voltage is 17.5 and the voltage giving a thick film yield of $17.5-0.35$ is 254.7 kv. Protons with an energy of 254.7 kv will penetrate a distance d into a thick target of lithium before being stopped and will give a yield of $17.5-0.35=17.15$. Protons with an energy of 256 kv will have their energy decreased to 254.7 kv in going through a film of thickness x and from there on will go the same distance d and give the same yield as the 254.7 kv protons. The increase in yield of 0.35 is therefore due to a film of thickness x sufficient to decrease the energy of 256 kv protons to 254.7 kv. A thin film of lithium giving a yield of 0.35 at 256 kv will therefore decrease the energy of 256 kv protons by 1.3 kv. Since for a given yield lithium hydroxide has four times the stopping power of pure lithium the film used for the data of Fig. 5 decreased the energy of 256 kv protons by 5.2 kv. This film was therefore sufficiently thin to give accurate values for the true thin film yield.

A thin film of lithium metal, coated by evaporation onto a nickel sheet, was studied with the apparatus shown in Fig. 1. Determinations of the absolute yield of this film showed that it was sufficiently thick to decrease the energy of 256 kv protons by 9 kv. The data obtained from two runs on this film are shown in Fig. 5 by circles and triangles. Further considerations such as those of the last paragraph show that two films may be sufficiently different in stopping power to give quite different absolute yields but nevertheless the curves showing yield as a function of voltage would be of practically the same form for both. Thus if the yields obtained from the lithium film on nickel are multiplied by a properly chosen constant factor the curve obtained for yield as a function of voltage should coincide with the curve determined by the lithium hydroxide film data. An inspection of Fig. 5 shows that within the limit of accuracy of the measurements the data from these two thin films give identical yield curves. Over the straight part of the yield curve (above 180 kv) the rate of increase of yield with voltage can be specified by the ratio $Y_{250}/Y_{200}=1.64$, where Y_{250} and Y_{200} are the yields at 250 kv and 200 kv respectively, determined from the curve of Fig. 5.

A thin film yield curve has been determined from the thick target data of curve A, Fig. 3 assuming the law $R=KV^{\frac{3}{2}}$ for the range of protons in lithium where R is the range and V the energy of the protons. Let Y_v be the thick film yield at voltage V determined from curve A, Fig. 3. The differences $Y_{130}-Y_{110}$, $Y_{150}-Y_{130}$, $\cdots Y_{410}-Y_{390}$ were determined from the curve. Each difference $Y_{v2}-Y_{v1}$ gives the yield of a lithium film of sufficient thickness T_{v2v1}, to decrease the energy of the protons by 20 kv. Using the law $R=KV^{\frac{3}{2}}$ this film thickness is given by $T_{v2v1}=K(V_2^{\frac{3}{2}}-V_1^{\frac{3}{2}})$. If each difference of yield $Y_{v2}-Y_{v1}$ is divided by a value T_{v2v1} proportional to the thickness of lithium effective, the thin film yields over the entire voltage range will be reduced to the yields which would be obtained from a film of constant thickness. The values $Y_{v2}-Y_{v1}/V_2^{\frac{3}{2}}-V_1^{\frac{3}{2}}$ are shown plotted in Fig. 6 (large dots) as the thin film yields for the voltages $(V_2+V_1)/2$. The continuous line drawn in is the experimentally determined thin film curve of Fig. 5 transferred to Fig. 6 for comparison. At 340 kv the derived yield value

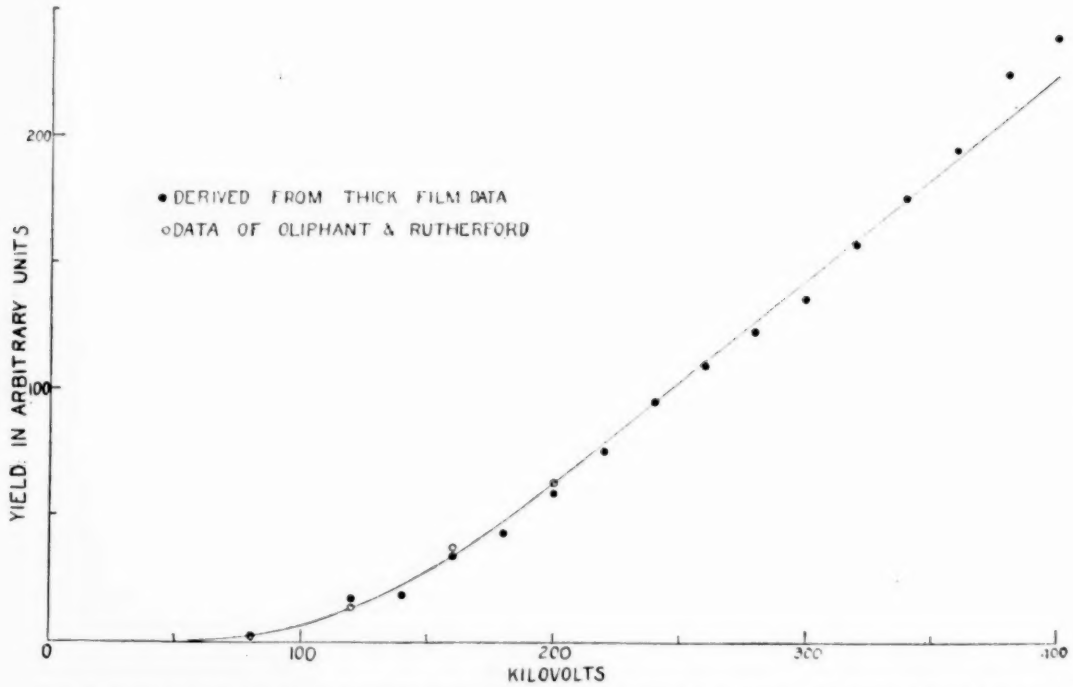

FIG. 6. Yield of alpha-particles from thin films of lithium. The large dots show data derived from the thick film yield curve of Fig. 3. The curve drawn in is the direct experimental curve of Fig. 5 transferred to this figure for comparison.

was made to fall on the experimental curve by multiplying all derived values by a suitable constant. In obtaining the yield values of Fig. 6 from the thick film curve of Fig. 3 slight inaccuracies in measuring the differences $Y_{v2} - Y_{v1}$ caused the rather large irregularities observed in the yield values given by large dots. If these irregularities are neglected the curve determined by the derived data falls quite accurately on the curve drawn in, which is the thin film curve determined by direct experiment. This excellent agreement of the data derived from a thick film curve with the experimentally determined thin film curve is a very satisfactory check on the accuracy of the yield measurements on both the thick and thin lithium films.

The circles of Fig. 6 show yield values determined from a curve obtained by Oliphant and Rutherford on a thin film of lithium oxide. If their curve is assumed to be a straight line at high voltages and is extrapolated up to 250 kv, the rate of increase of yield with voltage determined from their curve is given by $Y_{250}/Y_{200}=1.51$. The value obtained for this ratio from the curve of Fig. 5 and Fig. 6 is 1.64. Thus the thin film yields determined at this laboratory show a more rapid rise with voltage than the yields given by Oliphant and Rutherford.

CONCLUSION

Although our measurement of the absolute yield of alpha-particles from a thick target of lithium bombarded by protons seems fairly satisfactory we hope to check the results soon with a new target chamber and a different sample of lithium.

Our work on thin targets is quite conclusive in showing an increasing yield up to 400 kv. All of our data indicate that above 180 kv the yield is quite accurately a linear function of voltage with a rate of increase which can be specified by giving the yield ratio found, $Y_{250}/Y_{200}=1.64$. Within our limits of accuracy no resonance levels could be detected.

We wish to express our indebtedness to Professor C. E. Mendenhall who directed this research and to Professor G. Breit for much valuable advice. We also wish to thank Mr. E. J. Bernet for his work on the linear amplifier and Mr. G. R. Sears for advice and helpful discussions. One of us (R. G. H.) wishes to acknowledge the generous grant of a fellowship from the Wisconsin Alumni Research Foundation.

Cloud Chamber Studies of the Gamma-Radiation from Lithium Bombarded with Protons

H. R. CRANE, L. A. DELSASSO, W. A. FOWLER AND C. C. LAURITSEN, *Kellogg Radiation Laboratory, California Institute of Technology*

(Received April 30, 1935)

The gamma-radiation emitted when lithium is bombarded with protons has been studied by means of a cloud chamber operating in a magnetic field of 2000 gauss. The spectrum consists of at least eleven lines, the highest of which is 16 MEV. The voltage excitation curve for the gamma-radiation shows a maximum at 650 kv proton energy, and is very different from the excitation curve for the 8.4-cm alpha-particles emitted under the same conditions. An attempt is made to interpret these results. The experimental procedure and methods of measuring the cloud chamber tracks are also discussed.

INTRODUCTION

THE gamma-radiation emitted when lithium is bombarded with protons has been the subject of considerable discussion, mainly concerning its quantum energy, but in some instances concerning the existence of the radiation itself. The lack of agreement among experimenters working at various voltages as to the existence of the lithium radiation is, however, fully explained by the peculiar shape of the voltage excitation curve, which is not at all similar to the shape of the curve for the yield of long range alpha-particles produced under the same conditions of bombardment.[1]

Lauritsen and Crane[2] first measured the absorption coefficient of the radiation in lead and found it to be the same as that of gamma-radiation from radium, and hence supposed that its quantum energy was also the same, namely about 1.6 MEV. Later,[3] with the knowledge of the way in which the absorption coefficient for high energies is modified because of the creation of electron pairs, it was necessary to reinvestigate the absorption coefficient of the lithium radiation, with absorbers of at least two different atomic numbers. Lead and copper were used, and the combination of absorption coefficients found was such as to place them on the ascending branch of the curve at about 6.3 MEV, instead of on the descending branch at 1.6 MEV as previously supposed. At the same time Crane, Delsasso, Fowler and Lauritsen obtained Wilson cloud chamber photographs of the recoil electrons ejected from a thick lead plate by the radiation, and bent in a magnetic field. Their results indicated that the spectrum was complex, consisting of at least two lines, one at 4 and one at 12 to 13 MEV and this composite radiation was consistent with the observed value of the absorption coefficient which corresponded to 6.3 MEV.

It is mainly the results of a continuation of these cloud chamber studies which we propose to discuss in this paper.

APPARATUS

The vacuum tube used for accelerating the positive ions, the high voltage source and the ion source used in these experiments are essentially the same as described in a previous paper.[4] A horizontal Wilson cloud chamber 15 cm in diameter by 2 cm effective depth is operated at the center of a pair of Helmholtz coils capable of producing a magnetic field of 3000 gauss, constant to about 2 percent. In the present work fields up to 2000 gauss were used, requiring up to 180 amperes at 100 volts, hence to avoid excess heating the circuit is closed only for about 1 second, at the time of the expansion. By means of a system of solenoids and relays separated by long insulating strings the ion source is also operated in synchronism with the cloud chamber. All relays are actuated from a central contact drum, driven by a motor, and the sequence of events is as follows:

1st contact: Filament in ion source raised to emitting temperature; small amount of hydrogen (H^1 or H^2) admitted into ion source; magnetic field circuit closed.

[1] Henderson, Phys. Rev. **43**, 98 (1933).
[2] Lauritsen and Crane, Phys. Rev. **45**, 63 (1934).
[3] Crane, Delsasso, Fowler and Lauritsen, Phys. Rev. **46**, 531 (1934).
[4] Crane, Lauritsen and Soltan, Phys. Rev. **45**, 507 (1934).

2nd contact: Chamber expanded; anode circuit of ion source closed, producing ion current of 100 microamperes at target.
3rd contact: Arc light flashed; camera shutter opened.
4th contact: Everything off.

The chamber is allowed 15 seconds to reach equilibrium before the next expansion.

By operating the ion source intermittently, as described, it can be considerably overloaded during the short time it is actually used. Also the tube can be run at higher voltages (it will run steadily at 1000 kv with 100 microamperes intermittent ion current) because less gas is set free by ion bombardment of the inside of the tube and bombardment of the target. This has been found especially advantageous in using targets of chemical compounds which are decomposed into gases by the ion stream. When bombarding with deuterons a considerable saving of heavy hydrogen is effected, since the gas is allowed to flow into the ion source for only about one-fifteenth the total time of running.

Choice of Absorbing Material

In our first cloud chamber studies of the radiation from lithium a thick lead plate was used as the material on the inner wall of the chamber, from which the observed electrons were ejected. Because of the rapidly increasing probability of the creation of electron pairs with increasing quantum energy, quanta of high energy have a greater chance of ejecting electrons into the chamber from a lead absorber than quanta of low energy (all above 3 MEV). Therefore the high energy end of a gamma-ray spectrum will experience greater absorption, and hence be responsible for a greater number of electrons in the chamber than will the lower end of the spectrum. In addition, there is the possibility of measuring the combined energy of both members of many of the pairs, and this, plus 2 mc^2, should give directly the energy of the quantum which produced the pair. However, several effects attend the use of a heavy absorber which tend greatly to reduce the intensity of the upper end of the electron spectrum, and tend to destroy any line structure which may exist below the upper energy limit of the radiation. Some of these effects are listed below.

(1) The increased absorption for high energy quanta is due entirely to increased pair formation. Since the quantum energy (less 2 mc^2) is shared between the two members of each pair, with the greatest probability for equal division, the average energy of members of pairs is less than half the quantum energy, thus contributing little to the upper end of the electron energy spectrum, and, in addition, tending to mask any line structure within the spectrum.

(2) The probability of electrons suffering large radiative energy losses in passing through lead is much greater, per electron in the absorber, than it is in the case of lighter elements. Theory[5] gives the following energy loss per cm path for 5, 10 and 20 MEV electrons due to electron collisions and to radiative collisions with nuclei:

		5 MEV	10 MEV	20 MEV
H_2O	Radiation	0.07	0.16	0.36
	Collisions	1.98	2.15	2.32
Pb	Radiation	6.4	14.4	31.4
	Collisions	12.5	13.9	15.3

Because of this a large number of electrons originating below the surface in the lead absorber may lose a large and undetermined part of their energy, and their only effect is then to mask any line structure that may exist lower in the spectrum. Fortunately large radiative losses are usually accompanied by large angle deviations, and hence many of these electrons can be recognized and discarded in the measuring process.

(3) Pairs, of which both members are measurable likewise suffer radiative energy loss and scattering, so the total energy of the pair (plus 2 mc^2) is seldom equal to the full quantum energy. Nevertheless, this perhaps remains the best indicator of the quantum energy, where a lead absorber is used.

Hence in cases where good resolution is necessary to reveal the line structure of a spectrum, an absorber must be chosen which will produce, in the chamber, as large a ratio of Compton recoil electrons to pair electrons as possible, and also give rise to a minimum of radiative energy loss and large angle scattering.

We have plotted in Fig. 1, from theoretical data,[6] the energy spectra of negative electrons

[5] Bethe and Heitler, Proc. Roy. Soc. **A146**, 83 (1934).
[6] Data on pairs taken from Bethe and Heitler, reference 5.

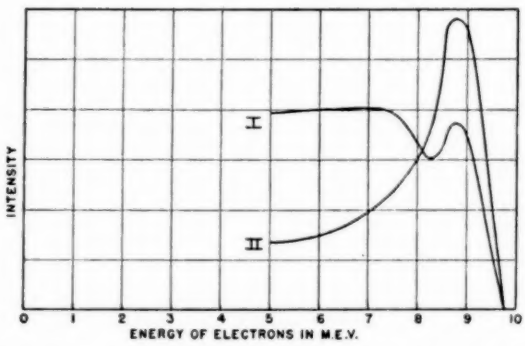

FIG. 1. Theoretical energy spectra of negative electrons which would be produced by a monochromatic gamma-ray of 10 MEV falling on a lead absorber (curve I), and on a glass absorber (curve II), each of thickness corresponding to 1 MEV stopping power for 10 MEV electrons, neglecting the effect of scattering.

which would be produced by a monochromatic gamma-ray of 10 MEV falling on a lead absorber and on a glass absorber, each of thickness corresponding to 1 MEV stopping power for 10 MEV electrons, neglecting scattering. The advantage of using an absorber of light material is evident from these two curves. For these reasons we have used the glass wall of the cloud chamber as the absorber in most of the work described in this paper.

SELECTION AND MEASUREMENT OF TRACKS

The general character of the electron spectrum and resolving power depend to a large extent upon the selection of the tracks which are to be measured and recorded. The more closely the counting is restricted to tracks in the forward direction, the sharper will be the maxima and minima in the electron spectrum, but also the smaller will be the number of tracks measured. Such a selection should not influence the final value of the gamma-ray energy obtained except as to accuracy. In our present apparatus the spread in angle in the vertical plane is limited by the depth of the visible part of the chamber. If a track is visible for a distance of 2/3 the diameter of the chamber, it necessarily makes an angle of less than 7.5 degrees with the direction of the radiation. Arbitrarily, we allow about the same spread in angle in the horizontal plane (plane of the chamber). This rule of selection permits the measurement of a reasonably large number of tracks, and at the same time eliminates the following kinds of electrons which are undesirable:

(a) Compton recoil electrons which come off at a large angle to the direction of the quantum.

(b) Electrons which have suffered a large radiative energy loss and accompanying large angle deviation.

(c) Those members of pairs which receive only a small share of the energy of the quantum.[7]

A rigorous elimination of the above kinds of electrons is of course not accomplished, but the effect of such a selection is very much in the direction of increasing the resolution in the resulting electron spectrum. We have demonstrated this experimentally by comparing spectra obtained from the same photographs, using several different rules of selection of the tracks. Each track is inspected carefully for scattering by the gas along its path and rejected if it is visibly deflected. About 1/5 to 1/3 of the total number of measurable tracks in the chamber satisfy the above requirements as to direction, etc., the fraction depending somewhat upon the hardness of the radiation. The calculated limits in energy of Compton electrons which fall within the cone of half-angle 7.5 degrees are given below:

Photon energy (MEV)	Compton electron energy (MEV)
5	4.75 to 4.40
10	9.75 to 8.05
15	14.75 to 11.30

Measurement of the tracks is accomplished by projecting the photograph of the chamber, full size, onto a card on which is drawn a series of circles varying in radius by 1/2 cm steps. The radius of the circle which most nearly fits the track is recorded.

STRUCTURE OF THE GAMMA-RAY SPECTRUM

In accordance with the methods outlined in the preceding paragraphs we have measured a total of 1576 negative electron tracks and 57 pairs resulting from the lithium radiation, using a magnetic field of 2000 gauss and using the 5 mm glass wall of the chamber as the absorbing material. This has, theoretically, a stopping power of about 2.5 MEV for 10 MEV electrons. In some cases a $\frac{1}{2}$-mm lead foil was fixed to the inner side of the glass wall, in order to obtain a greater number of pairs. The results obtained with only glass as the

[7] The average lateral component of energy of a member of a pair is mc^2, independent of the energy of the quantum.

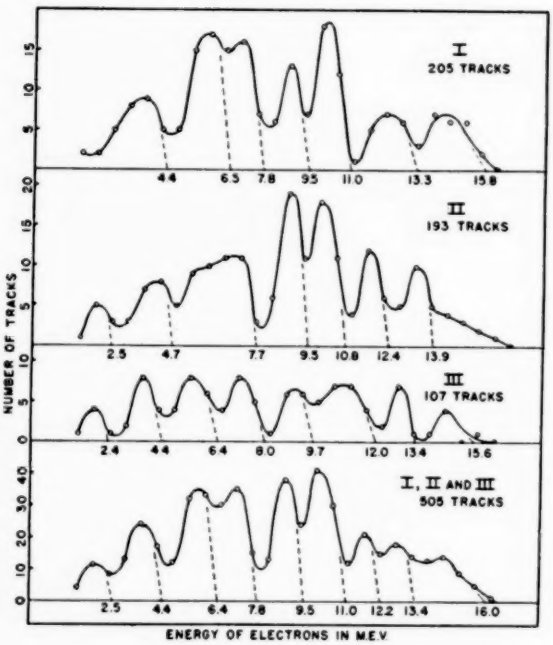

FIG. 2. Electron spectra resulting from three independent runs of 400 photographs each, plotted separately and added. The source of the electrons was the glass wall of the cloud chamber.

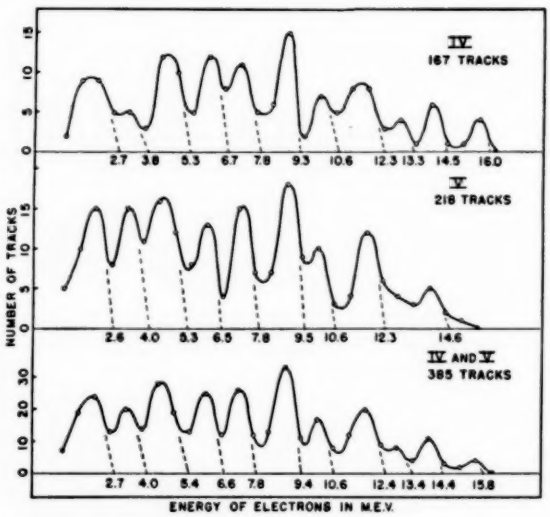

FIG. 3. Electron spectra resulting from two independent runs of 600 photographs each, plotted separately and added. The source of the electrons was the glass wall of the cloud chamber.

absorber are shown in Figs. 2 and 3. In Fig. 2 the results of three independent runs of 400 photographs each are plotted separately and then added together. In Fig. 3 two runs of 600 photographs each are plotted separately and added. It is seen that the principal features of the spectrum are the same in all the independent groups of data, and therefore are probably not due to statistical fluctuations. The fronts of the peaks are extended downward (dotted lines) and the energies corresponding to the intercepts noted on the diagram.[8]

The data obtained with the $\frac{1}{2}$-mm lead foil in the chamber were plotted in two groups, each consisting of the tracks from 800 photographs. The plots of these two groups, together with their sum, are reproduced in Fig. 4. In these measurements a $\frac{1}{2}$-cm radius of curvature (about 0.25 MEV energy) interval was used; hence the ordinates of the spectrum are only about half as high as those in the former set, where a 1-cm interval was used.

There are several possible ways in which the above data may be combined or averaged to give the probable values for the energies of the gamma-ray lines comprising the spectrum. The problem of extending the fronts of the peaks down to the axis is largely a matter of personal judgment, and subject to error, since the exact theoretical shape which the component peaks should have is not known. If all the data were plotted together as a single curve, the values which would be obtained for the energies of the gamma-ray lines would be dependent upon a single extrapolation. We have thought it more

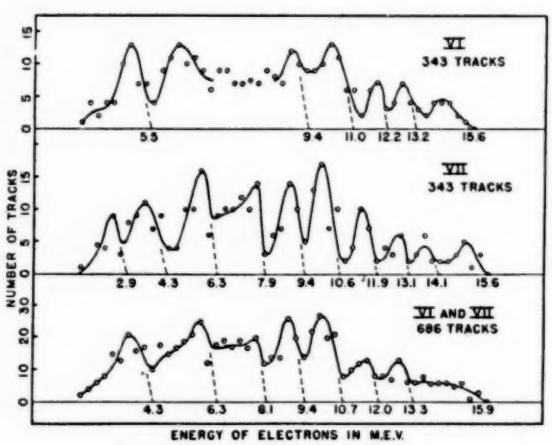

FIG. 4. Electron spectra resulting from two independent runs of 800 photographs each, plotted separately and added. The source of the electrons was the glass wall of the cloud chamber, plus a $\frac{1}{2}$-mm lead foil on the inner wall.

[8] It should be noted that the dotted lines should not necessarily be parallel, even for adjacent lines, unless the lines are of equal height and uniformly spaced.

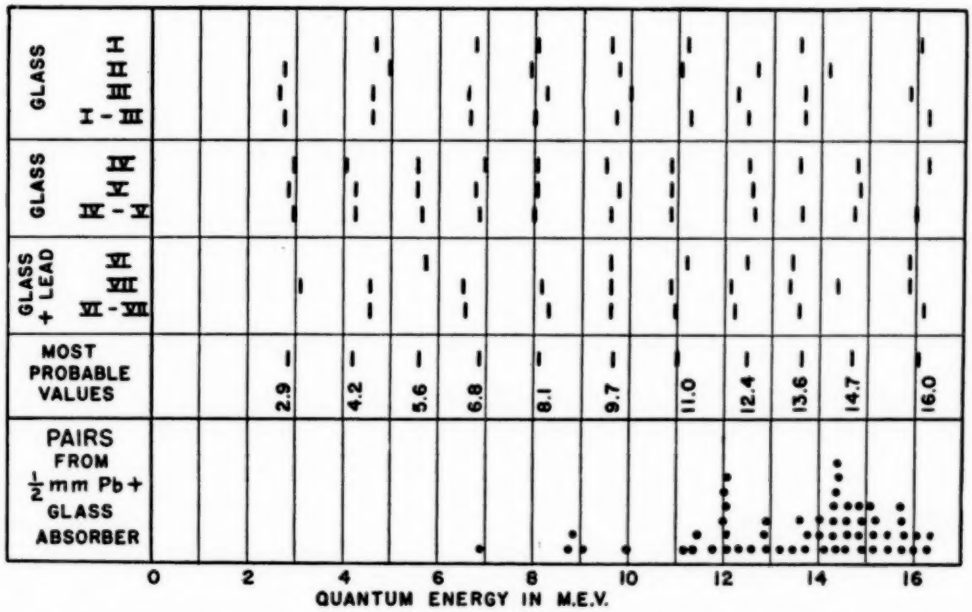

FIG. 5. Upper plot: Values of the gamma-ray energies, as indicated by each of the spectra in Figs. 2, 3 and 4. Lower plot: Total energies of pairs (2 mc^2 included), obtained when the ½-mm lead foil was placed in the chamber. Each dot represents a pair.

trustworthy, therefore, to draw the intercepts on each curve separately and average all the intercepts for a given line. In Fig. 5 are shown the values for the gamma-ray energies obtained from each spectrum, and also the average for each of the lines. All the values plotted in Fig. 5 are ½ mc^2 (0.25 MEV) higher than the corresponding intercepts in Figs. 2, 3 and 4, as required by the theory of Compton collisions.

An independent check, especially on the upper limit of the spectrum, can be obtained from the electron pairs. From the photographs in which the chamber was lined with ½-mm lead foil 57 pairs were found, both members of which could be measured with the required accuracy. The total energies of these pairs, with 2 mc^2 added in accordance with the theory of pair formation, are plotted in Fig. 5. Although the number of pairs is too small to give detailed structure within the spectrum, the upper limit is quite clearly indicated at 16 MEV, in agreement with the upper limit given by the plots of single electrons.

Division of Energy Between the Members of Pairs and the Ratio of Positive to Negative Electrons

We can obtain an interesting by-product of this work by plotting the pairs according to the fraction of the total energy carried away by one of the members, as shown in Fig. 6. This plot need not be restricted to the pairs from the lithium radiation, so we have included all the pairs we have accumulated from our measurements of various gamma-rays, and divided them into two groups according to total energy. A third curve is added to show the theoretical distribution for pairs produced by 10 MEV quanta, as given by Bethe and Heitler.[5] The shape of the curve is not sensitive to quantum energy in this region. It should be emphasized, however, that only the center portion of these plots can have any meaning, as far as checking the theory is concerned. Because of the experimental conditions, the chance of observing a pair in which one member has very low energy is small; therefore the ends of the experimental curve may be expected to drop off faster than those of the theoretical curve.

In order to obtain the ratio of the numbers of positive and negative electrons ejected from the glass absorber we took 400 photographs with a weak magnetic field (500 gauss), just sufficient to distinguish positives from negatives. In counting an arbitrary line was drawn across the projected image of the chamber perpendicular to the direc-

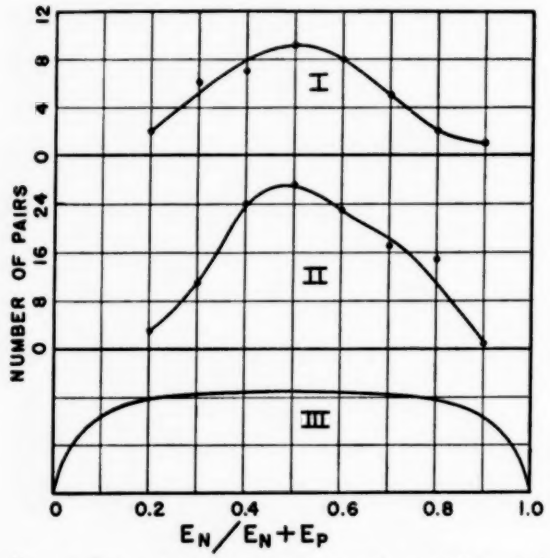

FIG. 6. Pairs, plotted according to the fraction of the total kinetic energy carried away by the negative number. Curve I: 42 pairs having total energy (2 mc^2 included) between 5 and 10 MEV. Curve II: 121 pairs having total energy between 10 and 16 MEV. Curve III: Theoretical distribution for 10-MEV pairs, according to Bethe and Heitler.

tion of the radiation. All tracks which intersected the line were recorded according to polarity, but regardless of their energy or the angle at which they crossed the line. The use of a very low field eliminates the ambiguity about the polarity of tracks of low energy, which, in a strong field, would appear as half circles beginning and ending on the same side of the chamber. The ratio of positives to negatives obtained is not entirely independent of the rules adopted for counting, because the angular distribution of members of pairs and of Compton electrons is not exactly the same, and at best a very limited solid angle can be made use of. The result of the count was 408 positives and 930 negatives. Only 60 positives had negatives visibly associated with them. Assuming, nevertheless, that each positive indicates the existence of a pair, the ratio of pairs to Compton electrons can be obtained simply. It is 0.78 pair per Compton electron. Calculating the ratio of pair absorption to Klein Nishina absorption for glass (taking 11 for the average atomic number) from Bethe and Heitler's theoretical curves, we find that the ratio 0.78 corresponds to 15 MEV radiation. Considering the actual spectrum of the lithium radiation, this value for the effective quantum energy seems rather high.

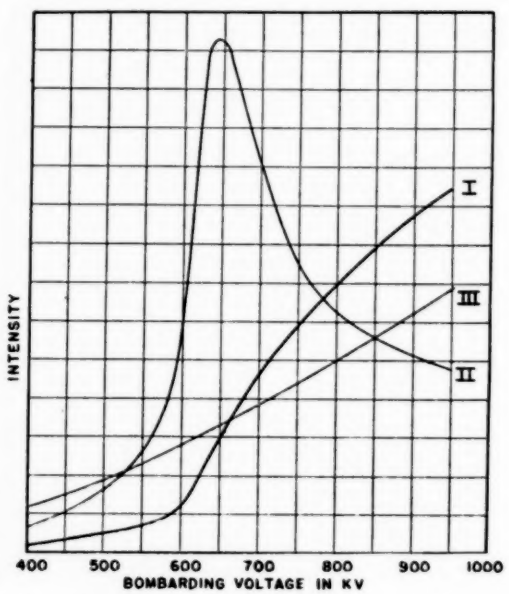

FIG. 7. Voltage excitation curves of the radiation from lithium bombarded with protons. Curve I: Experimentally observed intensity of gamma-radiation from a thick target. Curve II: curve I differentiated, to approximate a thin target. Curve III: Yield of 8.4-cm alpha-particles from a thick target, as obtained by Henderson.

VOLTAGE EXCITATION CURVE

The curve for the variation of intensity of the lithium radiation with the energy of the bombarding protons was found to have a rather striking character, as shown in Fig. 7. The intensity was measured with a lead-lined ionization chamber, shielded with enough lead to exclude stray radiation from the tube. A thick[9] target of LiCl was used, and a target of $CaCl_2$ was also bombarded as a check on the possibility of an effect from chlorine, and found to give negative results. The curve, as obtained under our experimental conditions, is necessarily an integral curve, since both a thick target and an ion beam of heterogeneous velocities were used. By differentiating this curve we may derive a curve which represents approximately the results which would have been obtained from a very thin target. Correction for the heterogeneity in velocity of the ion beam is more complicated and is not attempted here, for the reason that it would not modify the essen-

[9] The LiCl on the surface of the target is decomposed by the ion beam, so that after a short time the target actually consists of a thin Li metal film on a LiCl background. The excitation curve resulting from this should then be considered as due to a "partially thin" target.

tial character of the curve. Although the ion beam is not monochromatic, there is a preponderance of ions having velocity near the maximum, as has already been pointed out.[4] The differentiated curve shows clearly a sharp maximum in efficiency at 650 kv, and a decreasing efficiency above that voltage. The possible meaning of this will be discussed in the following section. Henderson's[1] curve for the yield of 8.4-cm alpha-particles from lithium bombarded with protons is drawn in for comparison, but without regard to relative intensity.

Discussion of Results

Although the values of the energies of the various lines in the gamma-ray spectrum are not known precisely enough to permit theories to be made about series relations, something pertinent may be said at least in regard to the upper limit of energy. There can be little doubt that the observed effect is due to the lithium isotope of mass 7. No reaction can be imagined involving Li^6 which can release sufficient energy to make possible the emission of a 16-MEV gamma-ray. The reaction which gives the required energy is

$$Li^7+H^1+E_H \rightarrow He^4+He^4+17.0\ \text{MEV}+E_H \quad (1)$$

where the 17.0 MEV is the energy available due to the difference in mass on the two sides of the equation, and E_H is the energy contributed by the bombarding proton, because of its kinetic energy.

Alpha-particles are the only products in reaction (1); therefore, if gamma-rays are emitted, it is reasonable to suppose that they come from an excited alpha-particle, and hence are characteristic of transitions between energy levels in the alpha-particle.[10] We shall therefore write the reaction with one of the alpha-particles excited to 16 MEV (indicated by a bar), and with the energy left over for kinetic energy indicated as before.

$$Li^7+H^1+E_H \rightarrow He^4+\overline{He^4}+1.0\ \text{MEV}+E_H. \quad (2)$$

The experimental excitation curves show that the reaction occurs with greatest probability when the proton bombarding energy is 650 kv. The maximum in the differentiated curve is quite sharp and has a half-breadth of about 100 kv, although part of this breadth is undoubtedly instrumental. Such a behavior is clear indication of resonance, or the existence of a virtual quasi stable level for the products of the reaction at the corresponding energy, which is equivalent to saying that the product particles separate through a resonance tunnel. Using the energy of the protons at the observed resonance peak, we find from reaction (2) that the position of the quasi stable level for the two alpha-particles is at 1.5 MEV.[11] This will be a level for the system consisting of one excited and one normal, or of two normal alpha-particles, according to whether the separation takes place before or after radiation. Such a level is possible only if the height of the potential barrier between the particles is considerably greater than 1.5 MEV. A half-breadth as small as 100 kv for the peak in the excitation curve would be understandable if the barrier height were about 2.5 MEV. For two normal alpha-particles the data on the anomalous scattering of alpha-particles in helium[12] and on the disintegration of boron by protons[13, 14] indicate a barrier height between 1.6 and 2 MEV. This value seems rather low to account for the observed sharpness of the resonance, but our data for the excitation energy of the alpha-particle are hardly of sufficient precision to settle this point.[15]

Recently Hafstad and Tuve[16] have obtained, independently, the excitation curve for this reaction over about the same range of voltage, using a monochromatic ion beam and a thin target. Their curve exhibits a sharp maximum at 450 kv and a

[10] Lauritsen and Crane, Phys. Rev. **46**, 537 (1934).

[11] Where the mutual energy of the two alpha-particles is considered, only 7/8 E_H is available, on account of the kinetic energy imparted to the system as a whole.

[12] Rutherford and Chadwick, Phil. Mag. **4**, 605 (1927).

[13] Lauritsen and Crane, Phys. Rev. **45**, 493 (1934).

[14] Cockcroft, Int. Conf. Phys. London, Oct. 1934.

[15] An analogous separation of the two products of disintegration through a resonance tunnel is clearly exemplified in the excitation curve of the gamma-rays from fluorine bombarded with protons, obtained by Hafstad and Tuve[16] which shows maxima at 350, 600 and 800 kv proton bombarding energy. The gamma-ray energy is 5.5 MEV, and the reaction is probably

$$F^{19}+H^1+E_H \rightarrow O^{16}+He^4+\gamma+2.6\ \text{MEV}+E_H.$$

The energy left over for kinetic energy is clearly not enough to make possible the escape of the alpha-particle over the O^{16} barrier, so it is reasonable that the three maxima correspond to resonance tunnels for the escaping alpha-particle.

[16] Hafstad and Tuve, Phys. Rev. **47**, 506 (1935).

steep rise beginning at about 800 kv and continuing to the end of their scale, which is 900 kv. Allowing for a possible difference in absolute voltage calibration between the two laboratories, the two sets of data are in good agreement. The second rise in Hafstad and Tuve's curve may indicate the process in which the two alpha-particles separate *over* their mutual barrier. However, it is not yet known whether this is a continued rise or another maximum like the first.

On the basis of theoretical estimates of the lifetime for radiation and for separation of the two alpha-particles, we must think of the radiation as being emitted predominantly after the excited alpha-particle has escaped from the field of the other alpha-particle. The gamma-rays are thus characteristic of a free alpha-particle, and only the probability of excitation will depend upon the mechanism by which the reaction occurs, and upon the temporary proximity of the two alpha-particles. For the time required for the separation of the two alpha-particles through the tunnel indicated by the above data we have to expect

$$T \sim \hbar/10^{-7} \sim 10^{-20} \text{ sec.}$$

On the other hand, the time required for the emission of a 16-MEV gamma-ray is

$$\tau = (\hbar/10^{-7}) \cdot (100) \sim 10^{-18} \text{ sec.},$$

assuming dipole radiation, which gives the shortest time. Thus if these estimates are to be believed, the time which the two particles remain together is very short compared to the lifetime for radiation. The gamma-rays thus come from an essentially unperturbed alpha-particle, and the peak in the excitation is to be attributed to resonance between the excited and the normal alpha-particle.

However, since this inference rests upon no very certain foundation, it is worth while considering an alternative limiting hypothesis: namely, that the radiation is characteristic of the composite unstable Be^8 nucleus, and that this nucleus has a lifetime long compared to the radiation time τ. This would make the process analogous to the capture of a proton on a quantized level by Be^9 or B^{11} and the subsequent emission of gamma-radiation (discussed in a succeeding paragraph), with the one important difference that the unstable Be^8 nucleus after radiation disintegrates into two alpha-particles. On this view it would be equally possible to attribute the resonance to the two normal alpha-particles which are left after radiation. In this case the theoretical estimates of both T and τ would be smaller by a factor of about 100. On this view it would be hard, however, to account for the complex character of the gamma-ray spectrum. If the ground level to which the system radiated were a quasi stable combination composed of two normal alpha-particles, the radiative transition down to this level would be about 100 times as probable as a transition to an intermediate level (which would presumably not be quasi stable for the two particles), and we should therefore expect only the 16-MEV line to appear with appreciable intensity. The situation is not helped by supposing the resonance to occur for the two particles before radiation, since if this were so we should expect the Be^8 to disintegrate readily after a part of its energy, corresponding to a transition to one of the intermediate levels, had been radiated. Both these mechanisms should give rise to a number of homogeneous groups of alpha-particles, related to the intermediate levels in the alpha-particle or in Be^8. No such groups have been found, and their absence must mean that the transfer of energy between the "inner" degrees of freedom of the alpha-particle and the inter alpha-particle kinetic energy must be slow compared to the rate of radiation. This again is theoretically very hard to accept, and furnishes a further argument against Be^8 as the origin of the gamma-rays.

Returning to the hypothesis that the gamma-rays come from the excited alpha-particle after disintegration, it is clear that their structure must be related to the energy levels of the free-alpha-particle. We must assume that the alpha-particle is nearly always excited initially to the full 16 MEV, and that it falls, usually by more than one step, to the ground state, thus giving rise to the observed softer lines. In order to account for the eleven observed lines it is necessary to assume that the alpha-particle has a series of at least seven levels between 0 and 16 MEV. It is not possible, however, to construct a unique level scheme on the basis of the present data.

If any level lower than the 16-MEV level could be excited, enough kinetic energy would remain

for the two alpha-particles to clear any reasonable potential barrier, even for quite low proton bombarding voltages. The absence, experimentally, of any appreciable radiation at low voltages indicates that the excitation of the 16-MEV level is far more likely than that of any other. In part this can be accounted for by the effect of resonance between the two alpha-particles when this level is excited, but the relative probability of exciting this level seems rather large to be accounted for on the basis of the resonance alone. It might suggest that the 16-MEV level corresponds to an internal structure which is not radically different from that of Li^7 plus the bombarding proton. From the excitation curve, and from experiments made by Oliphant, we can be sure that lower levels are not excited with an efficiency greater than about 5 percent of that of the 16-MEV level at full resonance.

We have observed several instances in which a proton seems to be captured by a nucleus, forming a new nucleus in a quantized state, with subsequent emission of gamma-radiation only. In two of these, beryllium and boron, the upper limits of energy of the gamma-ray spectra are so high that they can be accounted for only by the processes $Be^9+H^1\rightarrow B^{10}$ and $B^{11}+H^1\rightarrow C^{12}$, respectively. The formation of N^{13} when carbon is bombarded by protons exhibits the characteristics of a capture process: Hafstad and Tuve[16] have found that the voltage excitation curve has one, and possibly two, maxima between 400 and 500 kv, and we have found indications of a weak gamma-radiation of quantum energy as high as 6 MEV, although very few tracks were obtained. The formation of C^{11} when boron is bombarded with protons is probably another capture process:

$$B^{10}+H^1\rightarrow C^{11}$$

and doubtless has a sharp maximum in the excitation curve, accounting at least in part for the lack of agreement as to the ratio of the proton and deuteron effects.

Assuming, as is indicated by the results presented in this paper, that even the lightest nuclei possess a large number of quantized energy levels spaced at rather small intervals, we should expect that in general within the available range of a half million volts in the bombarding energy we should find some particular energy at which the proton is captured by the bombarded nucleus with the emission of gamma-radiation.

The yields found for such processes indicate that the levels on which the protons can be captured are at least of the order of 10,000 volts wide. This is in rough agreement with the calculations of Breit and Yost.[17]

We wish to thank Professor J. R. Oppenheimer for many helpful discussions during the preparation of this paper. We are grateful to the Seeley W. Mudd Fund for the financial support of this work.

[17] Breit and Yost, Phys. Rev. **46**, 1110 (1934); **47**, 508 (1935).

JULY 15, 1935 PHYSICAL REVIEW VOLUME 48

Intensities of Satellites of $K\alpha$

ANNA W. PEARSALL, *Cornell University*

(Received May 23, 1935)

By use of a Siegbahn vacuum spectrograph, the intensities relative to that of the parent line, were measured for the satellites of the $K\alpha_1$ line for elements in the atomic number range 16–29; but these intensities are in general much lower than those reported for the satellites of the line $L\beta_2$. The variation in this range is from approximately 0.7 percent to about 5 percent while the maximum found for the satellites of $L\beta_2$ was 52 percent. These results are in agreement with the prediction of Coster and Kronig as to low intensities for $K\alpha$ satellites; but, contrary to the Coster-Kronig theory, we find a possibility of a maximum of intensity which could not be explained on their assumption that the satellites originate in an Auger effect.

ALTHOUGH the existence of x-ray satellites has been known since 1916 and their wavelengths have been a source of study since that time, very little attention has been paid to their intensities. In 1931, R. D. Richtmyer[1] noted qualitatively a variation in the intensities of the satellites of $L\beta_2$ in the atomic number range 40–70. Richtmyer and Taylor[2] used an ionization chamber to study the Cu $K\alpha$ doublet and estimated the intensity of accompanying satellites relative to that of the parent to be of the order of a half of one percent; and DuMond and Hoyt[3] made a similar study and confirmed these results. In 1934 the present author reported an investigation of intensities of the $L\beta_2$ satellites by the photographic method for elements from Zr(40) to I(53) inclusive. This report[4] showed a definite variation in the intensities of satellites with atomic number, a maximum of intensity occurring at Ag(47). The variation was from four percent for Zr(40) to 52 percent for Ag(47), dropping suddenly to nearly zero for I(53). Existing theories of satellite origin could not account for the great intensities observed and particularly for the variation with atomic number.

Following the publication of the $L\beta_2$ results, Coster and Kronig[5] suggested that satellites may be due, in part, to Auger effects. On this basis they account qualitatively for the shape of the curve showing the intensities of the satellites of $L\beta_2$ as a function of atomic number, as well as for the large intensities observed. They also predict that there should not be high intensities, and no such variation of intensities, for the satellites of the K lines since there can be no Auger effect there. The present paper is a report of an experimental investigation of intensities of the satellites $K\alpha_{3,4}$ relative to $K\alpha_1$ for elements in the atomic number range 16–29. The results agree with the prediction of low intensity for the satellites of the K lines but, contrary to the Coster-Kronig theory, it appears that there may be a maximum of intensity for K satellites also.

The method employed is the same as that described in the report[4] on the $L\beta_2$ lines. The element to be studied was used on the anticathode of the x-ray tube, either as a wedge of the pure element or as a powdered compound pounded into a roughened wedge blank of copper or aluminum. Table II, column 2 shows the form in which the element was used. Tube voltage was from three to five times that needed for the excitation of the parent line and is shown in Table II, column 3. Tube current and time of exposure were varied so as to produce a plate of such density that intensity was proportional to photographic density. Microphotometer records were made from each suitable plate and these records changed to intensity plots in the usual manner. Fig. 1 shows a microphotometer record for the doublet $K\alpha_{1,2}$ of Fe(26) with accompanying satellites $K\alpha_{3,4}$, and Fig. 2 shows the corresponding density plot. The ratio of areas under the satellite curve and parent line, respectively, was taken as the relative intensity. There are some inaccuracies in the method employed and these results must be considered as exploratory rather than accurately quantitative. More precise results, now being obtained in the Cornell laboratory by Dr. Parratt and Dr. Kaufman by the ionization chamber method, agree well in most cases with those herein given. In our method, a number of plates was made for each element and the average of all values of relative intensity for any element taken as better than a single value. Table I shows the results obtained from eight exposures for Fe(26).

Relative intensities are given in Table II for the elements studied. The ratio given is that of

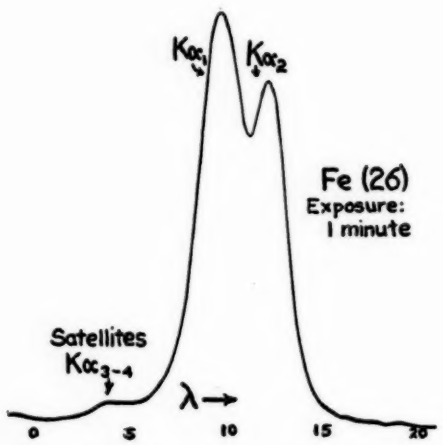

FIG. 1. Microphotometer record of $K\alpha$ lines for Fe(26).

[1] R. D. Richtmyer, Phys. Rev. **38**, 1802 (1931).
[2] Richtmyer and Taylor, Phys. Rev. **36**, 1044 (1930).
[3] DuMond and Hoyt, Phys. Rev. **36**, 1702 (1930).
[4] Anna W. Pearsall, Phys. Rev. **46**, 694 (1934).
[5] Coster and Kronig, Physica **2**, 13 (1935).

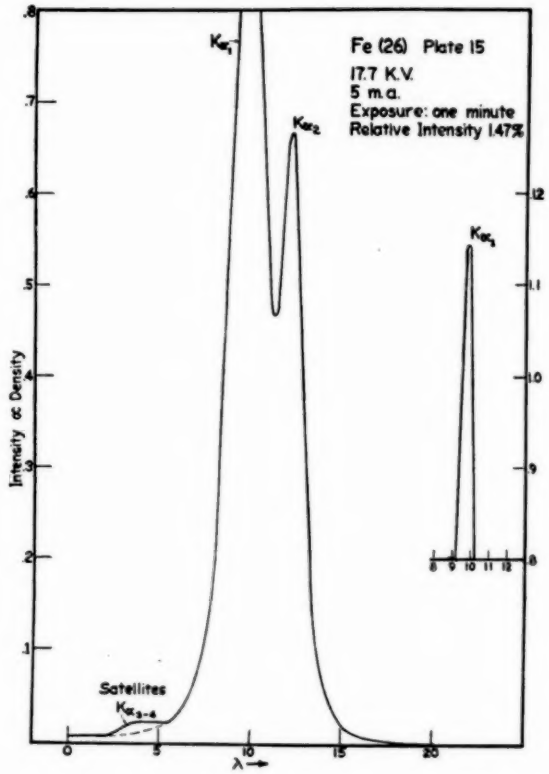

FIG. 2. Satellite intensity for $K\alpha$ lines for Fe(16); intensity curve plotted from record shown in Fig. 1.

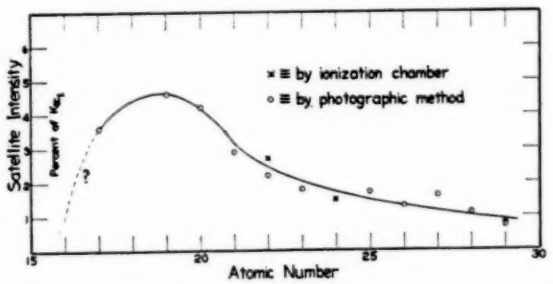

FIG. 3. Variation in intensities of satellites of $K\alpha$ lines with atomic number.

the intensities of $K\alpha_{3,4}$ to that of $K\alpha_1$. The satellites of S(16) were not strong enough to be measured by this method although several plates were taken for this element. The results are shown graphically in Fig. 3.

The $K\alpha$ satellites are relatively weak. Even on much over-exposed plates, they are not as prominent as in the case of the L series. There is a variation with atomic number of intensities relative to that of the parent line, a possible maximum* appearing between Cl(17) and Ca(20) with a gradual decrease toward higher atomic numbers. There is good agreement for Cu(29) with the earlier (1931) work of Richtmyer and Taylor and with recent unpublished data of Dr. Kaufman.

Appreciation is expressed to Dr. F. K. Richtmyer for his valuable advice and continued interest throughout the progress of the work.

TABLE I. *Plate data for Fe(26). Tube voltage, 17.7 kv.*

EXPOSURE NO.	EXPOSURE TIME	TUBE CURRENT	MAXIMUM DENSITY OF $K\alpha_1$	RELATIVE INTENSITY $K\alpha_{3,4} : K\alpha_1$
3a	2 min.	12 m.a.	1.01	1.05%
3b	8	12	1.63	0.80
5a	5	5	1.31	1.40
5b	12	5	1.46	1.30
5c	20	5	2.32	1.10
15a	1	5	1.36	1.45
15b	5	5	2.30	1.20
15c	10	5	1.73	2.20

TABLE II. *Intensity of satellites $K\alpha_{3,4}$*

ELEMENT	FORM USED	TUBE POTENTIAL	RELATIVE INTENSITY $K\alpha_{3,4} : K\alpha_1$
S(16)	Powdered S[1] and Al_2S_3[1]	12.3 kv	see text
Cl(17)	NaCl[2]	14.1	3.60%
K(19)	K_2SO_4[2]	14.4	4.65
Ca(20)	CaO[2]	16.1	4.22
Sc(21)	Sc_2O_3[2]	17.9	2.35
Ti(22)	TiO[2]	19.8	2.23
V(23)	$H_4V_2O_7$[2]	21.8	1.86
Cr(24)	Cr metal	24.0	1.49
Mn(25)	Powdered Mn[2]	16.4	1.73
Fe(26)	Fe wedge	17.7	1.25
Co(27)	Co wedge	19.3	1.65
Ni(28)	Ni strip on Cu	21.7	1.10
Cu(29)	Cu wedge	22.1	0.71

[1] On aluminum wedge.
[2] On copper wedge.

* Subsequent measurements by the ionization chamber method by Dr. L. G. Parratt give a relative intensity of eight percent for S(16). This result, if confirmed, removes the suggested maximum of intensity in the neighborhood of Ca(20).

Spectrum of Aluminum Vapor Distilled by a Tungsten Coil in Vacuum

E. GAVIOLA[1] AND JOHN STRONG, *California Institute of Technology*

(Received May 6, 1935)

If a tungsten coil, charged with aluminum, is brought to incandescence in a vacuum of the order of 10^{-5} mm Hg, it evaporates a cloud of metal, which has been observed to emit a violet-blue light. The luminosity has been analyzed and found to be mainly a line spectrum containing Al I, Al II, W and impurity lines. The excitation is produced by collisions with the electrons emitted by the incandescent filament and accelerated by the potential drop across it. λ3443.6 behaves as an Al arc and not as an Al II line, as commonly listed.

ONE of the authors,[2] during his work on the deposition of aluminum films on the surfaces of astronomical mirrors, or of diffraction gratings, by evaporating the aluminum from electrically heated tungsten coils, observed that while the metal remained in the gas phase (a time of 10^{-4} to 10^{-3} sec. for each atom), it emitted a violet-blue luminescence, that can be seen with the naked eye. This work had as its purpose to study this luminescence.

Apparatus and Results

The experimental arrangement consists of a tungsten coil, made of wire of 0.030 inch in diameter, containing about 10 full turns of 1/4-inch diameter, loaded with small aluminum *U*'s, one in each turn, of 1 mm wire of 99.9 percent purity. The length of wire in each *U* is 10 to 12 mm. The coil is placed in a glass or metal bell jar, its ends being connected with terminals of a transformer, from which any alternating potential in steps of 1 volt can be drawn, up to 110 volts. The bell jar is in communication with a two-stage oil diffusion pump by means of a tube 12 cm in diameter. An intermediary liquid air trap was generally used.

The luminescence is observed through a glass or quartz window, protected from the distilling aluminum by a screen. (Otherwise it would become opaque in a few seconds.)

When the vacuum is of the order of 10^{-5} mm or better, the tungsten coil is heated to a moderate temperature, in order to allow the Al *U*'s to melt and distribute along its surface. At the same time, the aluminum is partially outgassed and cleaned of its oxide surface. Then, a potential difference of from 10 to 40 volts is applied across the coil and the luminescence observed or photographed through the window. The whole process of evaporation lasts from 10 to perhaps 50 sec., depending on the voltage applied.

The first visual observations, with a hand spectroscope, indicated that the luminescence consists of a line spectrum, containing many lines in the visible, among which the violet doublet 3961.5 – 3944.0 of Al is conspicuous. The spectrum was then photographed through a fast glass spectrograph and with the small Hilger quartz instrument, varying the potential difference applied across the coil. The plates show mainly lines of Al I, Al II and W. The aluminum oxide bands in the green, conspicuous in the air arc, are totally absent. The hydride bands, on the other hand, appear with great intensity. The following heads have been identified: 4405, 4368, 4354, 4345, 4259, 4241, 4067.

The measurement of the plates indicates the presence of the lines listed in Table I. As im-

TABLE I. *Wavelengths of lines observed in Al vapor from W coil.*

Al I	Al II	W	Al I	Al II	W
3961.5	4663.1	5071.7	2372.1	3586.5	4551.8
3944.0	4585.8	5069.2	2367.1	3458.2	4546.5
3480.5	4485.8	5054.6	2321.6	3057.2	4294.6
3443.6	4447.8	5053.3	2317.5	3050.1	4215.4
3092.8	4227.5	5015.3	2313.5	2816.2	4137.5
3082.2	4226.8	5006.2	2312.4	2669.2	4102.7
2660.4	3900.7	4982.6	2269.1	2631.7	4089.0
2652.5	3859.3	4886.9	2263.5	2475.3	4074.4
2638.2	3842	4843.0	2258.0	2369.3(?)	4008.8
2575.1	3703.2	4693.7(?)	2210.1		3881.4
2568.0	3655.0	4680.5	2204.6		3868.0
2378.4	3651.1	4659.9(?)	2174.0		2944.4
2373.1	3587.1	4613.3	2168.8		

[1] Fellow of the John Simon Guggenheim Memorial Foundation.

[2] John Strong, Publ. A. S. P. **46**, 18 (1934).

purities, appear the strongest lines of the Fe spectrum; 4924.0 of Zn II; 4810.5, 4722.2, 4680.1 and 3075.9 of Zn I; 4172.0, 4033.0, 2943.7 and 2874.2 of Ga; 3493.0 of Ni; 3274.0 and 3247.5 of Cu; 2881.6, 2516.1 and 2506.9 of Si; 2852.1 of Mg I; 2802.7 and 2795.5 of Mg II; 4046.6 of Hg; 2840.0(?) of Sn; 4861.3 of H; 3280.7 of Ag and 3261.0 of Cd. The last two were not in all the plates.

Discussion of Results

The presence of many lines of W is due to the fact that this metal dissolves partially in the molten Al coat of the filament and is carried away by the rapid evaporation of it. A quantitative determination of the concentration of W in the deposited Al films indicates the value. The other metals appearing as impurities are probably contained in the commercial Al wire used for the *U*'s, with the exception of Ag and Cd which are contaminations of the bell jar and Hg, which comes from the McLeod gauge. The presence of the AlH bands and of Hβ indicate that the initial melting of the aluminum on the filaments leaves still a large amount of hydrogen occluded in it. This hydrogen then evaporates with the metal.

The intensity relation of the Al II to the Al I spectrum varies with the potential applied across the coil. With 10 volts, practically only the arc lines are present, with 40 volts the spark lines are nearly as strong as the former. It varies also with the distance from the coil: A photograph taken using a 40-inch bell jar, for which the spectrograph was focused to a region about 30 cm away from the coils, does not show the otherwise strongest Al II lines 2816.2 and 2669.2, although 20 volts were applied across the filament. The Al I spectrum appears as usual. This would indicate that recombination of the ions takes place rapidly, demanding the existence of a great number of free electrons. It is remarkable that in this case the line 3443.6, which is listed in Kayser among the Al II lines, but not classified, is present, in the absence of 2816.2 and 2669.2, as mentioned. This shows that 3443.6 does not belong to the Al II spectrum.

The doublets of the diffuse series of the Al arc are notably sharp and perhaps displaced in our case. This is in agreement with observations of other authors in low pressure or vacuum sources of Al light.[3]

The main question to be answered is how the spectra are excited. The foregoing observations pointed clearly to electronic collisions. The electrons are emitted by the hot filament and accelerated by the potential gradient along it. To test this assumption, we constructed an equipotential source of thermoelectrons, by coating a tantalum capsule with CaO, BaO and SrO and heating it internally, and an analogous equipotential source of Cd vapor. A suitable constant potential difference was set up between the two sources. The plate obtained shows Cd I and Cd II lines. Among the last, 2144 and 2265, which spring from the lowest excited level, appear clearly; 2749, which is the strongest Cd II line under normal conditions, is very weak, and the strong line 2313 does not show at all. This corroborates the assumption that the excitation is due to electronic collisions, controlled by the potential drop.

The method of controlled step by step excitation, by collisions with electrons, requires, usually, in order to obtain sufficient vapor density, the heating of the whole containing vessel to a suitable temperature. In this case the container is at room temperature and the density is determined by the number and temperature of the coils, exclusively. This may be an experimental advantage in some investigations.

During the Cd test experiment, it was remarked that the thermionic source of electrons had to be heated to a rather high temperature, in order to obtain enough intensity in the spectra. Dr. R. M. Langer suggested to us, that this observation indicates a high thermionic emissivity for the aluminum coated tungsten filament. This suggestion has been verified by us. The results of this investigation will appear in another publication.

[3] M. Bögemann, Dissert. Münster 1917; J. Barnes, Astrophys. J. **34**, 159 (1911); J. H. Pollock, Proc. Roy. Soc. Dublin **13**, 202 (1912).

The Spectrum of AgD

PHILIP G. KOONTZ,* *Sloane Physics Laboratory, Yale University*

(Received April 29, 1935)

The spectrum of AgD has been photographed at high dispersion with an Ag arc in an atmosphere of deuterium as a source. Quantum analyses of the 0,0 and 1,1 bands are presented. The value $B_e = 3.2595$ is found for the lower state. Comparing this with the corresponding value for AgH, the ratio B_e^i/B_e for the two isotopic molecules is 0.50511, whereas the ratio of the reduced masses, by using Aston's latest values for the masses of the H and D atoms, is 0.50497. Calculation of the corrections to B_e for the anharmonic oscillator as given by J. L. Dunham shows them to affect the B_e ratio inappreciably.

INTRODUCTION

RECENT investigations of the spectra of AlD[1] and CaD[2] have stimulated considerable interest in an accurate comparison of the spectra of hydrides with those of the corresponding deuterides. Because of the large differences in the spectra of the two isotopic molecules, the validity of the isotope theory can be determined to a high degree of accuracy. The above investigations have shown that, in certain cases at least, an appreciable discrepancy exists between the values of ρ^2 and the ratio of the rotational constant B_e for the nonrotating, vibrationless isotopic molecules, whereas simple theory predicts their equality. Two different views[1, 3] of the explanation of this discrepancy have developed and it is desirable to obtain additional data from other molecules. The results of an analysis of the spectrum of AgD are here presented.

EXPERIMENTAL PROCEDURE

The $^1\Sigma \rightarrow {}^1\Sigma$ band system of AgH with the system origin near 3300A is well known.[4–8] Spectrograms of the corresponding bands of AgD were taken in the third order of a 21-ft. concave grating in a stigmatic mounting. The dispersion was 1.58A/mm. The light source was a d.c. arc between two silver electrodes, one of which was water-cooled, in an atmosphere of deuterium gas at about 6 cm of Hg pressure. Currents of 5–6 amperes were used. The deuterium gas was obtained from the reaction in a vacuum of a gram of 99 percent deuterium oxide with Ca metal. Of course this reaction liberated only one-half of the deuterium. In this case no attempt was made to recover the remaining half as the CaOD was used as a target in some nuclear disintegration experiments in this laboratory. The AgH bands were present, the H_2 coming from the hot electrodes and electrode mountings, but they were weak and did not cause any difficulties in the analysis.

ROTATIONAL ANALYSIS

The spectrum of AgH may be described as consisting of a few sequences of bands, the spacing of the sequences being much wider than the distance between any adjacent bands forming the sequence. The bands degrade to the red, the R branch forming a head at about $J = 18$. The vibrational part of the isotope theory predicts only a small change toward the violet in the position of the 0,0 band origin of AgD relative to the origin of the corresponding band of AgH, as the difference of the ω_e values for the upper and lower states of AgH is known to be small. The rotational isotope effect predicts a change of nearly 2 to 1 in spacing of the individual lines of the P and R branches for the two isotopic molecules, the heavier isotope forming the smaller pattern. It is found for the 0,0 band, that both the band origin and the head of the R branch of the AgD band lie in the interval between the

* Portion of a dissertation presented for the degree of Doctor of Philosophy at Yale University.

[1] Holst and Hulthén, Nature **133**, 496 (1934); Nature **133**, 796 (1934); Zeits. f. Physik **90**, 712 (1934).

[2] Watson, Phys. Rev. **47**, 27 (1935).

[3] R. deL. Kronig, Physica **1**, 617 (1934).

[4] Bengtsson and Svensson, Comptes rendus **180**, 274 (1925).

[5] Hulthén and Zumstein, Phys. Rev. **28**, 13 (1926).

[6] Bengtsson and Hulthén, Trans. Faraday Soc. **25**, 752 (1929).

[7] Bengtsson and Olsson, Zeits. f. Physik **72**, 163 (1931).

[8] Bengtsson: Nova Acta Reg. Soc. Sci. Uppsala (IV) **8**, 23 (1932).

TABLE I. *Assignment of frequencies for* $^1\Sigma \rightarrow {}^1\Sigma$ *AgD bands* (cm^{-1} *units*).

	0,0		1,1			0,0		1,1	
	P	*R*	*P*	*R*		*P*	*R*	*P*	*R*
1					24	692.17	984.81	542.69	822.74
2	29897.86	29928.91			25	680.08	983.47	528.00	818.50
3	890.91	934.70		29807.48	26	667.75	981.97	512.99	813.66
4	883.83	939.60		812.11	27	655.07	979.92	497.43	807.90
5	876.60	944.61	29750.65	816.47	28	642.06	977.53	481.44	801.92
6	868.78	949.27	742.93	820.37	29	629.87	974.80	464.93	795.27
7	860.97	953.83	734.79	823.86	30	615.31	971.72	447.95	787.92
8	852.94	957.86	726.39	827.10	31	601.61	967.96	430.58	779.92
9	844.65	961.86	717.37	829.80	32	587.33	963.73	412.38	770.64
10	836.21	965.44	708.04	832.50	33	572.89	959.00	393.72	761.06
11	827.10	968.62	698.42	834.64	34	557.80	953.83	374.39	750.65
12	818.50	971.72	688.77	836.21	35	542.69	948.08	354.24	739.37
13	809.08	974.80	678.44	837.50	36	527.06	941.78	333.83	727.08
14	799.70	977.31	667.75	838.74	37	511.09	934.70	312.57	713.76
15	789.90	979.46	656.90	838.74	38	494.61	927.22	290.45	699.39
16	779.92	981.37	645.59	838.74	39	477.73	919.16	267.30	684.15
17	769.94	982.79	633.99	838.74	40	460.40	909.96	243.65	667.75
18	759.52	984.07	622.19	837.50	41	442.31	900.37	218.92	650.71
19	749.05	985.93	609.87	836.21	42	423.68	889.93	193.32	630.42
20	738.01	985.93		834.64	43	404.64	878.56	166.13	
21	727.08	985.93	584.09	832.50	44	385.06	866.30	139.07	
22	715.66	985.93	570.85	829.80	45	364.57	852.94	108.40	
23	704.05	985.93	556.83	826.48	46	343.57	838.74		
					47	321.51	823.86		

origin and the *R* branch head of the AgH band. Table I gives the assignment of frequencies to the *P* and *R* branches for the 0,0 and 1,1 bands of AgD. The rotational constants B_v and D_v are evaluated in the usual semi-graphical way from the $\Delta_2 F(J)$ values. Table II gives the values obtained for AgD. The values of α_e and B_e are determined from the relation $B_v = B_e - \alpha_e(v+1/2)$ when B_0 and B_1 are known. Simple isotope theory predicts that the ratio of the B_e values for the isotopic molecules should be exactly equal to ρ^2, the ratio of the reduced masses. Using Bengtsson's[8] value $B_e = 6.453$ for the ground state of AgH and the value $B_e = 3.2595$, this ratio is 0.50511.[9]

In calculating the value for ρ^2, Casimir[10] has shown that the masses of the electrons in closed shells should be included with the mass of the nucleus (the effect of adding one electron to the silver atom is negligible), but there is some uncertainty about the proper method of including the mass of the electron associated with the hydrogen atom. If we use the atomic weight of silver, 107.880, and Aston's[11] latest values of atomic masses for hydrogen and deuterium, H = 1.0081 and D = 2.0148, we find $\rho^2 = 0.50497$. By assuming all of the electrons associated with the silver and by using values for the proton and deuteron, $\rho^2 = 0.50485$. A comparison shows that the ratio of the *B* values is larger than the first value of ρ^2 by nearly 0.03 percent and that the discrepancy is a little larger in the second case. This difference is small and is in agreement with Kronig's[3] prediction concerning molecules whose united atom (a concept applicable only in the case of hydrides) is in a ^1S state for which $L = 0$. If one assumes Kronig's explanation this discrepancy could be attributed to the interaction of nearby states, the magnitude of which cannot be calculated. The alternative explanation[1, 9] assumes that a few of the outermost electrons are constrained by the nucleus to take part in the rotation and give an additional contribution to the moment of inertia of the molecule. Data

TABLE II. *Rotational constants for AgD.*

LOWER $^1\Sigma$ STATE	UPPER $^1\Sigma$ STATE
$B_0 = 3.2229$	$B_0 = 3.1015$
$B_1 = 3.1497$	$B_1 = 2.9854$
$D = -8.7 \times 10^{-5}$	$D = -10.1 \times 10^{-5}$
$\alpha_e = 0.0732$	
$B_e = 3.2595$	

[9] According to L. Hulthén (Nature **135**, 543 (1935)) E. Hulthén and E. Bengtsson Knave have obtained 0.50527 for the ratio of the B_e's for AgH and AgD.

[10] Casimir, Physica **1**, 1073 (1934).

[11] Aston, Nature **135**, 541 (1935).

obtained recently by the writer[12] on the constants of the BeD and BeD^+ spectra would seem to favor Kronig's interpretation of such discrepancies.

In making accurate comparisons of the B_e constants one should of course consider the correction to B_e given by Dunham[13] in his extended treatment of the rotating vibrator. Calculation of the Dunham constants for AgH shows that this correction is of the order of one part in 75,000. The evaluation of the corresponding Dunham constants for AgD requires the analysis of at least one additional band, but approximate values may be obtained by application of regular isotope relations. This approximate solution gives a correction to B_e of the order of one part in 100,000. These corrections are too small to be of importance in the comparison of these spectra.

The author wishes to thank Professor W. W. Watson, who suggested the problem, for many helpful discussions during its progress.

[12] Koontz, Phys. Rev. **47**, 641 (1935).
[13] Dunham, Phys. Rev. **41**, 721 (1932).

JULY 15, 1935 PHYSICAL REVIEW VOLUME 48

The Theory of $^3\Sigma^+ - {}^3\Sigma^-$ Transitions in Band Spectra[1]

RICHARD D. PRESENT, *Research Laboratory of Physics, Harvard University*

(Received May 20, 1935)

G. Herzberg has recently studied certain faint absorption bands in O_2 which show Q branches ($\Delta K=0$) but not the customary P and R branches ($\Delta K=\pm 1$). These bands he attributes on the basis of the configuration theory to a "forbidden" transition $^3\Sigma_g^- - {}^3\Sigma_u^+$. There exist two alternative explanations for the occurrence of these bands: (1) spin-orbit interaction, (2) rotational distortion. For the case of spin-orbit interaction the intensities have been calculated in case (a) and transformed to case (b) where the theory predicts twelve branches with $\Delta K=\pm 2,0$, provided that the J structure is resolved. When this structure is unresolved it is found that transitions with $\Delta K=0$ should be more intense than transitions with $\Delta K=\pm 2$ in the ratios: 6 : 1 for $K\doteq\infty$, 5 : 1 for $K=4$ and 4 : 1 for $K=1$. In view of the faintness of the observed bands this appears to be sufficient to account for the absence of branches with $\Delta K\neq 0$. With rotational distortion, calculations show that only Q branches will occur. The intensities with spin-orbit interaction vary asymptotically as the first power of K, while for rotational distortion they increase asymptotically as K^3. Further experiments are needed to decide between the two explanations, although theory would favor the first from considerations of relative intensity. An explanation is given of the non-enhancement of the $^3\Sigma_g^- - {}^3\Sigma_u^+$ bands in O_4, despite the proximity of the triple-headed ultraviolet bands of Wulf, Finkelnburg and Steiner which we attribute to a $^3\Pi_g$ upper state. Transitions of the type $^1\Sigma^+ - {}^1\Sigma^-$ are also discussed.

INTRODUCTION

SEVERAL years ago Herzberg[2] discovered an unusual system of faint absorption bands in O_2 which appear between 2600 and 2400A and consist of but one branch apiece under the available dispersion of the quartz spectrograph. It appears conclusively from the experimental data that these bands have Q branches ($\Delta K=0$) but not the customary P and R branches ($\Delta K=\pm 1$)[3] and that they correspond to a "forbidden" transition between the ground state $^3\Sigma_g^-$ and an upper state $^3\Sigma_u^+$.[4]

[1] Presented at the Washington meeting of the American Physical Society, April, 1935.
[2] G. Herzberg, Naturwiss. **20**, 577 (1932).
[3] This is apparently the first time that such bands have been observed. In accordance with the positive-negative selection rule the only states which can combine with $^3\Sigma_g^-$ to give Q branches but no P or R branches are the states $^3\Sigma_u^+$ and $^1\Sigma_u^+$, of which only the former is a configuration arising from normal O atoms in a ^3P state. Since it can be shown from the experimental data that the upper state must dissociate into normal atoms, this leads to the interpretation of these bands as $^3\Sigma_g^- - {}^3\Sigma_u^+$.
[4] There is the possibility that these bands may be due to magnetic dipole radiation. The selection rules for this type of radiation require that positive levels should combine only with positive levels and negative only with negative (since the magnetic moment is invariant to reflection) and in consequence even (g) states will combine only with even states and odd (u) with odd. Then the only states which can combine with $^3\Sigma_g^-$ in the desired way are $^3\Sigma_g^-$ and $^1\Sigma_g^-$, of which the former alone is a configuration arising from normal atoms. Since but one $^3\Sigma_g^-$ state, *viz.*, the ground level, can arise in this way, we may conclude that magnetic dipole radiation is not responsible for the appearance of these bands.

$\Sigma^+ - \Sigma^-$ transitions do not ordinarily occur because their appearance for $\Delta K = \pm 1$ would violate the selection rule that "forbids" positive-positive and negative-negative combinations, whereas for $\Delta K = 0$ the integral of the electric moment over the rotational "symmetrical top" functions is of zero amplitude. The positive-negative selection rule holds rigorously for electric dipole radiation in the absence of external fields; the vanishing of the rotational integral is valid so long as the molecular wave function satisfies the equation for the symmetrical top, i.e., so long as the perturbing matrix elements due to the components of angular momentum perpendicular to the internuclear axis are negligible. When this is no longer strictly true, i.e., when the distortion due to molecular rotation becomes appreciable, the exact dependence of the electronic wave function Φ on φ through the factor $e^{\pm i\Lambda\varphi}$ is destroyed, for the internuclear line is no longer an axis of symmetry when the "perpendicular components" are taken into account. Then the usual classification of molecular states into Σ, Π, Δ states is no longer exact, for Λ ceases to be a "good quantum number." Thus rotational distortion causes the Σ states to "borrow" some of the characteristics of Π states and since Σ–Π transitions do not yield vanishing "symmetrical top" amplitudes, the forbidden bands will appear.

A second cause for the appearance of these bands may be the spin-orbit interaction by which the electron spins are coupled to the axis of figure of the molecule. This interaction will also destroy the dependence of Φ on φ through the factor $e^{\pm i\Lambda\varphi}$, for the matrix elements of the interaction energy are diagonal in Ω rather than in Λ. This would appear to be the first known case where spin-orbit interaction may lead to transitions which are not between states of different multiplicities, i.e., not intersystem combinations. Our calculation is in many respects similar to Schlapp's spin-orbit treatment of the intersystem bands.[5]

Spin-Orbit Interaction in Case (a)

Although we shall make use of a molecular model with two valence electrons in our derivation of the relative phases, the same arguments should apply to a system of any number of electrons and the phases so determined will be perfectly general. The molecule is referred to a system of moving axes (ξ, η, ζ) which are related in the usual way to the fixed axes (x, y, z); it will also be convenient to use a system of cylindrical coordinates (ρ, φ, ζ) where the azimuth φ is measured about the ζ axis from the plane $\eta = 0$. Then reflection in the plane $\eta = 0$ is equivalent to replacing φ by $-\varphi$. The wave function for the stationary molecule in a state characterized by the quantum number Λ, will be a linear combination of terms of the sort:

$$[e^{i\lambda_1\varphi_1}g(1)e^{i\lambda_2\varphi_2}h(2) \pm e^{i\lambda_2\varphi_1}h(1)e^{i\lambda_1\varphi_2}g(2)], \tag{1}$$

where g and h are real functions independent of φ_1 and φ_2 and where $\lambda_1 + \lambda_2 = \Lambda$. For Σ states the wave function is real and of the form $G\cos\lambda(\varphi_1 - \varphi_2)$ or $H\sin\lambda(\varphi_1 - \varphi_2)$, where G and H are independent of φ, depending on whether the state is Σ^+ or Σ^-, i.e., even or odd to reflection in the plane $\eta = 0$. In addition there will be the usual spin functions, three of which are symmetrical in the spin coordinates $(S = 1; \Sigma = \pm 1, 0)$ and are to be combined with the orbital factors (1) with the lower sign; and the fourth of which is antisymmetrical $(S = 0; \Sigma = 0)$ and is to be combined only with factors (1) having the upper sign. Since Λ and Σ are both good quantum numbers in case (a), their sum Ω will also be a good quantum number and may be affixed as a subscript to the term symbol, *viz.*, ${}^3\Sigma_1$, ${}^3\Sigma_0$, ${}^3\Sigma_{-1}$.

We introduce as a small perturbation the interaction energy between the orbits and spins of the individual electrons. This is known to be of the form:

$$H' = a_1(l_1 \cdot s_1) + a_2(l_2 \cdot s_2) \quad (a_i = (e/2m^2c^2)(1/r)dV/dr),$$

where a_1 and a_2 are real constants, s_1 and s_2 are the Pauli spin operators and l_1 and l_2 are the angular-momentum operators whose components are given by: $l_\xi = h/2\pi i(\eta\partial/\partial\zeta - \zeta\partial/\partial\eta)$ etc. The matrix ele-

[5] R. Schlapp, Phys. Rev. **39**, 806 (1932).

ments of the perturbing energy H' between the wave functions for the stationary molecule are readily found to be diagonal in Ω and to have $\Delta\Lambda=0,\ \pm1$, when use is made of the well-known properties of l and s by virtue of which:

$$(l\cdot s)\Phi_{\frac{1}{2},\ m_l}\rightarrow\Phi_{-\frac{1}{2},\ m_l+1},\quad (l\cdot s)\Phi_{-\frac{1}{2},\ m_l}\rightarrow\Phi_{\frac{1}{2},\ m_l-1}.$$

The perturbed wave functions will therefore consist of the following linear combinations:

$$\begin{aligned}\Phi'(^3\Sigma_0{}^{\pm})&=a_{\pm}\Phi(^3\Sigma_0{}^{\pm})+b_{\pm}\Phi(^3\Pi_0{}^1)+b_{\pm}'\Phi(^3\Pi_0{}^{-1}),\\ \Phi'(^3\Sigma_1{}^{\pm})&=c_{\pm}\Phi(^3\Sigma_1{}^{\pm})+d_{\pm}\Phi(^3\Pi_1{}^1),\\ \Phi'(^3\Sigma_{-1}{}^{\pm})&=e_{\pm}\Phi(^3\Sigma_{-1}{}^{\pm})+f_{\pm}\Phi(^3\Pi_{-1}{}^{-1}),\end{aligned}\tag{2}$$

where the superscript to the right of the term symbol for the Π states gives the value of Λ. The transformation matrices, whose elements give the constants a, c, e, b, b', d and f are, in the first order approximation of perturbation theory, of the form: $S=1+S'$ where 1 stands for the unit matrix and S' is a matrix consisting entirely of nondiagonal terms: $S_{mn}'=-H_{mn}'/(W_m{}^0-W_n{}^0)$. Here H_{mn}' is the matrix element of the perturbation energy between the mth and nth states which have unperturbed energies $W_m{}^0$ and $W_n{}^0$. Without an exact knowledge of the molecular wave functions it is impossible to determine the amplitudes of the constants b, b', d and f; for our present purposes, however, it is sufficient to determine their relative phases, which are the same as those of the corresponding matrix elements H_{mn}'.

The matrix elements of the spin-orbit interaction energy are readily obtained from the well-known properties of the spin operators:

$$(^3\Pi_0{}^{\pm1}|H'|^3\Sigma_0)=(^3\Pi_{\pm1}{}^{\pm1}|H'|^3\Sigma_{\pm1})=2^{-3/2}[a_1(^3\Pi^{\pm1}|l_{1\xi}\pm il_{1\eta}|^3\Sigma)+a_2(^3\Pi^{\pm1}|l_{2\xi}\pm il_{2\eta}|^3\Sigma)].\tag{3}$$

A change of variables corresponding to the reflection $\eta'=-\eta$, $\varphi'=-\varphi$ reveals phase relations between the orbital integrals which are

$$(^3\Pi^1|l_{1\xi}|^3\Sigma^{\pm})=\mp(^3\Pi^{-1}|l_{1\xi}|^3\Sigma^{\pm}),\quad (^3\Pi^1|l_{1\eta}|^3\Sigma^{\pm})=\pm(^3\Pi^{-1}|l_{1\eta}|^3\Sigma^{\pm});$$

$$\therefore(^3\Pi_0{}^1|H'|^3\Sigma_0{}^{\pm})=\mp(^3\Pi_0{}^{-1}|H'|^3\Sigma_0{}^{\pm}),\quad (^3\Pi_1{}^1|H'|^3\Sigma_1{}^{\pm})=\mp(^3\Pi_{-1}{}^{-1}|H'|^3\Sigma_{-1}{}^{\pm}).$$

Consequently there will exist between the transformation matrix elements the following relations:

$$a_{\pm}=c_{\pm}=e_{\pm}=1,\quad b_{\pm}=d_{\pm},\quad b'_{\pm}=f_{\pm},\quad d_{\pm}=\mp f_{\pm},\tag{4}$$

since $W_m{}^0-W_n{}^0$ will be the same for all matrix elements between the same two electronic states.

The complete wave function includes in addition to the electronic part just discussed, a factor to represent the solution of the vibrational equation and the symmetrical top function which describes the rotational motion. Since we are interested only in the J structure of one particular band, corresponding to a definite vibrational level in each of the two states, it will be unnecessary to consider the vibrational function at all, for this merely introduces a factor independent of J into the intensities. The characteristic functions of the top are denoted by $u_{\Omega JM}(\theta,\ \omega)$ where θ is the angle between the z and ζ axes and ω is the angle giving the azimuth of the ξ axis around the z axis to which it is perpendicular. There is an arbitrary phase factor connected with each of these functions which will be chosen in conformity with the convention adopted by Van Vleck in a treatment of the rotational distortion problem.[6] This is done for the sake of consistency, since we shall later have occasion to use some of the results of this treatment. From the definition of the symmetrical top function and the convention adopted for the phase factor, the following reflection property may be readily verified:

$$u_{\Omega JM}(\pi-\theta,\ \omega+\pi)=(-1)^J u_{-\Omega JM}(\theta,\ \omega).\tag{5}$$

[6] J. H. Van Vleck, Phys. Rev. **33**, 467 (1929). Cf. footnote 25.

The Amplitudes in Case (a)

Let us now form the matrix elements of the z component of the electric moment for which $\Delta M=0$. If we recall that $\Delta\Sigma=0$ for transitions in case (a) and that Σ^+ does not combine with Σ^- in first approximation, then upon neglecting second-order terms the following expressions are obtained for the case (a) amplitudes:

$$\begin{aligned}
(^3\Sigma_0{}^+-{}^3\Sigma_1{}^-)JJ'&=f_+(^3\Pi^{-1}-{}^3\Sigma^-)(0J,\,1J')+d_-(^3\Sigma^+-{}^3\Pi^1)(0J,\,1J')=A\,|\,(0J,\,1J')\,|,\\
(^3\Sigma_0{}^+-{}^3\Sigma_{-1}{}^-)JJ'&=d_+(^3\Pi^1-{}^3\Sigma^-)(0J,\,-1J')+f_-(^3\Sigma^+-{}^3\Pi^{-1})(0J,\,-1J')=B\,|\,(0J,\,-1J')\,|,\\
(^3\Sigma_1{}^+-{}^3\Sigma_0{}^-)JJ'&=d_+(^3\Pi^1-{}^3\Sigma^-)(1J,\,0J')+f_-(^3\Sigma^+-{}^3\Pi^{-1})(1J,\,0J')=C\,|\,(1J,\,0J')\,|,\\
(^3\Sigma_{-1}{}^+-{}^3\Sigma_0{}^-)JJ'&=f_+(^3\Pi^{-1}-{}^3\Sigma^-)(-1J,\,0J')+d_-(^3\Sigma^+-{}^3\Pi^1)(-1J,\,0J')=D\,|\,(-1J,\,0J')\,|,
\end{aligned}\tag{6}$$

where $(^3\Pi^{-1}-{}^3\Sigma^-)(0J,\,1J')=\int\Phi^*(^3\Pi^{-1})\eta\Phi(^3\Sigma^-)d\tau\int u^*{}_{0JM}u_{1J'M}\sin^2\theta d\theta d\omega$

$$+\int\Phi^*(^3\Pi^{-1})\zeta\Phi(^3\Sigma^-)d\tau\int u^*{}_{0JM}u_{1J'M}\sin\theta\cos\theta d\theta d\omega,$$

with corresponding expressions for the other transitions. The second integral will vanish for all the transitions concerned because ζ can have no matrix elements which are nondiagonal in Λ. The integrals $(0J,\,1J')$ etc. are just the amplitude factors for the symmetrical top and their relative phases may be obtained from (5). Transformation of each integral by reflection gives the phase relations:

$$\begin{aligned}
(^3\Pi^{-1}-{}^3\Sigma^-)&=(^3\Pi^1-{}^3\Sigma^-),\quad (0J,\,1J')=(-1)^{\Delta J}(0J,\,-1J'),\\
(^3\Sigma^+-{}^3\Pi^1)&=-(^3\Sigma^+-{}^3\Pi^{-1}),\quad (1J,\,0J')=(-1)^{\Delta J}(-1J,\,0J').
\end{aligned}\tag{7}$$

If A, B, C and D represent, respectively, the quotients of each line of (6) by the modulus of the corresponding symmetrical top amplitude factor, then from (4) and (7) we have:

$$A/B=C/D=(-1)^{\Delta J+1}.\tag{8}$$

The relative phases of B and C, i.e., of $(0J,\,-1J')$ and $(1J,\,0J')$, may be determined by examining the appropriate Rademacher-Reiche integrals[7] and the phase conventions in the definition of $u_{\Omega JM}$, from which it is seen that $(0J,\,-1J')$ and $(1J,\,0J')$ are in phase for all M and ΔJ.

We may now write down the amplitude matrices for $^3\Sigma^+-{}^3\Sigma^-$ transitions in case (a), taking the well-known amplitude factors from Rademacher and Reiche:

$$\begin{array}{r}
\\ \Omega=\\ \Omega_-=1\\ 0\\ -1
\end{array}
\begin{array}{c}
\begin{array}{ccc} J-J'=0 & & \end{array}\\
\begin{array}{ccc} 1 & 0 & -1 \end{array}\\
\begin{pmatrix} 0 & -Ad & 0 \\ Ad & 0 & -Ad \\ 0 & Ad & 0 \end{pmatrix}
\end{array}
\begin{array}{c}
\begin{array}{ccc} J-J'=1 & & \end{array}\\
\begin{array}{ccc} 1 & 0 & -1 \end{array}\\
\begin{pmatrix} 0 & Af & 0 \\ Ae & 0 & Ae \\ 0 & Af & 0 \end{pmatrix}
\end{array}
\begin{array}{c}
\begin{array}{ccc} J-J'=-1 & & \end{array}\\
\begin{array}{ccc} 1 & 0 & -1 \end{array}\\
\begin{pmatrix} 0 & Ag & 0 \\ Ah & 0 & Ah \\ 0 & Ag & 0 \end{pmatrix}
\end{array},\tag{9}$$

$$M=M',\quad d=\frac{(J'(J'+1))^{\frac{1}{2}}M'}{2J'(J'+1)},\quad e=\left[\frac{J'(J'+1+M')(J'+1-M')}{4(J'+1)(2J'+1)(2J'+3)}\right]^{\frac{1}{2}},$$

$$f=\left[\frac{(J'+2)(J'+1+M')(J'+1-M')}{4(J'+1)(2J'+1)(2J'+3)}\right]^{\frac{1}{2}},\quad g=\left[\frac{(J'-1)(J''^2-M''^2)}{4J'(2J'-1)(2J'+1)}\right]^{\frac{1}{2}},\quad h=\left[\frac{(J'+1)(J''^2-M''^2)}{4J'(2J'-1)(2J'+1)}\right]^{\frac{1}{2}}.$$

[7] F. Reiche and H. Rademacher, Zeits. f. Physik **41**, 453 (1927). It may be seen from their Table III, as applied to their case (6), that the phases of the integrals corresponding to $(1J,\,0J')$ and $(0J,\,-1J')$ are such as to ensure that when account is taken of our sign convention for $u_{\Omega JM}$, then $(1J,\,0J')$ and $(0J,\,-1J')$ will be in phase for all M and ΔJ.

The Amplitudes in Case (b)

The amplitudes which have just been calculated are of no direct experimental significance, for a $^3\Sigma$ state of the rotating molecule comes under case (b) where the spin has been uncoupled from the figure axis through the influence of molecular rotation and the quantum number Ω no longer has meaning. To pass from case (a) to case (b) we introduce as a perturbation the rotational distortion that is due to the components of spin perpendicular to the molecular axis. The matrix elements should really be calculated with respect to the perturbed wave functions ψ' which take into account the spin-orbit interaction, but since this is small compared with the spin distortion we may use the unperturbed functions ψ instead. The appropriate transformation matrix for this case has been obtained by Schlapp[5] and is (for complete uncoupling of the spin):

$$S=\begin{pmatrix} 1/\sqrt{2} & 0 & 1/\sqrt{2} \\ a & ib\sqrt{2} & -a \\ -b & ia\sqrt{2} & b \\ \Omega=1 & 0 & -1 \end{pmatrix}\begin{matrix} K=J \\ J-1, \\ J+1 \end{matrix} \qquad \begin{matrix} a=\left(\dfrac{J+1}{2(2J+1)}\right)^{\frac{1}{2}}, \\ \\ b=\left(\dfrac{J}{2(2J+1)}\right)^{\frac{1}{2}}. \end{matrix} \tag{10}$$

If we denote the amplitude matrices in case (a) by q_a and in case (b) by q_b, then the matrix equation: $q_b=S_+q_aS_-^{-1}=S_+q_a\tilde{S}_-^*$ will express the transformation of the amplitudes from case (a) to case (b). The matrices q_a are given by (9) and S_+ and S_- are, respectively, the transformation matrices for the $^3\Sigma^+$ and $^3\Sigma^-$ states. The quantum number Ω of the hypothetical case (a) states enters only as an index of summation. In case (b) as in case (a) there will be three amplitude matrices corresponding to transitions for which $\Delta J=0,\ 1,\ -1$. Instead of writing these down we shall give immediately the final intensities which are obtained from the amplitudes for the z component by taking three times the square of the modulus and summing over M from $-J$ to J. We characterize the J resolved branches of case (b) by the following notation: the letters P, Q and R correspond to $\Delta J=1,\ 0,\ -1$ and a superscript O, P, Q, R, S written to the left denotes that $\Delta K=2,\ 1,\ 0,\ -1,\ -2$; e.g., ${}^SQ$ means $\Delta J=0,\ \Delta K=-2$.

The intensity formulae are:[8]

$$\begin{array}{lc} & \begin{matrix} K= & K'=J'-1 & J' & J'+1 \end{matrix} \\ \Delta J=J'-J & \begin{matrix} J-1 \\ J \\ J+1 \end{matrix}\begin{pmatrix} 2A^2J(J+1)/(2J+1)({}^QQ) & 0 & A^2/2(2J+1)({}^OQ) \\ 0 & 0 & 0 \\ A^2/2(2J+1)({}^SQ) & 0 & 2A^2J(J+1)/(2J+1)({}^QQ) \end{pmatrix}, \\ =0 & \end{array}$$

$$\begin{array}{lc} & \begin{matrix} J-1 \\ J \\ J+1 \end{matrix}\begin{pmatrix} 0 & A^2J(J+2)/2(2J+1)({}^OP) & 0 \\ A^2J(J+1)/2(2J+3)({}^QP) & 0 & A^2J(J+2)/2(2J+3)({}^OP) \\ 0 & A^2(J+1)(J+2)/2(2J+1)({}^QP) & 0 \end{pmatrix}, \\ \Delta J=1 & \end{array} \tag{11}$$

$$\begin{array}{lc} & \begin{matrix} J-1 \\ J \\ J+1 \end{matrix}\begin{pmatrix} 0 & A^2J(J-1)/2(2J+1)({}^QR) & 0 \\ A^2(J^2-1)/2(2J-1)({}^SR) & 0 & A^2J(J+1)/2(2J-1)({}^QR) \\ 0 & A^2(J^2-1)/2(2J+1)({}^SR) & 0 \end{pmatrix}. \\ \Delta J=-1 & \end{array}$$

If we add up all the individual intensities corresponding to a single level J of either state, the result will be proportional to $2J+1$ in accordance with the usual sum rules. The branches which appear are those to be expected from the positive-negative selection rule.

Comparison with Experiment

In the experimental work the J structure was not resolved. We must therefore sum over the resolved J components to determine the relative intensities of the transitions with $\Delta K=0,\ \pm2$

[8] J, K refer to the $^3\Sigma^+$ and J', K' to the $^3\Sigma^-$ state. Consequently the branch notation used here is appropriate when the upper state is $^3\Sigma^+$; if it be $^3\Sigma^-$ then P and R and also O and S must be interchanged.

(there are no branches for $\Delta K=\pm 1$). This is done by expressing the formulae (11) in terms of K and by adding separately the components for which $\Delta K=0,\ \pm 2$. The relative intensities are:

$$\begin{aligned}
&\Delta K=0 \quad (Q) \quad (12K^3+18K^2-2K-4)/(2K+3)(2K-1),\\
&\Delta K=2 \quad (O) \quad (2K^3+5K^2+K-2)/(2K+3)(2K-1),\\
&\Delta K=-2 \quad (S) \quad (2K^3+K^2-3K)/(2K+3)(2K-1),
\end{aligned} \tag{12}$$

from which it may be seen that the ratio of the intensity of the $\Delta K=0$ branch to the more intense branch with $\Delta K=\pm 2$ is as 6 : 1 for $K\doteq\infty$, 5 : 1 for $K=4$, 4 : 1 for $K=1$ and 2 : 1 for $K=0$. Because of the great faintness of the observed bands it appears that the $\Delta K=\pm 2$ branches could very well have passed unnoticed if they occurred with a fifth or sixth of the intensity of the $\Delta K=0$ branch.[9] This would then account for Herzberg's failure to observe branches with $\Delta K=\pm 1,\ \pm 2$.

Rotational Distortion

There is another possible explanation for the occurrence of these bands: the rotational distortion which is due to the perpendicular components of the orbital angular momentum. This problem is most readily treated from the standpoint of case (b) since the spin should play no essential part in the calculation and since the states concerned belong actually to case (b). The new linear combinations for the complete wave functions are:

$$\psi'(^3\Sigma^{\pm})=a_{\pm}\psi(^3\Sigma^{\pm})+b_{\pm}\psi(^3\Pi^1)+c_{\pm}\psi(^3\Pi^{-1}),$$

where $a\sim 1$ and $b_{\pm}$ and $c_{\pm}$ are proportional to the corresponding matrix elements of the perturbing energy. The matrix elements for rotational distortion in case (b) are similar to those in case (a)[10] with K, Λ replacing J, Ω:

$$II(\Lambda, v;\ \Lambda\pm 1, v')=2(BP_{\eta})(\Lambda, v;\ \Lambda\pm 1, v')[K(K+1)-\Lambda(\Lambda\pm 1)]^{\frac{1}{2}} \qquad K'=K,$$

where P_{η} is the η component of the total electronic angular momentum. Since II is nondiagonal in Λ and connects different electronic states, it must contain a vibrational factor[11] depending on v and v' (the Franck-Condon integral). However in obtaining the relative J dependence of the several branches we may leave the vibrational function out of consideration altogether. Then

$$II(\Lambda,\ \Lambda\pm 1)=2B[K(K+1)-\Lambda(\Lambda\pm 1)]^{\frac{1}{2}}[l_{1\eta}(\Lambda,\ \Lambda\pm 1)+l_{2\eta}(\Lambda,\ \Lambda\pm 1)].$$

If we now determine the relative phases of the transformation matrix elements and of the integrals appearing in the z component of the electric moment, then the latter is found to take on the simple form:

$$(^3\Sigma^+-{}^3\Sigma^-)KK=CM_K, \quad (^3\Sigma^+-{}^3\Sigma^-)KK'=0, \quad K'-K=\pm 1,\ \pm 2, \tag{13}$$

where M_K is the magnetic quantum number for case (b) and C is a constant, similar to A of Eq. (6), whose value depends only on the electronic and vibrational characteristics of the motion.

To obtain the intensity of the $\Delta K=0$ transition we must as before take three times the square of the modulus of the z component given by (13) and sum over the magnetic quantum number. Because of the unresolved spin degeneracy there will occur an additional factor of $2S+1$. Therefore the total intensity is:

$$I=9C^2\sum_{-K}^{K}M_K{}^2=3C^2K(K+1)(2K+1). \tag{14}$$

[9] Confirmed by a letter from Dr. Herzberg to Professor Van Vleck.

[10] Reference 6.

[11] Because the Λ doubling is negligible in this approximation, the vibrational factor will be the same for both the nondiagonal terms $(^3\Sigma|II|^3\Pi^1)$ and $(^3\Sigma|II|^3\Pi^{-1})$ and will not alter the relative magnitudes of b and c. Neither will the vibrational factor affect the relative phases since it is invariant under reflection. For the same reasons the nondiagonality in v will not influence the relative magnitudes and phases of the transition amplitudes $(^3\Sigma-{}^3\Pi^1)$ and $(^3\Sigma-{}^3\Pi^{-1})$.

Resolution of the J Structure

The procedure used in resolving the J structure is analogous to that adopted by Hill and Van Vleck[12] in obtaining the case (b) amplitude factors and is strictly justified by the principle of spectroscopic stability. In case (b) the loosely coupled spin S precesses slowly with K about their resultant J in a fashion similar to the precession of L and S about J in ordinary atomic multiplets. The J dependent factors in the relative intensities for all the transitions consistent with a given value of ΔK, will then be given by the atomic formulae of Kronig, Russell and Sommerfeld-Hönl[13] if we substitute K for L throughout. The relative intensities for the resolved J structure of the given transition with $\Delta K=0$ may then be obtained by normalizing these factors to a total intensity of $3C^2K(K+1)(2K+1)$. The relative intensities are as follows:

$$
\begin{aligned}
&\Delta J=J'-J=0({}^qQ)\\
&\quad J=K \qquad C^2(2J+1)[J(J+1)-1]^2/J(J+1),\\
&\quad J=K+1 \quad C^2(J-1)^2(J+1)(2J+1)/J,\\
&\quad J=K-1 \quad C^2(J+2)^2J(2J+1)/(J+1),\\
&\Delta J=1({}^qP)\\
&\quad J=K \qquad C^2J(2J+3)/(J+1),\\
&\quad J=K-1 \quad C^2(2J+1)(J+2)/(J+1),\\
&\Delta J=-1({}^qR)\\
&\quad J=K \qquad C^2(2J-1)(J+1)/J,\\
&\quad J=K+1 \quad C^2(2J+1)(J-1)/J,
\end{aligned}
\tag{15}
$$

where J refers to the ${}^3\Sigma^+$ state. This is the final result and may be compared with the corresponding formulae (11) for the case of spin-orbit interaction. There are two striking points of difference: (1) For spin-orbit interaction the branches with $\Delta K=\pm 2$ are relatively faint; with rotational distortion they do not occur at all; (2) for spin-orbit interaction the total intensities vary asymptotically as the first power of J; with rotational distortion they increase asymptotically as J^3. Further experiments are needed to decide between these two explanations as applied to the ${}^3\Sigma_u^+-{}^3\Sigma_g^-$ bands of O_2. Since spin-orbit interaction is known to occur in neighboring states of the molecule giving rise to the intersystem bands: ${}^3\Sigma_g^--{}^1\Sigma_g^+$ and ${}^3\Sigma_g^--{}^1\Delta_g$,[14] we might also expect it to occur here if the perturbing Π terms were favorably located.

On theoretical grounds we should prefer the spin-orbit to the rotational distortion explanation, for an estimate of the relative intensities reveals that the spin-orbit bands should be more intense than the bands caused by rotational distortion when K is not too large. This result is obtained by comparing the explicit expressions for the constant A of (11) and the constant C of (15). A and C are found to depend on precisely the same matrix elements; if only the ${}^3\Sigma^+$ state is perturbed (presumably by ${}^3\Pi_u$ for the oxygen bands) then:

$$
\frac{\sqrt{2}}{a}|A|=\frac{1}{2B}|C|
$$

$$
=F({}^3\Sigma^+, v; {}^3\Pi^1, v')\frac{({}^3\Sigma^+|l_\eta|{}^3\Pi^1)}{W({}^3\Sigma^+)-W({}^3\Pi^1)}({}^3\Pi^1-{}^3\Sigma^-),
$$

where a is the spin-orbit interaction constant of Eqs. (3), B is the rotational constant of the vth vibrational level of ${}^3\Sigma^+$, and $F({}^3\Sigma^+, v; {}^3\Pi^1, v')$ is the Franck-Condon integral over the vibrational functions of the two states. According to Mulliken[15] a is roughly 150 cm^{-1} for atomic oxygen and probably somewhat less for molecular oxygen; B has been estimated by Herzberg[2] to range from 0.53 to 0.84 cm^{-1} for ${}^3\Sigma_u^+$. The ratio of A^2 to C^2 should then lie somewhere between 10^3 and 10^4, depending on the vibrational level of ${}^3\Sigma_u^+$ concerned. The rotational distortion bands will increase very rapidly in intensity with K, so that when $K=10$ for example, they will be roughly from 1/50 to 1/5 as intense as the spin-orbit bands. For higher values of $K(K\sim 30)$, the intensities become equal and from then on the rotational distortion bands will have the greater intensity. If the principal perturbation occurs in the ground state, the rotational distortion bands will be about three times more intense.

[12] E. L. Hill and J. H. Van Vleck, Phys. Rev. **32**, 250 (1928).
[13] Ruark and Urey, *Atoms, Molecules and Quanta*, p. 703.
[14] J. H. Van Vleck, Astrophys. J. **80**, 161 (1934).
[15] R. S. Mulliken, Rev. Mod. Phys. **4**, 1 (1932); Cf. Table XIV.

Interpretation of the Ultraviolet Bands in O_4

It is worthy of note that bands of the type $^3\Sigma_u^+ - {}^3\Sigma_g^-$ should not be enhanced by the perturbing influence of the polarization forces that come into play at high pressures. If we write the wave function for the polarization molecule O_4 as the product of the molecular functions for two O_2 molecules, then the lowest state will be represented by $\Psi_a = \psi_1(^3\Sigma_g^-)\psi_2(^3\Sigma_g^-)$. If the upper state has a configuration $^3\Sigma_g^- + {}^3\Sigma_u^+$, its wave function will be $\Psi_b = \psi_1(^3\Sigma_g^-)\psi_2(^3\Sigma_u^+)$. The perturbation is principally due to polarization forces[16] of the familiar dipole-dipole, dipole-quadrupole and quadrupole-quadrupole character, of which the first two are known from Margenau's work to be the most important.[17] It is immaterial which state we regard as being perturbed; let us suppose it to be the upper state. The matrix elements of the dipole-dipole interaction energy, which is of the form: $(e^2/R^3)(x_1x_2+y_1y_2-2z_1z_2)$, will connect only even (g) states with odd (u) states and will vanish for $\Sigma^+ - \Sigma^-$ combinations. Thus the perturbed wave functions are of the form:

$$\Psi_b' = \psi_1(^3\Sigma_g^-)\psi_2(^3\Sigma_u^+) + \sum_i a_i \psi_{1u}{}^i \psi_{2g}{}^i,$$

where $\psi_{1u}{}^i = \psi_1\ (^3\Sigma_u^-)$ or $\psi_1(^3\Pi_u)$ and $\psi_{2g}{}^i = \psi_2(^3\Sigma_g^+)$ or $\psi_2(^3\Pi_g)$. Then the electric moment is:

$$E = \int\int \Psi_b'^*[r_1+r_2]\Psi_a d\tau_1 d\tau_2 = \sum_i a_i [\int \psi_{1u}{}^{i*} r_1 \psi_1(^3\Sigma_g^-) d\tau_1 \int \psi_{2g}{}^{i*} \psi_2(^3\Sigma_g^-) d\tau_2 + \int \psi_{1u}{}^{i*} \psi_1(^3\Sigma_g^-) d\tau_1 \int \psi_{2g}{}^{i*} r_2 \psi_2(^3\Sigma_g^-) d\tau_2].$$

The first term will vanish because of the orthogonality of the functions in the second integral and the second term will vanish because both integrals are carried into their negatives by a reflection in the origin. The dipole-quadrupole terms give perturbed wave functions of the form:

$$\Psi_b' = \psi_1(^3\Sigma_g^-)\psi_2(^3\Sigma_u^+) + \sum_i a_i \psi_{1g}{}^i \psi_{2g}{}^i + \sum_i b_i \psi_{1u}{}^i \psi_{2u}{}^i.$$

The electric moment will vanish for this case also because both O_2 molecules have the same g–u symmetry in the upper and in the lower states, so that the orthogonality integral will vanish when the radiative integral does not and *vice versa*. Hence, except for weak quadrupole-quadrupole terms, the $^3\Sigma_u^+ - {}^3\Sigma_g^-$ bands will not be enhanced by polarization forces.

Finkelnburg and Steiner[18] have observed a system of triple-headed O_4 absorption bands in the neighborhood of 2500A which partly coincide with the Herzberg bands $^3\Sigma_u^+ - {}^3\Sigma_g^-$ in O_2. Since these bands are found to grow in intensity with increasing pressure, it is clear from the foregoing that *they cannot be due to the same transition as the Herzberg bands*, i.e., the upper state of the O_4 complex is not $^3\Sigma_g^- + {}^3\Sigma_u^+$. Experimentally Finkelnburg has come to the same conclusion from a comparison of the band heads with the Herzberg null-lines; however, we cannot accept his interpretation of these bands as due to transitions: $^3\Sigma_g^- + {}^3\Delta_u \rightarrow {}^3\Sigma_g^- + {}^3\Sigma_g^-$. When the triple-headed structure is attributed to vibrations of the O_4 complex rather than to a multiplet separation in the upper state, as has been made plausible by more recent work,[19] the *raison d'être* for this interpretation disappears. By an argument precisely analogous to that used to rule out the interpretation $^3\Sigma_u^+ - {}^3\Sigma_g^-$, we can show that $^3\Delta_u - {}^3\Sigma_g^-$ is equally untenable.

It is known from the experimental work that the upper state of the O_4 complex must dissociate into four normal O atoms. Since the matrix elements of the perturbing energy are diagonal in the spins, intersystem combinations will not be enhanced appreciably by the polarization forces. These two conditions restrict the permissible upper states to the following: $^3\Sigma_u^+(2)$, $^3\Delta_u$, $^3\Pi_u$,

[16] That the forces involved are principally of the van der Waals type is to be inferred from the small dissociation energy which is 0.0055 e.v. for the ground state of the O_4 complex (G. N. Lewis, J. Am. Chem. Soc. **46**, 2027 (1924)). $(O_2)_2$ would be a more appropriate designation, but usage favors O_4.

[17] H. Margenau, Phys. Rev. **38**, 747 (1931).

[18] Finkelnburg and Steiner, Zeits. f. Physik **79**, 69 (1932). These bands were first identified by Wulf, Proc. Nat. Acad. Sci. **14**, 609 (1928).

[19] W. Finkelnburg, Zeits. f. Physik **90**, 1 (1934).

$^3\Sigma_g^-$ and $^3\Pi_g$. $^3\Sigma_u^+$ and $^3\Delta_u$ have already been eliminated, $^3\Pi_u$ does not give a forbidden transition, and $^3\Sigma_g^-$ is preempted by the ground state. *This leads to the interpretation of the O_4 ultraviolet bands as* $^3\Sigma_g^- + {}^3\Pi_g \rightarrow {}^3\Sigma_g^- + {}^3\Sigma_g^-$. Examination of the perturbed wave functions and the electric moment integrals, as in the preceding, shows that such transitions are caused by the dipole-quadrupole terms in the polarization energy. There is another possible interpretation: excitation of both molecules in the upper state.[20] Although double jumps are much less probable than single jumps, the polarization forces can here be of the dipole-dipole variety and it may be easily seen that the molecules in the upper state must have opposite g–u symmetry. There are two significant arguments against the double excitation hypothesis. In the first place it is found that the convergence limit of these bands is, apart from a few hundred cm^{-1} which must be allowed for the dissociation energy of the O_4 complex, just the dissociation energy of the O_2 molecule in its normal state. In the second place one should expect that the intensity of double excitation processes would decrease as the proportion of foreign gas increases and would be very nearly independent of the nature of this gas. Salow[21] has found that the intensity varies in fact with the polarizability of the foreign gas in just such a way as one should expect from the single excitation hypothesis.

One last point may be made to support the interpretations given here. Evidence for the favorable location and stability of the $^3\Pi_g$ state, which has not been previously observed, is afforded by the observed intensity situation for the $^3\Sigma_g^- - {}^1\Sigma_g^+$ and $^3\Sigma_g^- - {}^1\Delta_g$ bands in atmospheric O_2. The fact that the former are much more intense than the latter[22] indicates that the most important "borrowing" effect in spin-orbit interaction is the borrowing from $^3\Pi_g$ by $^1\Sigma_g^+$.[14] This would support the view that the $^3\Pi_g$ state cannot be far above $^1\Sigma_g^+$ and is probably stable. Because of the proximity of the Herzberg bands to the O_4 bands, the potential curves for $^3\Sigma_u^+$ and $^3\Pi_g$ must lie close together with $^3\Pi_g$ below, but there will be no appreciable interaction because of the difference of symmetry.

Transitions of the Type $^1\Sigma^+ - {}^1\Sigma^-$

Finally we mention the possibility of transitions of the type $^1\Sigma^+ - {}^1\Sigma^-$. These could not occur through the medium of spin-orbit interaction because the perturbing energy is necessarily diagonal in Ω and will not connect a $^1\Sigma$ with a $^1\Pi$ term. Rotational distortion would explain such transitions. The derivations up to Eq. (14) are equally valid for a $^1\Sigma^+ - {}^1\Sigma^-$ transition and the result is simply that a single branch having $\Delta K = \Delta J = 0$ will appear with an intensity $C^2K(K+1)(2K+1)$.

I wish to thank Professor J. H. Van Vleck for suggesting this problem and for providing me with the opportunity for many stimulating discussions in the course of the work.

[20] The continuous O_4 bands in the visible have been partially attributed by Ellis and Kneser, Zeits. f. Physik **86**, 583 (1933), to double excitations to the $^1\Delta_g$ and $^1\Sigma_g^+$ states. Although this interpretation agrees with experiment, it is difficult to see how bands that violate the selection rules to the fifth order (second order in the polarization forces which must be of the dipole-quadrupole variety, second order in spin-orbit interaction and, on top of all this, double excitations with small coupling energy) can have any measurable intensity.

[21] H. Salow, Zeits. f. Physik **90**, 11 (1934).

[22] G. Herzberg, Nature **133**, 759 (1934).

The Transparency of the Air Between 1100 and 1300A

THEODORE LYMAN, *Research Laboratory of Physics, Harvard University*

(Received May 28, 1935)

It has long been predicted that the air possesses considerable transparency for light in the region between 1100 and 1300A. This paper deals with a very simple method of demonstrating this transparency by the use of a thermoluminescent screen. Secondary products of the investigation are *first*, a study of the selective sensitivity of the screen just mentioned; *second*, a determination of the nature of the so-called Entladungsstrahlen; and *third*, the description of a simple method of testing the transparency of lithium fluoride crystals.

SOME time ago Hopfield[1] pointed out that the air should possess considerable transparency between 1100 and 1218A even in a column about 4 cm thick. Later Ladenburg, Van Voorhis and Boyce[2] showed that for oxygen the gap should extend between 1100 and 1300. The most obvious method of testing the matter is to close a vacuum grating spectrograph with a window of lithium fluoride and then to photograph the spectrum of a condensed spark placed in air outside the window and a few centimeters from it.

In the actual experiment a piece of lithium fluoride was selected transparent in the extreme ultraviolet to the neighborhood of 1100A. The spectrograph was provided with a concave grating of one meter radius. The distance from the external window to the slit was about one centimeter. Condensed sparks about 3 mm in length, produced by a half kw transformer with a capacity of about 0.002 μf were employed. The potential across the gap, estimated by the sparking distance between spherical electrodes, was found to be of the order of 9000 volts. The spark was placed in air and about one and one-half to two cm from the window. Experiments were made with carbon, copper and silicon electrodes. The times of exposure varied between ten and forty minutes depending upon the width of the slit, etc. etc. Cramer Contrast plates were used treated with Cenco pump oil.

In every case the spectra were nearly independent of the material of the spark terminals. They consisted chiefly of nitrogen and oxygen lines lying between 1144 and 1311A. The wavelengths were determined by comparison with the values given in the Tables of MacInnes and Boyce.[3] Three lines are due to N_I, two to N_{II}, two to N_{III}, four to O_I; and one to hydrogen; one line was not identified. When the distance of the spark to the window was increased to about four and one-half cm, a few of the strongest lines between 1144 and 1185A were still present.

While this method is perfectly straightforward, the necessary apparatus is rather complicated. It is the chief purpose of this article to describe a much easier way of demonstrating the transparency of the air in this particular region. The simplified procedure was suggested by some old experiments of Wiedemann on what he termed "Entladungsstrahlen."[4]

The experiment is conducted as follows: A paste of calcium sulphate and water is thoroughly mixed with a little manganese sulphate. The exact amount of the second ingredient does not seem important; it may vary from one to five percent. The resulting thick broth is evaporated to dryness; the residue is ground to powder, mixed again with a little water and flowed on copper strips of suitable dimensions. The water is allowed to evaporate and the copper with its coating is heated to redness for a few minutes. The whole process is very much the same as that described by Hoffmann[5] many years ago.

The demonstration is carried out by placing one of these coated copper strips beneath a condensed spark of about 3 mm, between "V" shaped electrodes, and at a distance of two or three centimeters from the spark. Upon the surface of calcium sulphate are placed a small piece of fluorite known to be transparent to 1240A and a similar piece of the best lithium fluoride

[1] Hopfield, Phys. Rev. **20**, 587 (1922).
[2] Ladenburg, Van Voorhis and Boyce, Phys. Rev. **40**, 1018 (1932).
[3] MacInnes and Boyce, Palmer Physical Lab., Princeton, N. J., 1930.
[4] Wiedemann, Wied. Ann. **56**, 237 (1895).
[5] Hoffmann, Wied. Ann. **60**, 269 (1897).

known to be transparent to 1100A the spark is then excited for ten or fifteen seconds. The crystals are next removed and the coated copper strip is heated to a maximum temperature of about 180°. If the experiment is carried on in the dark, the calcium sulphate is seen to glow quite strongly before the maximum temperature is reached. The important facts to note are that the part of the surface which had been protected by the fluorite did not glow, while the portion which had been covered by the lithium fluoride was luminescent, though not to so great a degree as those parts of the surface which had been totally unprotected. The conclusion is clear: The observed thermoluminescence is produced by light which has passed several centimeters of air, to which fluorite is opaque and which is able to penetrate lithium fluoride at least to some degree. The luminescence is therefore due to the region of the spectrum between 1100 and 1250A.

It must be noted that if the calcium sulphate surface, part of which is protected by fluorite, be given a very long exposure to a spark; upon heating a faint luminescense appeared under the fluorite. This indicates that while the opacity of the air is considerable near the absorption limit of fluorite yet it shows some transparency, a fact which is in agreement with the results obtained with a spark in air and the vacuum spectrograph.

So much then for this simple demonstration. Next it is of interest to determine the spectral region to which the calcium sulphate-manganese-sulphate screen is sensitive.

To this end a strip of copper, properly coated, was inserted in the vacuum grating spectrograph in the position usually occupied by the photographic plate. The source was a hydrogen discharge tube. A long exposure proved necessary, the time being of the order of seven or eight hours. The spectral region covered by the plate extended from 900 to about 2100A. The calcium sulphate screen was next heated in a dark room and observed visually. The extent of the resulting luminescence indicated that the sensitivity of the thermoluminescent substance began quite abruptly near 1300A and was only limited on the side of the extreme ultraviolet by the end of the plate itself, that is by a point near 900A.

More precise measurements were made by placing an Eastman "33" photographic plate, film side down, upon the calcium sulphate screen after it had been withdrawn from the spectrograph; strips of thin asbestos being used to keep the plate about a millimeter from the screen. On heating, the resulting luminescence was recorded on the photographic plate. The results confirmed the visual observations. The group of hydrogen lines near 1280A was reproduced in luminescence; but the strong hydrogen spectrum from 1340 to 1640A produced no effect whatever.

To test the sensitivity of the substance under examination in the region beyond that which could be conveniently covered with the concave grating instrument, a spectrograph provided with a plane grating used at grazing incidence was employed. The general arrangement being that described by Osgood.[6] The source was a hot spark between a tungsten and a tungsten carbide terminal. The resulting spectrum extended to 140A. The calcium sulphate surface was exposed in this instrument for one and a half hours. On heating, eye observations showed that the sensitivity extended to the end of the spectral range of the instrument, namely to 140A.

We may conclude therefore that the mixture of calcium sulphate with a few percent of manganese sulphate shows thermoluminescence when excited by light in the region between 140A and 1300A. It may be activated by even shorter wavelengths. It is not excited by longer wavelengths, as is demonstrated by the fact that fluorite is opaque to the radiations which produce the effect. The properties of this and of kindred substances are well worth further investigation.

We may now proceed to our second sub-topic. To those who have read the papers of Wiedemann[4] and of Hoffmann[5] already quoted, the bearing of the experiment just described upon the nature of the so-called Entladungsstrahlen will be obvious. These same Entladungsstrahlen have been defined as a radiation proceeding from a spark to which both quartz and fluorite are opaque but which can penetrate several centimeters of air. It now seems clear that a great part of the thermoluminescent action attributed to these rays is produced by the region of the spectrum between 1100 and 1300A to which the air is relatively transparent.

---

[6] Osgood, Rev. Sci. Inst. **5**, 368 (1934).

Miss Laird[7] has pointed out that light of even shorter wavelength may also cause some of the luminescence. From the experiment just described it seems probable that the screen is sensitive in the region of the very shortest wavelength. But what we now know of the absorption of the air makes it improbable that light between 300 and 1100A could reach the thermoluminescent surface, and the character of the spark makes it unlikely that radiations of shorter wavelength were given out in the particular experiments here described. Obviously a very powerful spark might possibly produce soft x-rays which in turn might penetrate several centimeters of air.

Finally, the calcium-sulphate-manganese sulphate screen affords a simple method of testing the relative transparencies of various specimens of lithium fluoride. It is only necessary to place the unknown specimens, together with a piece of known quality, on the surface in question; expose for ten or fifteen seconds to the light from a 3 mm condensed spark at a distance of two or three centimeters, and then heat the screen in a dark room. The degree of transparency of the lithium fluoride can be quite accurately judged by the brightness of the thermoluminescence excited by the light which has passed through the specimen.

I am greatly obliged to Dr. H. M. O'Bryan and to Dr. E. G. Schneider who have made the observations involving the use of the vacuum spectrographs.

[7] Laird, J. Opt. Soc. Am. **13**, 39 (1926).

JULY 15, 1935 PHYSICAL REVIEW VOLUME 48

On the Half-Lives of Potassium, Rubidium, Neodymium and Samarium

ARTHUR RUARK AND KARL H. FUSSLER, *University of North Carolina*

(Received May 4, 1935)

The long apparent half-lives of K, Rb and Nd are in striking disagreement with theory. To relieve this discrepancy, at least in part, the suggestion has often been made that their activities are due to isotopes of small abundance, having half-lives small in comparison with the apparent ones. Using data on the relative abundance of the elements, it is shown that the half-life of the active fraction of K is greater than 10^7 years, and that the active fractions of Rb, Nd and Sm have half-lives greater than 10^8 years. It is pointed out that these activities may be caused by small radioactive fractions of well-known isotopes; RaD and stable Pb(210) constitute a similar case. Data are presented which show that it is possible for the active portions of Nd and Sm to be genetically connected.

1. INTRODUCTION

THE apparent decay constant, λ', of a radioactive element composed of several isotopes is the fraction of its atoms which disintegrates per unit of time. If only one isotope, whose atoms constitute a fraction A of all the atoms in the preparation, is active, then the actual decay constant is

$$\lambda=\lambda'/A, \tag{1}$$

and the actual half-life is

$$T=AT', \tag{2}$$

where T' is the apparent half-life. The apparent half-lives of K, Rb, Nd and Sm are of the order of 10^{12} to 10^{13} years and the question arises whether their activities are due to isotopes which have been detected with the mass spectrograph, or to undetected isotopes for which A is very small. The case of Sm has been discussed by Hevesy, Pahl and Hosemann.[1] Its apparent half-life agrees fairly well with the value computed from the range of the alpha-particles. Therefore it is probable that the alpha-particles are emitted by one of the known isotopes. It is also probable that there is only one active isotope, for Bearden and Kanne[2] have shown that all the alpha-particles have the same range, within 2 mm. On the other hand, the situation in regard to K, Rb and Nd is unsatisfactory. The theories of Beck and Sitte and of Fermi[3] yield half-lives much

[1] Hevesey, Pahl and Hosemann, Zeits. f. Physik **83**, 43 (1934).

[2] Bearden and Kanne, Phys. Rev. **47**, 639 (1935). See also Ortner and Schintlmeister, Zeits. f. Physik **90**, 698 (1934).

[3] Beck and Sitte, Zeits. f. Physik **86**, 105 (1933); Fermi, Zeits. f. Physik **88**, 161 (1934).

TABLE I.

ELEMENT	APPARENT HALF-LIFE, (YR.)	COMPUTED HALF-LIFE, (YR.)
K	1.4×10^{13}	0.01*
Rb	4.3×10^{11}	0.03
Nd	0.7 to 1.4×10^{12}	76

lower than the apparent ones. These theories are speculative and incomplete but since they yield a qualitative account of the main features of beta-ray emission by heavy radioactive elements, we should seriously consider their predictions in regard to K, Rb and Nd. We have computed the half-lives of these elements from Fermi's theory, the results being shown in Table I. Fermi's result contains an adjustable constant g; for this we employed a value found suitable for the heavy radioactive elements. In the present state of the theory it is not possible to say whether this is justifiable. Nevertheless, the data in Table I suggest that the activities of these elements may arise from isotopes which cannot be detected by the mass spectrograph. Fig. 1 will be helpful in discussing this matter. For Rb and Nd, there is no evidence as to the active isotopes but in the case of K, the fractionation experiments of Hevesy and his colleagues[4] showed that the activity must reside in the known isotope 41, or in hitherto unknown isotopes, 40 or 42. Recently Hevesy[5] has shown that K^{42} can be produced by bombarding scandium with neutrons, and that its half-life is about 16 hours. Therefore he believes that the naturally active isotope is either 40 or 41. He also states, without giving details, that the life of the active isotope is greater than 10^8 years.

Previous writers have not considered the interesting possibility that the beta-ray emission of these elements may be due to small active fractions of known isotopes. There are known instances of such behavior.[6] RaD and the stable Pb(210) found by Aston in common lead, are both isobaric and isotopic. Also, there is strong evidence that the isotopic beta-rayers UX_1 and

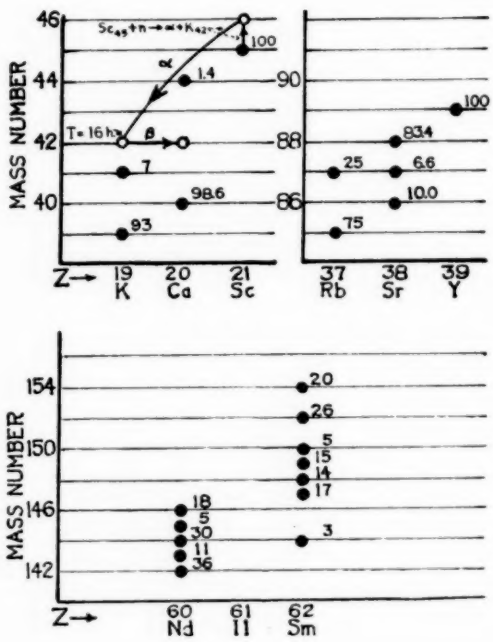

FIG. 1.

UZ have the same atomic weight, although they are quite different in radioactive behavior. It may be that UX_1 is merely UZ in an excited state, or *vice versa*.

2. MINIMUM HALF-LIVES OF THE ACTIVE ISOTOPES OF K, RB, ND AND SM

We shall show that *while undetected isotopes or small active fractions of well-known isotopes may be responsible for the activities of K, Rb, Nd, they cannot have half-lives less than 10^7, 10^8 and 10^8 years, respectively.* Similarly, the active isotope of Sm has a half-life superior to 10^8 years. Consider a mineral containing a large percentage of the radioactive element in question, and suppose that this element has only one active isotope, or alternatively, that only a part of the atoms of one isotope are active. In a sample of this mineral, let there be N atoms of the element, of which AN are active, and let the age of the mineral be t years. Neglecting intermediate products for the moment, the number of atoms of the end product which have accumulated during the life of the mineral is

$$n = AN(e^{\lambda t}-1). \qquad (3)$$

Some of the end-product atoms may have been present originally, so N_e, the total number of

[4] Hevesy and Logstrup, Zeits. f. anorg. Chemie **171**, 1 (1929); Hevesy, Seith and Pahl, Zeits. f. physik. Chemie, Bodenstein-Festband 309 (1931); Biltz and Ziegert, Physik. Zeits. **29**, 197 (1928).

[5] Hevesy, Nature **135**, 86 (1935).

[6] Ruark, Science Leaflet **7**, 16 (1934); Gamow, Nature **133**, 833 (1934).

TABLE II. *Calculated minimum half-lives for the active isotope.*

MATERIAL	MICROCLINE[1]	FELDSPAR[2]	PEGMATITE[2]
Percent Ca:	0.04	<0.3 (CaO)	<0.3 (CaO)
Percent K:	11	About 9 (K_2O)	About 9 (K_2O)
Probable age, (yr.)	$2\cdot10^8$	10^9	$6\cdot10^8$
10^9A	1	5	3
T, (yr.)	$1.7\cdot10^7$	$8\cdot10^7$	$4.5\cdot10^7$

[1] Frost and Frost, Nature **125**, 48 (1930).
[2] Kendall, Smith and Tait, Nature **131**, 688 (1933).

TABLE III. *Calculated minimum half-lives for potassium, rubidium, neodymium and samarium.*

HYPOTHETICAL TRANSITION	T' (YR.)	N_e/N	10^9A	T (YR.)
$K^{40}Ca^{40}$	$1.4\cdot10^{13}$	1.4	7	$1\cdot10^8$
$Rb^{88}Sr^{88}$	$4.3\cdot10^{11}$	12	270	$1\cdot10^8$
$Nd^{146}Il^{146}Sm^{146}Nd^{142}$	$2.8\cdot10^{12}$	0.37	100	$1.3\cdot10^9$
$Sm^{146}Nd^{142}Il^{142}Sm^{102}$	$1.3\cdot10^{12}$	0.78	100	$1.3\cdot10^8$

atoms of this substance now present, is greater than, or equal to, n:

$$N_e/N \geqq A(e^{\lambda' t/A}-1). \qquad (4)$$

Use of the equality sign gives an upper limit for the quantity $A(e^{\lambda' t/A}-1)$, and this yields the minimum possible value of A. Knowing A, we can obtain from (2) a lower limit for the half-life of the active isotope.

Computation for potassium

Attempts have been made to show that potassium produces Ca^{41}, by studying the atomic weight of calcium from old potassium minerals. However, Aston[7] has recently examined several samples of such calcium and finds that it does not contain as much as 0.1 percent of the isotope 41, although several times that quantity would be expected if K^{41} were the active potassium isotope. Aston concluded that two successive beta-ray disintegrations may be involved, the end product being scandium. Klemperer's experiments[8] make it more probable that the activity may be due to a hypothetical isotope K^{40}, but do not show whether the end product is calcium or scandium. Whatever the final solution may be, we can get a *minimum* half-life for the active isotope by applying Eq. (4) to the disintegration $K^{40}Ca^{40}$, since Ca^{40} is the most abundant isotope of calcium. Table II shows the necessary data for three potassium-bearing rocks, and the results.

Computation for Rb, Nd and Sm

For these elements a modified procedure is necessary. In the absence of data on minerals, we consider a one-gram sample of material having the average composition of the earth's crust, containing AN atoms of the active isotope and N_e atoms of the end product. Then relation (4) will hold if we take for t the age of the crust. At first sight it appears that our ignorance of the end products of Rb, Nd and Sm makes it impossible to use Eq. (4). However, detailed consideration shows that the minimum value of T is obtained by using the highest possible value of N_e/N and the smallest possible value of t. Accordingly, we shall apply this equation to *hypothetical* disintegrations which lead to an end product for which N_e is as large as possible. For example, we shall consider a disintegration $RB^{88}Sr^{88}$, *not* because we have any reason to believe that it is the one occurring, but simply because Sr^{88} is the most abundant isotope of Sr. If it is discovered later that the actual disintegration sequence is Rb, Sr, Y, our conclusion as to the minimum value of T for rubidium will not be disturbed because Sr^{88} is more abundant in the earth's crust than yttrium. We use the value $t=1.8\times10^9$ years, this being the smallest value for the age of the earth's crust consistent with the known ages of radioactive minerals. Table III gives the results. A figure for potassium is included, supporting the results already given. The values of N_e/N in Table III are based on the relative abundances of the elements in igneous rocks, as given by Hevesy,[9] and on the relative abundances of the isotopes given in Aston's *Mass Spectra and Isotopes*. The apparent half-lives of K and Rb are those of Mühlhoff. Libby[10] states that the half-life of neodymium is between 1.46×10^{12} years and half that value. He favors the smaller value, but we use a decay constant calculated from the higher one, because this gives a minimum half-life for the active isotope. As for samarium, four values[11] are available: Libby, 6.3×10^{11} yr.; Lyford 7.1×10^{11} yr.;

[7] Aston, Nature **133**, 869 (1934).
[8] Klemperer, Proc. Roy. Soc. **A148**, 638 (1935).
[9] Hevesy, *Chemical Analysis by X-Rays and its Applications*, McGraw-Hill, p. 277.
[10] Libby, Phys. Rev. **46**, 196 (1934).
[11] Libby, reference 10; Lyford, Thesis, The Johns Hopkins University, 1934; Hevesy, Pahl and Hosemann, reference 1; Hertzfinkiel and Wroncberg, Comptes rendus, **199**, 133 (1934).

Hevesy, Pahl and Hosemann, 1.2×10^{12} yr.; Hertzfinkiel and Wroncberg, 1.3×10^{12} yr. Without attempting to judge these values, we take the highest, for the same reason as in the case of neodymium. In calculating a minimum half-life for Nd, several cases have been considered:

Case I. If element 61 is the end product we get a T value of about 4×10^{8} years by making use of the fact[12] that in rare earth minerals the ratio of element 61 to neodymium is certainly less than 1/180. To get a lower T value we consider two other disintegration-sequences:

Case II. Nd to element 61 to a stable isotope of Sm.

Case III. Nd to element 61 to Sm to a stable isotope of Nd. In cases II and III it seems fair to assume that element 61 is in equilibrium with the active isotope of Nd. If so, half the beta-particles attributed to Nd really come from element 61 and the apparent decay constant of Nd must be divided by 2. This has been done in Table III, but if it were not done, the minimum value of T would still be of the order of 10^{8} years. Detailed study shows that whatever the half-lives of the intermediate products may be, we arrive at a minimum value of T if we use Eq. (4), replacing N_e by the *sum* of the numbers of atoms of the intermediate products and the end-product. Under Case III, the sequence Nd^{146}, Il^{146}, Sm^{146}, Nd^{142} is chosen because it makes this sum a maximum, and a similar consideration governs the choice of the hypothetical disintegration sequence in Table III, beginning with samarium.

The T values in Tables II and III constitute the proof of the assertions at the beginning of this section.

3. A Possible Genetic Relation Between the Active Isotopes of Nd and Sm

It is possible that the active portions of neodymium and samarium are members of short radioactive series, following either one of the schemes portrayed in Fig. 2. Evidence on this point may be obtained by finding out whether these elements are in radioactive equilibrium. Of course, if abundant isotopes of *both* elements

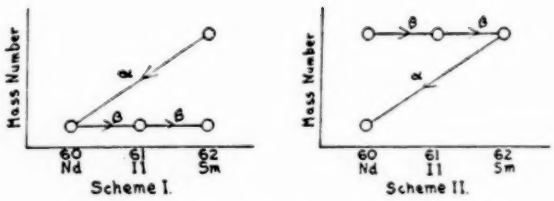

FIG. 2.

are active, equilibrium could not have been established in even the oldest rare-earth minerals. However, if the active fraction of neodymium in Scheme I, or the active fraction of samarium in Scheme II, has a life of the order 10^{8} years, a state approximating that of equilibrium would now exist in old minerals. The equation expressing such an equilibrium is $\lambda_{Nd}A_{Nd}N_{Nd}=\lambda_{Sm}A_{Sm}N_{Sm}$, but this may be written

$$\lambda_{Nd}'N_{Nd}=\lambda_{Sm}'N_{Sm} \qquad (5)$$

which means that the elements themselves are *apparently* in equilibrium.

To test this relation we require data on the apparent half-lives of Nd and Sm extracted from a given mineral, preferably of known age. An easier procedure consists in determining the activities of samples of these elements from sources of different geologic age. Libby found the same activity for two neodymium samples obtained from James and Hopkins, respectively, and Hevesy, Pahl and Hosemann showed that samarium preparations from four different sources of supply had the same activity, but nothing is said about the minerals from which these salts were prepared. In the absence of data suitable for a decisive test, the following points are worth attention. Probably most of the samples of Nd and Sm which have been used in studying their radioactive properties have come from monazite, a very common commercial source. It is known from the work of Goldschmidt and Thomassen[12] that in monazites the ratio Nd/Sm is about 3, and that the average value of this ratio for a number of rare earth minerals is about 2.1. On the other hand the ratio of the apparent half-lives ranges from 0.5 to 2.3, the latter value corresponding to Libby's determinations namely, 1.46×10^{12} yr. for Nd and 6.3×10^{11} yr. for Sm. Thus the abundance ratio and the ratio of apparent half-lives are in rough agreement.

[12] Goldschmidt and Thomassen, Kristiania Videnskapsselskapet Skrifter, I, Klasse, No. 5 (1924).

Calculation of the Elastic Scattering of Electrons in Krypton

A. L. HUGHES* AND S. BILINSKY, *Wayman Crow Laboratory of Physics, Washington University, St. Louis, Missouri*

(Received May 11, 1935)

In order to compute the elastic scattering coefficients for electrons colliding with atoms it is necessary to evaluate the wave-mechanics expression

$$I(\theta)=(1/4k^2)\left|\sum_{n=0}^{\infty}(2n+1)(e^{2i\delta_n}-1)P_n(\cos\theta)\right|^2.$$

Improvements in the method of summing the series and in evaluating the phases (particularly δ_0) have been effected. The computed scattering coefficients are in satisfactory agreement with the experimental values for electrons of energy 250, 350 and 510 volts; the agreement is less satisfactory for electrons of energy 780 and 950 volts. In the range over which satisfactory agreement is obtained, the Hartree field gave somewhat better results than the Fermi-Thomas field.

DURING the past few years, many studies of the scattering of electrons by gas atoms have been made, from both the experimental and theoretical standpoints. The agreement between the experimental results obtained by different investigators is, in many cases at least, highly satisfactory and justifies the confidence that the results are reliable and substantially free from experimental error. They may therefore be used with some assurance to test available theories. Wave mechanics leads to the following expression for the elastic scattering coefficient as a function of θ, the angle of scattering:[1]

$$I(\theta)=\frac{1}{4k^2}\left|\sum_{n=0}^{\infty}(2n+1)(e^{2i\delta_n}-1)P_n(\cos\theta)\right|^2, \quad (1)$$

where $P_n(\cos\theta)$ is the n-th Legendre polynomial, $k=2\pi/\lambda=(8\pi^2mE/h)^{1/2}$ in which λ and E are the wavelength and energy of the electron, and δ_n is a quantity called a phase of the n-th order (to be defined later). This expression is "exact" in the sense that no appoximations are made in deriving it from the initial assumptions. However, when we try to evaluate it numerically for specific electron speeds, angles and atoms we run into serious difficulties. The calculation of the phases to be used is a major problem. By direct numerical integration of the equation defining the phases (Eq. (8)), Holtzmark[2] has computed a few phases corresponding to the scattering of electrons of speeds 0, 13.5 and 54 volts by krypton atoms. This direct method of computing the exact values of the phases is excessively laborious and consequently when one needs many phases (of different orders and for different electron speeds), it is imperative to find a method which will give approximate values for the phases. Arnot and Baines,[3] using an approximation based on the work of Jeffreys have computed δ_0, δ_1, $\cdots$ δ_6 for 121-volt electrons scattered by krypton atoms.

Recently as part of the general program of work carried out in this laboratory on electron scattering, Mr. G. M. Webb[4] has obtained values for the elastic electron scattering coefficients for krypton which are believed to be unusually dependable. Over the limited range for which calculated phases were available, his results agreed satisfactorily with formula (1). However, in attempting to secure a more accurate comparison between theory and experiment, and over a wider range than heretofore, it became evident that improvements in the method of evaluating formula (1) by approximations were necessary. These improvements were worked out by one of us (S.B.). The result of these modifications is an extension of the agreement between experiment and theory to higher electron speeds.

In calculating $I(\theta)$ from (1), one encounters three practical difficulties: (a) the summation of the infinite series (1), (b) the determination of the field which best represents the atom, and (c) the evaluation of the phases δ_n.

* The senior author was aided in part by a grant from the Rockefeller Foundation to Washington University for research in science.

[1] N. F. Mott and H. S. W. Massey, *The Theory of Atomic Collisions*, (Oxford University Press, 1933), p. 24.

[2] J. Holtzmark, Zeits. f. Physik **66**, 49 (1930).

[3] F. L. Arnot and G. O. Baines, Proc. Roy. Soc. **A146**. 651 (1934).

[4] G. M. Webb, Phys. Rev. **47**, 379 (1935).

A. The Evaluation of Convergent Infinite Series with Oscillating Terms

We begin with a discussion of trigonometric series[5] of the form

$$\sum_0^\infty a_n(\theta)\cos n\theta. \tag{2}$$

The results obtained will apply by a natural extension to the complete trigonometric series involving also sine terms but for convenience we omit such terms here.

As usual we separate the series into two parts, the first of which contributes most of the value of the sum, so that the second (the "remainder") is either negligible or may be well approximated by a simple expression. In order to determine the best point of separation, we begin by finding an approximate remainder for an undetermined point of separation $n=L$, and then we shall choose L so that the value of the remainder is a minimum.

For this purpose we replace the summation of the discrete terms constituting the remainder by an integral

$$\int_L^\infty \varphi(x,\theta)dx,$$

where $\varphi(x)$ is such that $\varphi(n+\frac{1}{2},\theta)=a_n(\theta)\cos n\theta$. We shall now make several assumptions concerning the nature of $a_n(\theta)$. This is to be a function of n and θ such that it may be replaced by a continuous function $a(n,\theta)$ possessing any number of derivatives with respect to n, and, writing x in place of n, such that

$$(1/\theta^{r+1})(d^r/dx^r)a(x,\theta)=O(1/x^{r+\alpha}), \tag{3}$$

$$\alpha>0, \quad |\theta|\geq\rho>0$$

where the equation is to hold uniformly in θ, and for all values of r corresponding to the derivatives of $a(x,\theta)$ that exist, and for $r=0$. $O(\ )$ means, as usual, "of the order of." These conditions will insure the validity of the following results.

We now rewrite the integral as

$$\int_L^\infty a(x-\tfrac{1}{2},\theta)\cos(x-\tfrac{1}{2})\theta dx$$

and integrate successively by parts, obtaining

$$[a(x-\tfrac{1}{2},\theta)\sin(x-\tfrac{1}{2})\theta/\theta + a'(x-\tfrac{1}{2},\theta)\cos(x-\tfrac{1}{2})\theta/\theta^2-\cdots]_L^\infty.$$

All the terms vanish at the upper limit because of (3). Let us now choose L so that $(L-\frac{1}{2})\theta=m\pi$ where m is a positive integer. Then the terms which remain are

$$(-)^{m+1}a'(L-\tfrac{1}{2},\theta)/\theta^2 + (-)^{m+2}a'''(L-\tfrac{1}{2},\theta)/\theta^4+\cdots. \tag{4}$$

This way of choosing L imposes on the remainder the condition that the term of lowest order, i.e., the largest term asymptotically, vanishes. We are now able to write

$$\sum_0^\infty a_n(\theta)\cos n\theta \backsimeq \sum_0^{l_0-1} a_n(\theta)\cos n\theta + (L-l_0)a_{l_0}(\theta)\cos l_0\theta, \tag{5}$$

where l_0 is the largest integer less than L. It is easily seen that the last term is a fractional part of the l_0-th term in the given series. The remainder, which has a minimum value as a result of the way in which the series was divided, is omitted because it is not found to be of sufficient

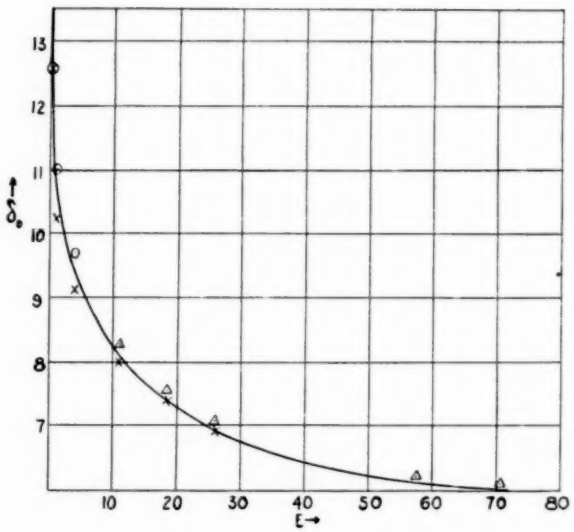

Fig. 1. Values of δ_0. *Continuous line*—Jeffreys' approximation with Hartree polarized field; *Crosses*—The same with Hartree unpolarized field; *Circles*—Holtzmark's exact values; *Triangles*—Including second approximation given by Eq. (15).

[5] Trigonometric series are generally defined with constant coefficients. We retain the name, although considering the coefficients to be functions of the argument.

TABLE I. $(1-2r\cos\theta+r^2)^{-\frac{1}{2}}=\Sigma r^n P_n(\cos\theta)$. $r(=1-10^{-10})<1$.

θ	Exact value $=(2(1-\cos\theta))^{-\frac{1}{2}}$	Σ at L	Σ at l_0	Σ at l_0+1	L
30°	1.932	2.037	2.242	1.832	7.50
60°	1.000	1.004	1.209	.940	9.76
90°	.707	.699	.562	.836	8.50
120°	.577	.561	.757	.534	7.88
150°	.518	.515	.306	.716	7.59

usefulness. (It should be noted, however, that the approximation (5) may not be entirely trustworthy for small values of θ, for then the terms in (4) may not be small enough to be neglected.)[6]

The method outlined above is applicable to any convergent infinite series whose general term is asymptotic to an expression of the form $a_n(\theta)\cos n\theta$ already discussed. In particular is this true of series of Bessel's and Legendre functions. In the latter case, we have

$$P_n(\cos\theta)\sim(2/n\pi\sin\theta)^{\frac{1}{2}}\cos[(n+\tfrac{1}{2})\theta-\pi/4]$$

and consequently for L we have[7]

$$L=(m+\tfrac{1}{4})\pi/\theta.$$

As an example of the usefulness of the method we give in Table I the exact values of the infinite sum $\sum_0^\infty r^n P_n(\cos\theta)$ (with $r=(1-10^{-10})$ to ensure convergence) for several values of θ, together with the values obtained by cutting off the series at L, at l_0 (the greatest integer less than L), and at l_0+1. In most cases the value obtained at L is better than the value obtained by cutting off the series even several terms later.

B. The Atomic Field

The calculation of the phases requires a knowledge of $V(r)$ the potential energy of the electron when in the field of the atom. Holtzmark[8] has computed the Hartree self-consistent field for krypton. The method of calculating the δ_n's corresponding to a given field is indicated in the next two sections. Henneberg[9] has given curves for δ_n's for mercury atoms, using the Fermi-Thomas field, together with a transformation formula whereby δ_n can be calculated for any other element. In this way δ_n's for krypton have been calculated. Our computed scattering curves, shown in Fig. 2, are given for both the Hartree field and the Fermi-Thomas field.

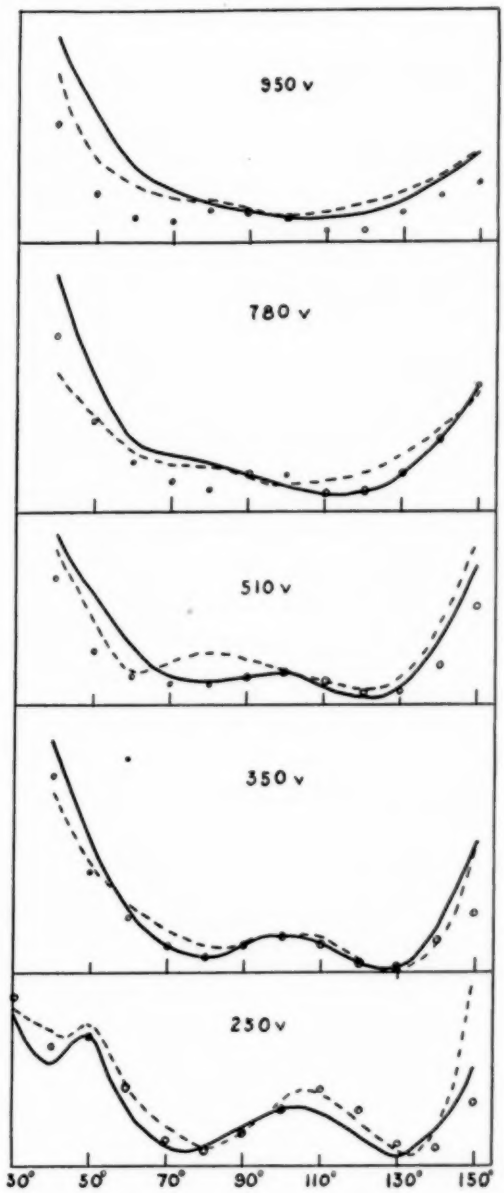

FIG. 2. Theoretical and experimental scattering curves. *Continuous line*—theoretical curve with Hartree field; *Dotted line*—theoretical curve with Fermi-Thomas field; *Circles*—Webb's experimental values.

An important assumption implicit in these calculations is that the velocity of the incident electrons is large enough to insure that the effects

[6] The actual lower limit depends upon the rapidity with which the derivatives of $a(x,\theta)$ diminish.
[7] The same expression is given by Henneberg.
[8] J. Holtzmark, Zeits. f. Physik **66**, 49 (1930).
[9] W. Henneberg, Zeits. f. Physik **83**, 555 (1933).

of polarization and exchange can be neglected. However, although we have no *a priori* means of determining at what velocities these effects are negligible, we have good reasons for supposing that they decrease in magnitude with increasing speeds, and conclude *a posteriori* from the fact that a good agreement is obtained at 350 and 250 volts that these effects have already become insignificant at these speeds. At speeds of 100 volts and below, Webb[4] obtained excellent agreement when he used Hartree's field corrected by Holtzmark for polarization. However, it should be stated that the more accurate method now available for computing the scattering does not give quite as good an agreement as he obtained for his 100-volt curve.

C. The Phase Constants, δ_n

The wave equation which must be solved to compute the scattering coefficients is

$$\nabla^2\psi+[k^2-8\pi^2 m V(r)/h^2]\psi=0. \tag{6}$$

The solution of this may be written

$$\psi=\sum_{n=0}^{\infty} A_n P_n(\cos\theta)(1/r)y(r), \tag{7}$$

when $y(r)$ is the solution of

$$d^2y/dr^2+\varphi^2(r)y=0, \tag{8}$$

in which

$$\varphi^2(r)=k^2-8\pi^2 m V(r)/h^2-n(n+1)/r^2.$$

If $V(r)$ is zero, a solution of (8) which is zero at the origin is the function $r^{1/2}J_{n+\frac{1}{2}}(kr)$, where $J_{n+\frac{1}{2}}(kr)$ is a Bessel function. Its asymptotic value is $(2/\pi k)^{\frac{1}{2}}\sin(kr-n\pi/2)$. If $V(r)$ is *not* zero, the asymptotic solution of (8) is presumably of the form $C\sin(kr-n\pi/2+\delta_n)$. (For this to be so, the field must fall to zero faster than the Coulomb field.)[10] This solution defines the phase constant δ_n: it is the phase difference between the asymptotic solutions of (8) when $V(r)$ is finite and when it is zero.

The phase δ_n may, of course, be obtained by direct numerical integration of (8). This has been done by Holtzmark for a few selected cases, but the work is so laborious that it is imperative to seek an approximate expression for a phase if we need a considerable number of phases. Contributions to the solution of this problem have been made by Jeffreys,[11] Kramers[12] and others.[13] These solutions have been obtained on the assumption that the roots of $\varphi^2(r)$ are separated by a sufficient distance and that in an appreciable neighborhood of each root $\varphi^2(r)$ behaves like r. Then, for $\varphi^2(r)>0$, the asymptotic solution to the right of r_0 is

$$y(r)=\varphi^{-\frac{1}{2}}(r)\cos(\xi+\pi/4),$$

where $\xi=\int_{r_0}^{r}\varphi(r)dr$, and r_0 is the root. The phase δ_n is given by the expression

$$\delta_n=\int_{r_0}^{r}\varphi(r)dr-\int_{r_1}^{r}\varphi_1(r)dr, \tag{9}$$

where $\varphi_1(r)=k^2-n(n+1)/r^2$, and r_1 is the positive root of $\varphi_1(r)$.

The assumptions made with respect to $\varphi(r)$ are probably valid in an interval at some distance from the nucleus. Close to the nucleus, however, it is more reasonable to suppose that $V(r)$ may behave like a Coulomb potential, so that when the root r_0 falls close to origin, as is generally true when $n=1$, 2 or 3, it is better to replace $V(r)$ in (8) by V_0-Z/r where V_0 is a constant and Z the atomic number. Kramers[12] has shown that this changes (9) by replacing $n(n+1)$ with $(n+\frac{1}{2})^2$. Since the difference between Kramers' method and Jeffreys' method is negligible for phases of higher order, we have used the former throughout our calculations, except for δ_0 which is discussed below.

At a considerable distance from the origin, however, it cannot be supposed that the region in which $\varphi^2(r)$ may be represented by r overlaps the region in which an asymptotic representation for the solution is valid. In fact, it has been pointed out by several writers that Jeffreys' approximation is unsatisfactory when $\delta_n<0.5$, and this occurs when the root of $\varphi^2(r)$ is far out ($r>2$ atomic units). For values of $\delta_n<0.5$, Born's approximation is more trustworthy; but we have not found it necessary to make use of this fact.

[10] Reference 1, p. 23.

[11] H. Jeffreys, Proc. London Math. Soc. (2) **23**, 428 (1923).

[12] H. A. Kramers, Zeits. f. Physik **39**, 828 (1926).

[13] A good discussion of the general problem is given by R. E. Langer, Bull. Am. Math. Soc. (8), 40 (1934).

Also for small values of δ_n, a fair estimate may be very simply obtained from a knowledge of the positive roots of $\varphi^2(r)$ and of $k^2-n(n+1)/r^2$. If the difference between the two roots is α, then $\delta_n \sim k\alpha$. The reason for this results from a consideration of the differential equations involved.

One cannot justify the extension of the methods of Jeffreys and Kramers to the case for $n=0$, because $\varphi^2(r)$ has no real root, since $V(r)$ is positive. In fact, it leads to incorrect results. In the following section we investigate the possibility of obtaining better results.

D. The Special Case of δ_0

We consider the function $u(x)$, where

$$u(x)=\varphi^{-\frac{1}{2}}(x)\sin\xi,$$

$\varphi(x)$ being the function appearing in (8) with $n=0$, and $d\xi/dx=\varphi(x)$. By differentiating twice it is found that $u(x)$ satisfies the differential equation

$$u''+(\varphi^2-\tfrac{3}{4}\varphi'^2/\varphi^2+\tfrac{1}{2}\varphi''/\varphi)u=0.$$

Now we may write (8) in the form

$$y''+(\varphi^2-\tfrac{3}{4}\varphi'^2/\varphi^2+\tfrac{1}{2}\varphi''/\varphi)y=\Phi y, \quad (10)$$

where

$$\Phi=\tfrac{1}{2}\varphi''/\varphi-\tfrac{3}{4}\varphi'^2/\varphi^2.$$

An integral of (10) which vanishes at the origin is given formally by the solution of the integral equation

$$y(r)=C\varphi^{-\frac{1}{2}}(r)\sin\xi_r+\int_0^r K(r,t)\Phi(t)y(t)dt, \quad (11)$$

where

(1) $\quad \xi_r=\int_0^r\varphi(t)dt,$

(2) $\quad K(r,t)=\varphi^{-\frac{1}{2}}(r)\varphi^{-\frac{1}{2}}(t)\sin(\xi_r-\xi_t).$

Assuming that the minimum of $\varphi^2(r)$ on the positive axis is sufficiently large, except perhaps at the origin, or where $\Phi(t)$ is very small,[14] an approximate solution of (11) is given by the equation

$$y(r)=C\varphi^{-\frac{1}{2}}(r)\{\sin\xi_r+\int_0^r[\sin(\xi_r-\xi_t)\sin\xi_t\Phi(t)/\varphi(t)]dt\}. \quad (12)$$

[14] This is quite generally satisfied.

The constant C, whose value is immaterial in this discussion, may be determined by a condition on the boundary.

The expression in braces in Eq. (12) may be written thus:

$$[1+g(r)]\sin\xi_r-f(r)\cos\xi_r$$

or

$$\sin[\xi_r-\epsilon(r)], \quad (13)$$

where

$$\epsilon(r)=\tan^{-1}[f(r)/(1+g(r))]$$

and

$$f(r)=\int_0^r[\Phi(t)\sin^2\xi_t/\varphi(t)]dt,$$

$$g(r)=\tfrac{1}{2}\int_0^r[\Phi(t)\sin 2\xi_t/\varphi(t)]dt.$$

An exact solution of (8) for $\varphi^2(r)=k^2$ is $\sin kr$. The difference in phase between this solution and the one already found (13) is obviously given by

$$\delta_0=\xi_r-kr-\epsilon(r)$$

for r large. In proceeding to the limit we find, where now $\varphi^2(r)=E+V(r)$, having written E for k^2,

$$\delta_0=\int_0^\infty((E+V(r))^{\frac{1}{2}}-E^{\frac{1}{2}})dr-\epsilon(\infty). \quad (14)$$

The integral in this last expression is that which is given as Jeffreys' approximation. We should expect more accurate results on subtracting the term $\epsilon(\infty)$. However, the evaluation of this term presents great difficulties. On the other hand, it is possible to show that for large values of E (the electron energy in atomic units), at which the solution (12) is also quite accurate, $\epsilon(\infty)$ has the form $\tan^{-1}[a\cdot E^{\frac{1}{2}}/(E+b)]$. Now if a and b are chosen so that $a=-0.67$ and $b=0.83$, we obtain the exact phases as calculated by Holtzmark for krypton at $E=1$ and $E=4$, which he got by numerical integration of (8). As a second approximation to δ_0, we therefore write

$$\delta_0=\int_0^\infty((E+V(r))^{\frac{1}{2}}-E^{\frac{1}{2}})dr+\tan^{-1}[0.67E^{\frac{1}{2}}/(E+0.83)]. \quad (15)$$

The approximation is to be applied only for values of $E>1$.

In Table II we give the values of the phase δ_0, (1) calculated by Jeffreys' approximation using the Hartree unpolarized field, (2) the same, but using the Hartree polarized field, (3) the latter after adding the correction developed in Eq. (15),

TABLE II. *Values of* δ_0.

E	V	1	2	3	4
ATOMIC UNITS	VOLTS	JEFFREYS' APPROX.; HARTREE UNPOLARIZED FIELD	J'S APPROX.; HARTREE POLARIZED FIELD	(2) PLUS CORRECTION	EXACT VALUES. HARTREE POLARIZED FIELD. (HOLTZMARK)
0	0	12.58	13.48	—	12.568
1	13.5	10.23	10.645	(10.996)	10.996
4	54	9.12	9.43	(9.696)	9.696
11	150	8.00	8.10	8.28	
18.45	250	7.41	7.41	7.56	
25.83	350	6.94	6.94	7.07	
57.56	780	6.13	6.13	6.22	
70.5	950	6.05	6.05	6.13	

and (4) the exact values as calculated by Holtzmark.

The results are plotted in Fig. 1. It may be noticed that at about $E=20$ (270 volts) and above, it is immaterial whether we use the polarized or the unpolarized field.[15]

The failure of Kramers' approximation for δ_0 at $E=4$ is even more appreciable than Jeffreys' for the exact value is 9.70, Jeffreys' approximation gives 9.43, while Kramers' gives 7.31.

The values that we have found for δ_0 with a polarized field and Jeffreys' approximation are different from those published by Arnot and Baines.[3] We are inclined to think that there is an error in their computation.

E. THEORETICAL SCATTERING CURVES

In calculating the curves shown in Fig. 2, Kramers' approximation was used for all the phases, except δ_0, for which we used Jeffreys' approximation together with the correction determined in the previous section (Eq. 15). The number of terms was, of course, determined by the value of L, which was chosen to be as close to 7 as possible, for ease in calculation and to obtain accurate results.

It is evident that the agreement between the experimental values and the calculated values is better for electrons of 250, 350, and 510 volts energy than for the faster electrons. As for the choice between the Hartree unpolarized field and the Fermi-Thomas field, the results are definitely in favor of the former for 350- and 510-volt electrons and possibly also for the 250-volt electrons. At 780 volts, and still more at 950 volts, however, the theoretical curves fail to account for the well-marked maxima in the experimental curve in the vicinity of 90°. The lack of agreement at the higher voltages calls for comment. In general the approximations used for the δ's become better with increase in electron energy. This is also true, to a certain extent, for the summation method for the infinite series (section A). The extent to which it is not true may account for the lack of agreement between the experimental and theoretical scattering curves in the following way. We may notice, in recalling the summation method that we first replace a sequence of discrete terms by a continuous curve, and then obtain an expression for the area under the latter. Now it is this last approximation which becomes better the more slowly the infinite series converges, a characteristic which is the more marked the higher the electron energy. But, on the other hand, since each single term involves an approximation, the error in the sum will be cumulative with the number of effective terms in the series, and since this number increases with the electron energy, this may account for the lack of agreement above 500 volts. At present it appears that, in order to get better agreement for the scattering of electrons of high energy, it is necessary to determine each δ to a higher degree of accuracy than heretofore and to use many more terms in evaluating the expression (1) for $I(\theta)$. This would appear to be necessary before concluding that the theory underlying (1) is inadequate to explain the scattering of faster electrons.

[15] It should be stated that the disappearance of the effect of polarization here is not the same kind of thing as that referred to in section B of this paper. There it was assumed that the scattering atoms were not appreciably polarized by very fast electrons, whereas in the calculation of δ_0, even if it is assumed that the polarization is the same for 1000-volt electrons as for 10-volt electrons, its effect on the value of δ_0 in either case becomes zero. This is not true for δ's of higher order.

Exact Solutions of the Schrödinger Equation

MILLARD F. MANNING, *Department of Physics, Massachusetts Institute of Technology*

(Received February 28, 1935)

In classical mechanics the problem of determining the forms of potential function which permit solution in terms of known functions received considerable attention. The present paper is a partial study of the same problem in quantum mechanics. A method is given for determining the forms of potential function which permit an exact solution of the one-dimensional Schrödinger equation in terms of series whose coefficients are related by either two or three term recursion formulas. The more interesting expressions for the potential energy have been tabulated. A correspondence is found between these solutions and the solutions of the corresponding Hamilton-Jacobi equation. It is shown that whenever the Hamilton-Jacobi equation is soluble in terms of circular or exponential functions, the corresponding Schrödinger equation is soluble in terms of a series whose coefficients are related by a two-term recursion formula. Whenever the Hamilton-Jacobi equation is soluble in terms of elliptic functions, the corresponding Schrödinger equation is soluble in terms of a series whose coefficients are related by a three-term recursion formula. For the first case the quantized values of the energy are found by restricting the series to a polynomial and in the second by finding the roots of a continued fraction. A brief discussion of the technique of solution of continued fractions is given.

EXACT SOLUTIONS IN CLASSICAL MECHANICS

IN either classical mechanics or in the Bohr-Sommerfeld formulation of quantum mechanics, the solution of a problem involves evaluation of an integral of the form:

$$\int[2m(E-V)(dr/dx)^2]^{\frac{1}{2}}dx \qquad (1)$$

where r is the coordinate and x is a function of r in terms of which the integration is simpler. If the integrand is expressed as a radical divided by a rational function of x, the degree of the expression under the radical determines the kind of function in terms of which the integral can be expressed. If the expression is quadratic in x, the integral can be solved in terms of circular functions; if the expression is of the third or fourth degree in x, the integral can be solved in terms of elliptic functions.

EXACT SOLUTIONS IN QUANTUM MECHANICS

If rotation is neglected, the one-dimensional Schrödinger equation has the form,

$$d^2R/dr^2+k[E-V(r)]R=0, \qquad (2)$$

where $k=8\pi^2mc/h$, E is the energy in cm^{-1}.

In order to obtain exact solutions of the differential equation for many interesting forms of potential functions, it is necessary to make a transformation of the independent variable. If the transformation $x=x(r/\rho)$ is carried out, the result is:

$$R''+\left[\frac{d^2x/dr^2}{(dx/dr)^2}\right]R'+\left[\frac{W-\Phi}{\rho^2(dx/dr)^2}\right]R=0, \qquad (3)$$

where $W=k\rho^2E$, $\Phi=k\rho^2V$.

If dx/dr has the form $x^{A_0}(1-x)^{-A_1}(a+x)^{A_2}$ the coefficient of R' becomes $A_0/x+A_1/(1-x)+A_2/(a+x)$.

The coefficient of R is, except for a constant, the same as the expression under the radical in Eq. (1).

The problem of obtaining an exact solution of the one-dimensional Schrödinger equation requires the solution of a linear second order differential equation. The methods of solution of such an equation depend upon the number and character of the singular points of the differential equation. For the purposes of the present study, six types of equations will be considered. These six types are all special cases of a more general equation. This more general equation is:

$$R''+\left[\frac{A_1}{1-x}+\frac{A_2}{a+x}+\frac{A_0}{x}\right]R'+\left[\frac{B_0}{x^2}+\frac{B_1}{(1-x)^2}+\frac{B_2}{(a+x)^2}+\frac{C_1x+C_2}{x(1-x)(a+x)}+\frac{C_3}{x}+\frac{C_4}{1-x}-\mu^2+C_6+C_5x-\epsilon^2x^2-\frac{\delta^2}{x^4}+\frac{B_3}{x^3}\right]R=0, \qquad (4)$$

of which there is a solution of the form:

$$R=x^\alpha(1-x)^\beta(a+x)^\gamma e^{-\delta/x-\mu x-\epsilon x^2/2}\sum a_nx^n. \qquad (5)$$

TABLE I. *Classification of equations.*

TYPE	CONSTANTS OF EQS. (4) AND (5) WHICH ARE ZERO	REG. SING. PTS.	IRREG. SING. PTS. 2ND SPECIES	IRREG. SING. PTS. 4TH SPECIES	KNOWN EXAMPLES
I	$A_2, B_2, C_2-C_1a, C_3, C_4, C_6, \mu, C_5, \epsilon, \delta, B_3, \gamma$	$0, +1, \infty$			Hypergeometric
II	$A_1, A_2, B_1, B_2, C_1, C_2, C_4, C_6, C_5, \epsilon, \delta, B_3, \beta, \gamma$	0	∞		Confl. hypergeometric
IIIa	$C_3, C_4, C_6, \mu, C_5, \epsilon, \delta, B_3$	$0, +1, a<-1, \infty$			Lamé
IIIb	" "	$0, +1, a>+1, \infty$			"
IVa	$A_2, B_2, C_1, C_2, C_6, C_5, \epsilon, \delta, B_3, \gamma$	$0, +1,$	∞		Spheroidal
IVb	" "	$0, -1,$	∞		"
V	$A_1, A_2, B_1, B_2, C_1, C_2, C_4, C_5+2\mu\epsilon, \delta, B_3, \beta, \gamma$	0		∞	
VI	$A_1, A_2, B_1, B_2, C_1, C_2, C_4, \beta, \gamma, C_6, C_5, \epsilon$		0, ∞		Mathieu

The above table gives the essential characteristics of the six types of equations. In the first column is the number by which that type of equation will be referred to; in the second column are listed the constants of Eqs. (4) and (5) which are zero for that type of equation; in the third column the regular singular points of the equation are listed; in the fourth column the irregular singular points of the second species[1] are listed, and in the fifth column the essential singular points of the fourth species[1] are listed. Many of these equations, or their special cases, have been studied and named. These names are given in the last column of Table I.

For the first two types of equation the recursion relation involves only two of the a_n's. For the other four types of equations the recursion involves three of the a_n's. For the first five types of equation, there will be two roots of the indicial equation, although it may be that only one of the roots gives a solution satisfying the boundary conditions. For the sixth type of equation, there will be at most only one root of the indicial equation.

FORMS OF POTENTIAL FUNCTIONS PERMITTING AN EXACT SOLUTION

From Eq. (3) it follows that if a differential equation of a given type is to be a transformed Schrödinger equation, one term in the coefficient of R must have the form of a constant divided by a function of x. If this constant is taken to be W and the denominator set equal to $\rho^2(dx/dr)^2$, a differential equation is obtained which can be solved for r as a function of x and by inversion for x as a function of r. The remaining terms in the coefficient of R are then taken to be $-\Phi/\rho^2(dx/dr)^2$. By this method Φ can be found as a function of r. A very large number of transformations can be found but for many of them x can be obtained from r only as a table of values. In the table which follows, consideration is limited to those transformations where x is defined as either a power of r or as an exponential function of r. In the adjoining table, the first column gives the type of differential equation considered, the second gives the constant which is taken to be W, the third gives the expression for $\rho dx/dr$, the fourth gives the expression for x as a function of r, the fifth column gives the expression for the potential energy, and the last column gives the reference for the cases that have been investigated.[2] For the sake of brevity, the various constants in the expression for Φ have been combined and the following substitutions used: $z=r/2\rho$, $u=1/x$, $v=1/1-x$, $w=1/1+x$, $s=1/a+x$.

The first list includes the cases for which valid solutions (for certain values of the energy) can be found in terms of convergent series about the origin. The second list includes those cases for which it may be necessary to join solutions about different singular points to obtain valid solutions. In any case the solutions for potential functions given in the second list must be examined in detail for each special case. For the potential functions which lead to Eq. III there

[1] For a discussion of the "species" of an irregular singular point, see Ince, *Ordinary Differential Equations*, Chap. 20.

[2] Essentially this method has been used by Rosen to determine the forms of potential function soluble in terms of hypergeometric or confluent hypergeometric functions. Since these results have not been published, they are included here for completeness.

TABLE II. *Potential functions permitting exact solutions.*

TYPE	W	$\rho dx/dr$	x	Φ	REFERENCES
I	B_0	$-x$	$\pm e^{-2z}$	$K_1x^2v^2+K_2xv+K_3v+K_4v^2$	1, 2, 3, 4
I	B_0	$x(1-x)^{\frac{1}{2}}$	$\operatorname{sech}^2 z$	$K_1x+K_2x^2v$	5
II	$-\mu^2$	1	$2z$	$K_1u+K_2u^2$	6, 7
II	C_3	$x^{\frac{1}{2}}$	z^2	K_1u+K_2x	6, 8
II	B_0	$-x$	e^{-2z}	$K_1x+K_2x^2+K_3v+K_4xv$	9
III	B_0	$-x$	$\pm e^{-2z}$	$K_1x^2v^2+K_2x^2s^2+(K_3x+K_4x^2)vs$	
III	B_0	$x(1-x)^{\frac{1}{2}}$	$\operatorname{sech}^2 z$	$K_1x+K_2xs+K_3x^2v+K_4x^2(1-x)s^2$	
IVa	B_0	$-x$	$\pm e^{-2z}$	$K_1x+K_2x^2+K_3x^2v+K_4x^2v^2$	
IVa	B_0	$x(1-x)^{\frac{1}{2}}$	$\operatorname{sech}^2 z$	$K_1x+K_2x^2+K_3x^3+K_4v$	10
V	C_2	$x^{\frac{1}{2}}$	z^2	$K_1u+K_2x+K_3x^2+K_4x^3$	11
V	B_0	$-x$	e^{-2z}	$K_1x+K_2x^2+K_3x^3+K_4x^4$	
V	C_5	$x^{-\frac{1}{2}}$	$(3z)^{\frac{2}{3}}$	$K_1u^3+K_2u^2+K_3u+K_4x$	
V	$-\epsilon^2$	$1/x$	$2z^{\frac{1}{2}}$	$K_1u^4+K_2u^3+K_3u^2+K_4u$	
V	B_3	1	$2z$	$K_1u^2+K_2u+K_3x+K_4x^2$	
IVa	$-\mu^2$	± 1	$\pm 2z$	$K_1u^2+K_2u+K_3v+K_4v^2$	
IVa	C_3	$x^{\frac{1}{2}}$	$\pm z^2$	$K_1u+K_2x+K_3xv+K_4xv^2$	
IVb	C_3	$(x(1+x))^{\frac{1}{2}}$	$\sinh^2 z$	$K_1x+K_2x^2+K_3xw+K_4u$	
VI	B_2	$-x$	e^{-2z}	$K_1u^2+K_2u+K_3x+K_4x^2$	
VI	C_3	$x^{\frac{1}{2}}$	z^2	$K_1u^3+K_2u^2+K_3u+K_4x$	
VI	$-\mu^2$	1	$2z$	$K_1u^4+K_2u^3+K_3u^2+K_4u$	

[1] Eckart, Phys. Rev. **35**, 1303 (1930).
[2] Rosen and Morse, Phys. Rev. **42**, 210 (1932).
[3] Manning and Rosen, Phys. Rev. **44**, 953 (1933).
[4] Newing, Phil. Mag. **19**, 759 (1935).
[5] Poeschl and Teller, Zeits. f. Physik **83**, 143 (1933).
[6] Schrödinger, Ann. d. Physik **76**, 361 (1926).
[7] Shortley, Phys. Rev. **38**, 120 (1931).
[8] Davidson, Proc. Roy. Soc. **A135**, 459 (1932).
[9] Morse, Phys. Rev. **34**, 57 (1929).
[10] Manning, J. Chem. Phys. **3**, 136 (1935).
[11] Morse and Stückelberg, Helv. Phys. Acta **4**, 337 (1931).

will also be the cases when a is replaced by $-a$ and the case when $a=-1$. For the case $a=-1$ there is a possible transformation $x=\operatorname{sech} 2z$ for which the corresponding potential function belongs in the second group.

If, in Eqs. I and II, the coefficient of R is written over a common denominator, the numerator is quadratic in x. By comparison of Eqs. (1) and (3), it follows that whenever the Hamilton-Jacobi equation is soluble in terms of circular functions,[3] the corresponding Schrödinger equation is soluble in terms of functions characterized by a two term recursion relation. If in Eqs. III, IV, V, VI, the coefficient of R is written over a common denominator, the numerator will be of the fourth degree in x. Hence, it follows that whenever the Hamilton-Jacobi equation is soluble in terms of elliptic functions,[3] the corresponding Schrödinger equation is soluble in terms of functions characterized by a three-term recursion relation.

[3] In accordance with what has been said, it follows that the classical solutions for the potential functions listed here can be found in terms of either circular or elliptic functions. The transformations of the form $x=r^n$ are discussed in the fourth chapter of Whittaker's *Analytical Dynamics*, but the other transformations have received little attention in textbooks on classical mechanics.

BOUNDARY CONDITIONS AND METHOD OF DETERMINING ENERGY LEVELS

The solutions for all forms of potential function which lead to differential equations of the first two types have been given in the literature. It turns out that, for these cases, whenever the total energy is less than the potential energy at both plus and minus infinity, solutions satisfying the boundary conditions can be found only for those values of the energy for which the infinite series reduces to a polynomial.

For the last four types of equation, the recursion relation between coefficients has the form

$$H_n b_{n+1}+1+M_n/b_n=0, \tag{6}$$

where $b_n=a_n/a_{n-1}$ and H_n and M_n are expressible in terms of the various constants and the running number n. The convergence of such a series can be tested by a method given by MacLaurin.[4] The essential feature of this method is the assumption (which can be justified) that at large n, $b_{n+1}=b_n[1+0(1/n)]$. When this substitution is made, Eq. (6) reduces to a quadratic equation which can be solved for b_n. If one of the roots of this equation satisfies the ordinary convergence test, a series solution satisfying

[4] MacLaurin, Trans. Camb. Phil. Soc. **17**, 33 (1898).

the boundary conditions can be found for certain values of the energy. For Eq. III, Eq. IV when the range of the variable to from zero to unity, and Eq. V the necessary conditions are fulfilled. For Eq. VI and Eq. IV when the range of the variable includes infinity, the series will converge in only a restricted region and it is necessary to use some method of joining solutions which are valid about different expansion points.

The series solution must satisfy two conditions. There must be no terms containing negative powers of x, and at large n the ratio of two successive coefficients must approach the allowed limiting value found by the method just described. If Eq. (6) is written for $n=0$, the first condition causes this relation to reduce to:

$$0=1+H_0b_1. \tag{7}$$

By using Eq. (16) to solve for b_1 in terms of H_1, M_1 and b_2 and then to find b_2 in terms of succeeding values of H, M and b, the result is

$$0=1-\cfrac{Q_0}{1-\cfrac{Q_1}{1-\cfrac{Q_2}{1\cdots\cfrac{Q_{t-1}}{1-H_tb_{t+1}}}}} \tag{8}$$

where $Q_n=H_nM_{n+1}$.

At sufficiently large n the asymptotic value of b_n can be substituted without appreciable error, and the continued fraction terminated. For a given set of constants in the potential function and an arbitrary value of the energy, the result found by carrying out the process of repeated divisions and subtractions will not be zero but will be a function of the value assumed for the energy. This function will be zero only for certain values of the energy—these are the values of the energy for which the boundary conditions are fulfilled. The problem of determining these values must, except for the simplest cases, be carried out numerically. The method used is similar to that used in finding the roots of an algebraic equation of degree higher than the fourth and consists of evaluating the left-hand side of Eq. (8) for two values of W and interpolating or extrapolating for a better approximation to the value of W which makes the left-hand side of Eq. (8) vanish. The process can be repeated until the desired accuracy is reached. The value of the continued fraction as a function of the value of W has a number of branches and when extrapolating or interpolating care must be taken that the points used are all on the same branch.

The form given in (8) is not always satisfactory for numerical solution. By repeated inversions (8) can be transformed into

$$\cfrac{Q_m}{1-\cfrac{Q_{m+1}}{1-\cfrac{Q_{m+2}}{1\cdots}}}=1-\cfrac{Q_{m-1}}{1-\cfrac{Q_{m-2}}{1-\cdots\cfrac{Q_1}{1-Q_0}}}. \tag{9}$$

The values of the energy which make these two expressions equal are the ones for which the boundary conditions are satisfied. The best form of Eq. (9) for numerical solution is when Q_m in the numerator of the left-hand side is the largest of all the Q's.

For Eq. VI it is necessary to expand about an essential singular point. Detailed examination shows that the boundary conditions at $x=0$ can be satisfied only by so choosing the root (there is only one) of the indicial equation that there are at most only a finite number of negative powers of x in the series expansion. The series so found will converge for finite values of x but will diverge at x equal infinity. If a similar series expansion about x equal infinity is found it will have the same properties in terms of $1/x$.

By properly choosing the scale factor ρ the continued fraction corresponding to the solution valid about x equal infinity can be made the same as the continued fraction corresponding to the solution valid about x equal zero. For the values of the energy obtained by solution of this continued fraction it will be possible to join the two solutions at some intermediate point (say x equal unity) and thus obtain solutions valid throughout the entire range of the independent variable. It may be pointed out that this method is somewhat similar to that used for the Mathieu equation which is a special case of Eq. VI.

The author wishes to acknowledge his indebtedness to Dr. Nathan Rosen for pointing out that it is possible to determine the allowable transformations by a systematic process, and to thank Professor P. M. Morse and Professor J. A. Stratton for many helpful discussions about the mathematical aspects of the problem.

LETTERS TO THE EDITOR

Prompt publication of brief reports of important discoveries in physics may be secured by addressing them to this department. Closing dates for this department are, for the first issue of the month, the twentieth of the preceding month; for the second issue, the fifth of the month. The Board of Editors does not hold itself responsible for the opinions expressed by the correspondents.

About the Structure of Crystalline Bismuth and Selenium Layers Produced by Condensation in Vacuum

In the course of experiments, undertaken independently by the authors for different purposes, an analogous habitus of crystalline condensations of Bi and Se evaporated in vacuum was observed which apparently has not been described before.

In the case of Bi the substance was evaporated from a vacuum furnace described previously[1] and condensed on a water-cooled surface of Pyrex for many hours. In case of Se[2] a simpler arrangement, though of the same principle, was used. In both cases the vacuum was of the order of $\leqq 10^{-5}$ mm, hence the m.f.p. was larger than the distance between the surfaces of evaporation and condensation. The layers thus obtained were 5 to 10 mm thick.

From the point of view of the habitus of the deposit the structure of these layers proved to be of interest, inasmuch as their cross section in the direction of crystallization showed *two* distinctly different structures: the layer which is deposited first shows a *microcrystalline* structure of such fineness that it has almost an amorphous appearance. This is especially true for Se. The layer is homogeneous throughout its whole thickness of 10^{-2} cm, then its structure changes suddenly into a *macrocrystalline* one with fibrous texture. This second layer is furthermore characterized by a homogeneous orientation of these fibers, hence the whole of this layer has the characteristics of a single crystal with a very regular mosaic structure.

For both substances [111] is parallel to the direction of growth, i.e., normal to the plane of condensation. This is not trivial in view of the fact that the direction of growth for both substances follows [100].

Figs. 1 to 3 represent photomicrographs of the surfaces and cross sections of such layers for Bi and Se, respectively. In case of Se (Fig. 3) the coherence among the two layers is so small that the "amorphous" layer separated itself in parts.

Seemingly the only interpretation of this phenomenon is in terms of the temperature of the surface of condensation. This temperature is low as long as the deposited layer is thin, and the heat of crystallization is easily transferred to the cooling medium. As the deposit grows thicker the heat transfer becomes less easy and the temperature of the surface increases. The fact that the transition between the two types of layer is as abrupt as the observations show, seems to indicate the existence of a definite temperature above which the homogeneous crystallization only is possible.

It is of interest to compare this result with the observation of Kapitza[3] that the production of Bi single crystals out of the vapor phase is not successful below 200°C.

A. GOETZ
California Institute of Technology
L. E. DODD
University of California at Los Angeles

July 8, 1935.

[1] A. Goetz, Zeits. f. Physik **42**, 329 (1927).
[2] L. E. Dodd, Abstract No. 1 of paper on program of Am. Phys. Soc., Los Angeles, June 28, 1935.
[3] P. Kapitza, Proc. Roy. Soc. **A119**, 428 (1928).

FIG. 1. Bi-layer. Right to left: outer surface of first layer; cross section; outer surface of second layer. (About 10 times.)

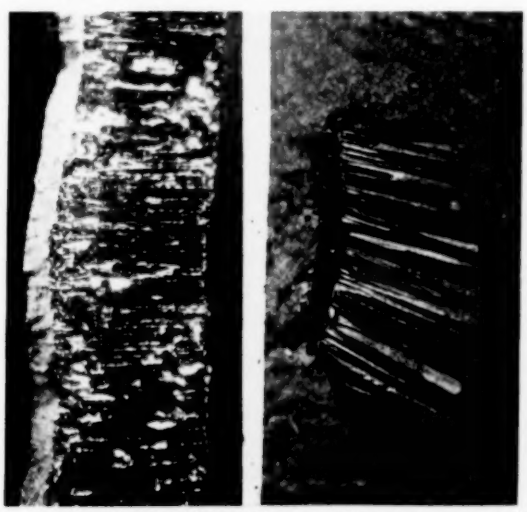

FIG. 2. Cross section of Bi-layer. Microcrystalline structure to the left. (About 30 times.)

FIG. 3. Cross section of Se-layer. Microcrystalline layer to the left. (About 20 times.)

The Relation Between the Thermal and Electrical Conductivities of Copper Alloys

Since 1929 an investigation has been in progress in the research laboratory of The American Brass Company to determine the thermal and electrical conductivities of all copper alloys of industrial importance or scientific interest. Some of the results have already been published[1, 2] and others are soon to appear.[3]

The conductivities of over one hundred alloys were determined, including binary series of alloys of copper with up to 50 weight percent of zinc, <10 percent Sn, <1 percent P, <4 percent Si, <12 percent Al, <20 percent Mn, <30 percent Ni, and a large number of ternary and more complex alloys. Some of these were in the cast state, and others were given special precipitation hardening heat treatments; but most of them were carefully homogeneized by extensive working and annealing before the conductivities were measured. The majority of the alloys were homogeneous α-phases (face-centered cubic in structure), although β brass (body-centered cubic) and several complex alloys were included. The thermal conductivity was assumed to be a linear function of temperature, and values at 20 and 200°C were read from the mean straight line through six or more experimental points for each alloy. The electrical conductivity was determined at 20 and 200°C on the identical specimens used for the thermal measurements. Full experimental details and complete analyses of the alloys are given in the papers referred to above.

When the thermal conductivity is plotted against the electrical conductivity at the same temperature, as in Fig. 1, the results for *all* the different alloys fall closely together and can be represented by a single curve, regardless of composition (within the limits named above), structure or heat treatment. The spread around the mean curve is rather greater than the supposed experimental error, and certain series of alloys lie uniformly below and others uniformly above the curve. Much more accurate determinations would be necessary, however, before the various series could be represented by separate lines. The curve at 200°C differs from that at 20°C in slope, but intersects the thermal conductivity axis at approximately the same value. All the results, representing all alloys at both 20 and 200°C, fall on a single curve if the thermal conductivity is plotted against the product of electrical conductivity and absolute temperature, as in Fig. 2. Much of the curve is straight, in agreement with the simple theory that thermal conductivity is composed of a metallic (electronic) and a nonmetallic part, i.e.,

$$K = k + c\lambda T,$$

K being the total thermal conductivity, k the nonmetallic part, λ the electrical conductivity and c a constant which may be regarded as a true Lorenz ratio for the metallic part of conductivity. In Fig. 2, $k = 0.018$ and $c = 5.71 \times 10^{-9}$ c.g.s. units. The deviation from this linear function becomes considerable for the alloys of high conductivity. The ordinary Lorenz ratio is obviously not a constant on account of the increasing importance of the factor k at low values of the conductivity. Alloys are represented in Fig. 2 in which the Lorenz ratio varies between 5.35 and 8.6.

The results of Schofield[4] for pure copper from room temperature up to 625°C fall closely on this K *vs.* λT curve, and those of Lees[5] at temperatures down to −170°C provide a smooth extrapolation of the curve with ever decreasing slope.

It is to be expected that curves of a similar type could be drawn for the alloys of other metals which form solid solutions, were a sufficient number of determinations available. The published figures for the conductivities for most of the other metallic elements fall more closely on the K *vs.* λT curve of Fig. 2 than on any curve of constant Lorenz ratio, and the alloy curves would be practically indistinguishable. Alloys between metals which do not form solid solutions would not lie on the curve unless the

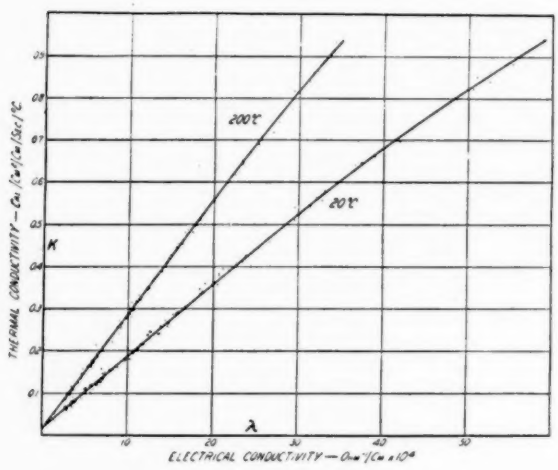

FIG. 1.

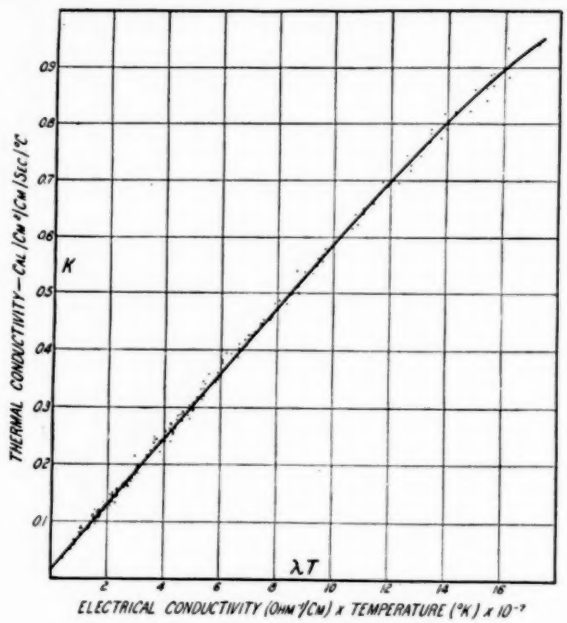

FIG. 2.

two elements did, but would lie on a line directly joining the points for the elements. The thermal conductivity of aluminum is definitely abnormal in its temperature variation, but the conductivities of all its usual alloys except those containing silicon are capable of close representation by a single curve at a given temperature.

CYRIL STANLEY SMITH

Copper Alloys Research Laboratory,
The American Brass Company,
Waterbury, Connecticut,
June 5, 1935.

[1] C. S. Smith, Trans. A. I. M. E. (Inst. Metals Div.) **90**, 84 (1930).
[2] C. S. Smith, Trans. A. I. M. E. (Inst. Metals Div.) **93**, 176 (1931).
[3] C. S. Smith and E. W. Palmer—Not yet published. Will be submitted to the Amer. Inst. Min. Met. Eng. for presentation at the October 1935 meeting.
[4] Schofield, Proc. Roy. Soc. **A107**, 206 (1925).
[5] Lees, Phil. Trans. Roy. Soc. **A208**, 381 (1908).

Statistical Fluctuations of Cosmic-Ray Ionization in New Recording Meter

The statistical fluctuations of the ionization due to cosmic rays inside a spherical chamber are related to the number of ionizing particles entering the chamber by the expression $\sigma = FI(N)^{-\frac{1}{2}}$, where σ is the standard deviation of a set of observations each extending over a time t, I is the total ionization and N the number of ionizing particles traversing the chamber during the time of one observation. The factor F is given by

$$F^2 = (9/8)\frac{\Sigma r_n \cdot \Sigma n^2 r_n}{(\Sigma n r_n)^2},$$

where r_n is the ratio of multiple to single rays and n is the number of associated shower particles.[1] If F were known accurately then it would be possible to determine N by measurements of σ. Actually F can only be approximated from drop track observations and the resulting value is certainly smaller than that which applies to shielded ionization chambers where the number of effective showers is undoubtedly larger than for the usual cloud chamber arrangement.

Recent analyses of records obtained from two precision recording cosmic-ray meters[2] running simultaneously side by side gave for the hourly statistical variation after elimination of bursts larger than 10^7 ions

$$\sigma_h = 33.4(10)^6 \text{ ions (meter No. 1)}$$
$$= 34.4(10)^6 \text{ " (meter No. 2).}$$

Since the collecting systems were insulated for 57.5 minutes out of each hour, the standard deviation for one minute was $\sigma_m = 33.9(10)^6 \times (57.5)^{-\frac{1}{2}} = 4.41(10)^6$ ions.

The observed total ionization was $I = 94.8(10)^6$ ions/minute.

The value of F as estimated from Anderson's cloud chamber observations[3] is 1.32 but in our case where we have a 35.6 cm diameter ionization chamber surrounded by 12 cm of lead, this factor would be considerably larger. If we take $F = 1.5$ then the calculated value of N comes out to be 1035 particles per minute or 1.04 per cm^2 per minute.

The total ionization is

$$I = (4/3)RsfN\Sigma n r_n / \Sigma r_n,$$

where R is the radius of the ionization chamber, s the number of ions per particle per cm in air at one atmosphere and f is the factor of proportionality between the ionization in one atmosphere of air and 50 atmospheres of argon ($f = 67.0$). Taking $\Sigma n r_n / \Sigma r_n = 1.42$ which is again an estimate from cloud chamber observations, the calculated value of s is 47 ions/cm.

The smallest burst which can be detected with reasonable certainty with this apparatus is about 10^7 ions, which corresponds to 132 ionizing particles on the basis of the above value of specific ionization. Obviously there are smaller bursts which occur but are not detectable as such and presumably this still holds true for apparatus capable of detecting bursts involving considerably fewer particles. This suggests that some of the bursts at least are simply large scale showers.[4]

RICHARD L. DOAN

Ryerson Physical Laboratory,
University of Chicago,
June 29, 1935.

[1] Evans and Neher, Phys. Rev. **45**, 144 (1934).
[2] Compton, Wollan and Bennett, R.S.I. **5**, 415 (1934).
[3] C. D. Anderson, Phys. Rev. **44**, 406 (1933).
[4] E. G. Steinke and H. Schindler, Naturwiss. **20**, 491 (1932).

On the Shape of the Distribution Curves of Electrons Emitted from Artificially Produced Radioactive Substances

No reliable method of finding the upper limit of the (momentum)-distribution curves of the electrons emitted from the nuclei of radioactive substances has as yet been devised. In the hope of finding a good statistical method of treating the histograms obtained from measurements of the curvatures of β-tracks in a cloud chamber we have been examining some experimental data in terms of the theory of Fermi[1] and also the modification of Fermi's theory introduced by Uhlenbeck and Konopinski.[2] We desire to give a brief account here of the ability of these theories to account for the shape of these distribution curves and to discuss their usefulness as methods of computation in getting the upper limits of such distributions without the arbitrariness usually involved in such work.

It appeared some time ago that the original Fermi theory gave a fairly good fit to our experimental curves and by using the theory in a form which will be indicated below we deduced the upper limits of several elements which were reported in April.[3] The tracks on which these results were based were photographed in a cloud chamber filled with oxygen. Feeling that our criterion of selection (that any track with a noticeable deflection was not measured) was discriminating against low energy tracks, we have repeated nearly all our previous work in a hydrogen-filled chamber which greatly reduces the scattering of the electrons. The new distribution curves have their peaks at a lower $H\rho$ and cannot be fitted by the old Fermi theory. At the suggestion of Dr. Arnold Nordsieck

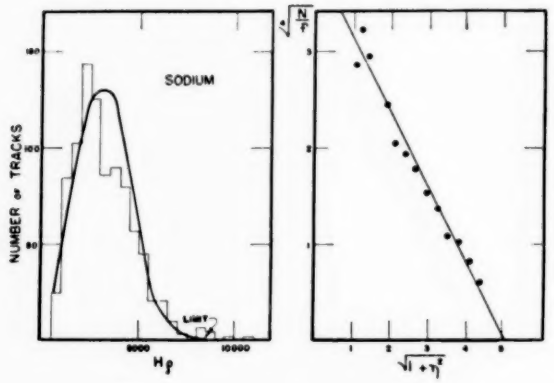

FIG. 1a. FIG. 1b.

FIG. 1 (a) The experimental histogram for the distribution in $H\rho$ of the electrons emitted from radio-sodium. The heavy smooth curve is a theoretical curve which has been fitted to the histogram by means of the plot in (b) where the same data are so plotted that a straight line is expected if the Uhlenbeck-Konopinski modification of the Fermi theory is valid. The few tracks beyond the upper limit are to be attributed to the strong γ-radiation emitted by radio-sodium.

we have tried fitting the Uhlenbeck-Konopinski formula to the data and found for the most part that the fits were gratifyingly good.

Fermi's formula for the probability that an electron of momentum $mc\eta$ be emitted may be written in the form

$$(1+\eta^2)^{\frac{1}{2}} = c - k[N/f(\eta, Z)]^{\frac{1}{4}}$$

where N is the number of tracks whose momenta lie within a certain class interval, $f(\eta, Z)$ is a function which may be computed from the Fermi theory, $c=(1+\eta_0^2)^{\frac{1}{2}}$ and k is a numerical constant. By plotting $(N/f)^{\frac{1}{4}}$ against $(1+\eta^2)^{\frac{1}{2}}$ one should get a straight line if the data conform to the theory. From the intercept c on the $(1+\eta^2)^{\frac{1}{2}}$ axis one may get the energy of the upper limit. The modification introduced by Uhlenbeck and Konopinski leads to a formula which differs essentially from this only in that the square root term of Fermi's formula becomes a fourth root. The immediate consequence of this is that the order of contact of the distribution curve with the $H\rho$ axis is raised to the fourth order and if this is true the difficulties of finding this upper limit directly—without having recourse to fitting a theoretical curve to the experimental data—become very great.

The elements on which we have fairly complete data are carbon, sodium, silicon, chlorine and potassium. The tracks of the electrons emitted from these elements after they have been activated by bombardment with deuterons have been photographed in hydrogen. The distribution curves for sodium and silicon are shown in Figs. 1a and 2a. Superimposed upon the experimental histograms are the theoretical (Uhlenbeck-Konopinski) curves which have been fitted by means of the straight line plots shown in Figs. 1b and 2b as explained above. In these straight line plots the excellence of the fit is perhaps more apparent

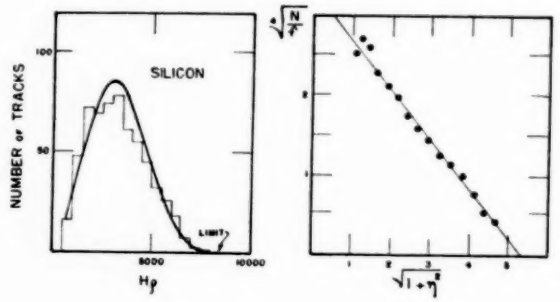

FIG. 2a. FIG. 2b.

FIG. 2 (a) The experimental histogram for the distribution in $H\rho$ of the electrons emitted from radio-silicon. Here again a theoretical curve has been fitted to the data by means of the plot in (b).

than real since the number of tracks in each column of the histogram enters the ordinate only as a fourth root. However the linearity of these plots is so much greater than a corresponding plot for the simple Fermi theory that one feels justified in attaching some value to the upper limits obtained in this way. We find in these two cases upper limits at $H\rho$ 8400 (2.1 mv) for sodium, and at $H\rho$ 8500 (2.1 mv) for silicon. In the case of sodium a few tracks from the hard γ-radiation emitted by this element make the determination of the upper limit from an inspection of the histogram very difficult, while for silicon no tracks have been found above $H\rho$ 8000.

For carbon an upper limit is indicated at $H\rho$ 7800 (1.9 mv) while no tracks have been found above $H\rho$ 7000.

Both chlorine and potassium are at present unsatisfactory in that they do not yield a single straight line but are readily decomposable into two straight lines and seem to indicate that the histograms are composed of two groups. A study of the γ-rays emitted from these substances is now being made in the hope of further unraveling these cases.

A more comprehensive and detailed account of the matters dealt with in this note will shortly be submitted to the *Physical Review*.

We are very grateful to Dr. Nordsieck for discussions and to Professor Uhlenbeck for private communications regarding his modifications to the Fermi theory.

FRANZ N. D. KURIE*
J. R. RICHARDSON
H. C. PAXTON

Radiation Laboratory, Department of Physics,
University of California,
Berkeley, California,
June 18, 1935.

[1] E. Fermi, Zeits. f. Physik **88**, 161 (1934).
[2] Uhlenbeck and Konopinski, Phys. Rev., this issue.
[3] Kurie, Richardson and Paxton, Washington meeting Am. Phys. Soc., April, 1935; Phys. Rev. **47**, 797A (1935).
* National Research Fellow.

Where Can Negative Protons Be Found?

The suggestion has variously been made, that in some distant stars or nebulae the identities of the carriers of positive and negative electricity might be reversed. A hydrogen atom in such regions would be built up of a negative proton and a positive electron.

If the above idea is correct, one should find negative protons which enter our atmosphere from interstellar space. We know indeed that elementary particles of all kinds are emitted from most of the nebulae which can be seen with the modern telescopes. *Common novae* and *super-novae* which from time to time flare up in these nebulae emit great numbers of fast elementary particles. Common novae, whose average absolute magnitude is −5.8 expel gaseous shells with velocities of the order of 100 to 2000 km/sec. Super-novae, whose average magnitude is of the order of −15 emit ions whose velocities are probably considerably greater than 10,000 km/sec. In any case, because of the generality of the nova phenomenon the earth atmosphere will be invaded by all kinds of ions, some of which have traveled hundreds of millions of light years.

A rough estimate indicates that on the top of the earth's atmosphere the number of atoms coming from novae is of the order of 0.1 per cm² and second. Because of the abundance of hydrogen in the stars many of these particles should be ordinary protons, as well as negative protons, provided that the latter exist in stars nearer than that critical distance ($>2\times10^9$ light years) through which the energy of elementary particles probably is radically reduced by "redshift" effects or absorption. We conclude: (1) Negative protons should be looked for in cloud chambers at high altitudes. (2) Hard γ-rays of the order of one to two billion volts will be produced in the upper atmosphere if mutual annihilation of positive and negative protons takes place. (3) An east-west effect of the observed sign can be expected due to the dissimilar penetration of positive and negative protons into the atmosphere.

F. ZWICKY

California Institute of Technology,
Pasadena, California,
June 6, 1935.

THE AMERICAN INSTITUTE OF PHYSICS

INCORPORATED

GOVERNING BOARD

For The American Physical Society:

KARL T. COMPTON, *Chairman*
Massachusetts Institute of Technology

GEORGE B. PEGRAM, *Secretary*
Columbia University

JOHN T. TATE
University of Minnesota

For The Optical Society of America:

E. C. CRITTENDEN
Bureau of Standards

PAUL D. FOOTE
The Gulf Companies

F. K. RICHTMYER
Cornell University

For The Acoustical Society of America:

HARVEY FLETCHER
Bell Telephone Laboratories

VERN O. KNUDSEN
University of California at Los Angeles

WALLACE WATERFALL
The Celotex Company

For The Society of Rheology:

E. C. BINGHAM
Lafayette College

A. STUART HUNTER
du Pont Rayon Company

S. E. SHEPPARD
Eastman Kodak Company

For The American Association of Physics Teachers:

HOMER L. DODGE
University of Oklahoma

PAUL E. KLOPSTEG
Central Scientific Company

FREDERIC PALMER
Haverford College

ADMINISTRATIVE STAFF

HENRY A. BARTON, *Director* JOHN T. TATE, *Adviser on Publications*

MADELINE M. MITCHELL, *Editorial Secretary*

Office: 11 East 38th Street, New York, New York

JOURNALS

THE PHYSICAL REVIEW

REVIEWS OF MODERN PHYSICS

PHYSICS
JOHN T. TATE, *Editor*
J. W. BUCHTA, *Assistant Editor*
E. C. BINGHAM, *Rheology Editor*

THE JOURNAL OF THE OPTICAL SOCIETY OF AMERICA

THE REVIEW OF SCIENTIFIC INSTRUMENTS
WITH PHYSICS NEWS AND VIEWS
F. K. RICHTMYER, *Editor*

JOURNAL OF THE ACOUSTICAL SOCIETY OF AMERICA
F. R. WATSON, *Editor*

THE JOURNAL OF CHEMICAL PHYSICS
HAROLD C. UREY, *Editor*

THE AMERICAN PHYSICS TEACHER
DUANE ROLLER, *Editor*

The American Institute of Physics is a membership corporation of which five societies are the founding members. These five societies are the principal national societies devoted to pure and applied physics in America. Their names, and those of their representatives who form the Governing Board of the Institute, are given above. The principal work of the Institute is the publication of journals sponsored by the societies or by itself. The names and the editors of the journals are also listed above.

The broad purpose of the Institute is to represent, in all matters of wide or common interest, the five thousand or more members and subscribers associated with the Founder Societies and the journals. It aims to advance the science and profession of physics, and to promote cooperation between pure research, the applied sciences and the industries. To achieve these aims, it is greatly in need of an endowment and is empowered by law to administer grants and funds of any kind.

CONTENTS

PHYS. REV. 48 (1935) JULY 15

Variation of Sparking Potential with Intense Ultraviolet Illumination . . . . . HARRY J. WHITE 113

Yield of Alpha-Particles from Lithium Films Bombarded by Protons . . . . . R. G. HERB, D. B. PARKINSON AND D. W. KERST 118

Cloud Chamber Studies of the Gamma-Radiation from Lithium Bombarded with Protons . . . . . H. R. CRANE, L. A. DELSASSO, W. A. FOWLER AND C. C. LAURITSEN 125

Intensities of Satellites of $K\alpha$ . . . . . ANNA W. PEARSALL 133

Spectrum of Aluminum Vapor Distilled by a Tungsten Coil in Vacuum . . . . . E. GAVIOLA AND JOHN STRONG 136

Spectrum of AgD . . . . . PHILIP G. KOONTZ 138

Theory of $^3\Sigma^+ - ^3\Sigma^-$ Transitions in Band Spectra . . RICHARD D. PRESENT 140

Transparency of the Air Between 1100 and 1300A . . THEODORE LYMAN 149

On the Half-Lives of Potassium, Rubidium, Neodymium and Samarium . . . . . ARTHUR RUARK AND KARL H. FUSSLER 151

Calculation of the Elastic Scattering of Electrons in Krypton . . . . . A. L. HUGHES AND S. BILINSKY 155

Exact Solutions of the Schrödinger Equation . MILLARD F. MANNING 161

Letters to the Editor:

About the Structure of Crystalline Bismuth and Selenium Layers Produced by Condensation in Vacuum. . . . . A. GOETZ AND L. E. DODD 165

Relation Between the Thermal and Electrical Conductivities of Copper Alloys . . . . . CYRIL STANLEY SMITH 166

Statistical Fluctuations of Cosmic-Ray Ionization in New Recording Meter . . . . . RICHARD L. DOAN 167

On the Shape of the Distribution Curves of Electrons Emitted from Artificially Produced Radioactive Substances . . . . . FRANZ N. D. KURIE, J. R. RICHARDSON AND H. C. PAXTON 167

Where Can Negative Protons Be Found? . . . . . F. ZWICKY 169

LANCASTER PRESS INC., LANCASTER, PA.